

AN ABSTRACT OF THE THESIS OF

Virgilio Asuncion Fernandez for the degree of Doctor of Philosophy

in Forest Products presented on December 13, 1977

Title: MODEL AND PROCEDURE FOR DETERMINATION OF

STRENGTH AND STIFFNESS OF WOOD STUDS

Redacted for privacy

Abstract approved: \_\_\_\_\_  
Anton Polensek

Elasticity properties of wood studs are essential inputs for  
the structural analysis of wood-stud wall systems.

A theoretical procedure was developed to determine the probability distributions for the deflection-load relations of stud samples. The procedure is based on the finite element analysis and a Monte-Carlo type simulation and accounts for the nonlinearity and local material variability caused by stud defects. The procedure was verified experimentally; the results displayed a good agreement between the theoretical and experimental values. A parameter study showed that the deflection-load curves were greatly affected by the local elasticity and strength of clear wood, grain angle, and knots.

A listing of the computer program prepared is included. The program allows various options as to the types and geometry of stud defects.

© Copyright by Virgilio Asuncion Fernandez 1978  
All Rights Reserved

**Model and Procedure for Determination of  
Strength and Stiffness of Wood Studs**

by

**Virgilio Asuncion Fernandez**

**A THESIS**

**submitted to**

**Oregon State University**

**in partial fulfillment of  
the requirements for the  
degree of**

**Doctor of Philosophy**

**June 1978**

APPROVED:

Redacted for privacy

---

Associate Professor of Forest Products  
in charge of major

Redacted for privacy

C

---

Head of Department of Forest Products

Redacted for privacy

---

Dean of Graduate School

Date thesis is presented December 13, 1977

Typed by Opal Grossnicklaus for Virgilio Asuncion Fernandez

COMMITTEE MEMBERS

Redacted for privacy

---

A. Polensek

---

Redacted for privacy

---

G. Atherton

---

Redacted for privacy

---

H. Laursen

---

Redacted for privacy

---

K. Rowe

---

Redacted for privacy

---

T. Ching

---

## ACKNOWLEDGMENTS

I wish to express my sincere thanks to Dr. Anton Polensek of the Forest Products Department for his advice and assistance in this study. I also thank Prof. George H. Atherton of the Forest Products Department, Dr. Harold Laursen of the Civil Engineering Department, and Dr. Kenneth Rowe of the Statistics Department for their helpful suggestions; Ken Bastendorff of the Forest Research Laboratory for his assistance in the collection of specimens and in the setting-up of the testing equipment; and my wife, Elvira, for typing the rough draft of the thesis.

I am grateful to the Oregon State University Forest Research Laboratory for financial support for this study.

## TABLE OF CONTENTS

I. INTRODUCTION . . . . .	1
1.1. Present Design Procedure . . . . .	2
1.2. Previous Works and Present Outlook . . . . .	2
1.2.1. Load Sharing . . . . .	3
1.2.2. Composite Action . . . . .	3
1.2.3. Nonlinear Behavior of Studs . . . . .	4
1.2.4. Finite Element Method . . . . .	7
1.3. Future Outlook . . . . .	8
1.4. Justification and Objectives . . . . .	9
II. METHOD OF ANALYSIS . . . . .	11
2.1. Finite Element Method . . . . .	11
2.2. Assumptions . . . . .	14
2.3. The Finite Elements and their Stiffness Matrices . . . . .	15
2.3.1. Rectangular Elements . . . . .	16
2.3.2. Triangular Elements . . . . .	21
2.4. Elasticity Parameters . . . . .	24
2.4.1. Modification of Elastic Properties by Axial Transformation . . . . .	25
2.5. Nonlinear Analysis . . . . .	31
2.5.1. Linear Step-by-Step Analysis . . . . .	32
III. VERIFICATION . . . . .	37
3.1. Selection, Preparation and Characterization of Specimens . . . . .	37
3.2. Flexure Test . . . . .	38
3.3. Compression and Tension Tests of Small, Clear Specimens . . . . .	43
3.4. Finite Element Mesh . . . . .	49
3.5. Comparison of Experimental and Theoretical Results . . . . .	55
IV. PARAMETER STUDY . . . . .	60
4.1. Procedure . . . . .	60
4.2. Results . . . . .	61

V. SIMULATION PROCEDURE .....	66
5.1. Generation of Material Properties .....	66
5.1.1. Diameter and Location of Knots .....	66
5.1.2. Grain and Ring Angles .....	70
5.1.3. Elastic and Strength Properties .....	70
5.2. Finite Element Mesh .....	72
VI. DISCUSSION .....	75
6.1. Finite Element Model and Simulation Procedure .....	75
6.2. Accuracy of Stud Properties for Verification and Effect on the Theoretical Results .....	75
6.2.1. Moduli of Elasticity .....	76
6.2.2. Shear Moduli and Poisson's Ratio.....	77
6.2.3. Grain and Ring Angles .....	77
6.2.4. Clear Wood Stresses .....	78
6.2.5. Knots .....	78
6.3. Applications of the Finite Element Model and Simulation Procedure .....	79
VII. CONCLUSIONS AND RECOMMENDATIONS .....	80
BIBLIOGRAPHY .....	82
APPENDICES	
Appendix A: Computer Program .....	88
Appendix B: Input File for Stud No. 1 .....	112
Appendix C: Input File for Stud No. 2 .....	117
Appendix D: Input File for Stud No. 3 .....	122
Appendix E: Input File for Stud No. 4 .....	127
Appendix F: Input File for Stud No. 5 .....	134
Appendix G: Input File for a Simulation Analysis..	140
Appendix H: Computer Output for Analysis of Stud No. 2 .....	142
Appendix I: Moisture Content and Specific Gravity of Studs .....	143
Appendix J: Moduli of Elasticity and Stresses of Small Clear Specimens .....	144

## LIST OF TABLES

<u>Table</u>		<u>Page</u>
2.1.	Direction cosines of the angles of rotation.	28
3.1.	Experimental and theoretical values of load, MOE and MOR.	58
4.1.	Magnitude of parameter increases used in parameter study.	61
4.2.	Moduli of elasticity and rigidity for deflection- load traces of control model and models with changed elasticity property.	64
5.1.	Generated value and the corresponding knot diameter used in simulating the stud model.	69
5.2.	Values of variable IP and the corresponding knot diameter ranges considered by the model.	69

## LIST OF FIGURES

<u>Figure</u>		<u>Page</u>
1.1.	Typical deflection-load curve of lumber.	5
2.1.	Rectangular plane stress element.	17
2.2.	Triangular plane stress element.	22
2.3.	Geometry and elasticity of studs.	26
2.4.	Rotation of axes.	29
2.5.	Flow diagram for linear step-by-step analysis.	33
2.6.	A strain-stress curve of an element.	35
3.1.	Characteristics of stud No. 5.	39
3.2.	Stud loading condition and location of LVDT's.	40
3.3.	A photograph of an LVDT and movable core.	41
3.4.	Dimensions of tension and compression specimens.	45
3.5.	The arrangement for tension tests in the Instron testing machine.	46
3.6.	The arrangement for compression tests in the Tinius Olsen testing machine.	47
3.7.	The two mesh refinements studied to determine the sizes and number of elements used in the analyses of the three clear wood studs.	50
3.8.	Deflection-load curves of stud No. 2 obtained experimentally and theoretically using two finite element models.	51
3.9.	Finite element models used to analyze stud numbers four and five.	53

3.10.	Deflection-load curves of stud No. 2 showing the experimental solution and three theoretical solutions using three different load increments (30-, 50-, and 200 lb).	54
3.11.	Deflection-load curves obtained experimentally and theoretically for stud numbers one, two, and three.	56
3.12.	Deflection-load curves obtained experimentally and theoretically for stud numbers four and five.	57
4.1.	Deflection-load curves for the control model, and for the model with increased MOE's, grain angle and clear wood stresses.	62
4.2.	Deflection-load curves for the control model, and for the model with increased Poisson's ratio, modulus of rigidity, and ring angle.	63
5.1.	Flow diagram for simulation procedure.	67
5.2.	Elements disturbed by knots.	71
5.3.	Finite element mesh used in the analyses of wood studs.	73

## MODEL AND PROCEDURE FOR DETERMINATION OF STRENGTH AND STIFFNESS OF WOOD STUDS

### I. INTRODUCTION

The present design method for wood-stud walls considers each stud as an independent beam-column carrying its own proportionate share of the load. This procedure neglects factors such as the non-linear nature and variability of stud stiffness, composite effect of covering materials and load sharing between studs of various strengths and stiffnesses, which combine to result in general over-design in currently-built walls. This method is uneconomical and puts wood in a poor competitive position with other construction materials. Research at the Forest Research Laboratory, Oregon State University, has resulted in a rational design procedure, based on an accurate theoretical analysis (37) and computer simulation method (38), that accounts for these factors. To use the rational procedure, however, properties and probability distribution of studs must be available. Currently, such information can only be obtained by in-grade testing of studs, which is an expensive and time-consuming method. There is, therefore, a need to develop an alternative non-destructive procedure to evaluate stud properties.

### 1.1. Present Design Procedure

The allowable stress,  $F_b$ , for a grade and species of studs is based on the ultimate bending strength or the modulus of rupture (MOR). First the MOR value is selected at the five-percent exclusion value on the cumulative probability distribution of the MOR for the small-size clear wood bending specimens from the species considered (3, 25). The selected value is then adjusted for the grade according to the effects of seasoning, strength-reducing defects, general adjustment factor and depth. The resulting value is the  $F_b$  for studs of grade and species considered.

The design modulus of elasticity (MOE) is based on the average MOE of species, which was determined from bending tests of small clear specimens (3, 25). The average MOE is then adjusted for the grade according to defects and effects of seasoning.

### 1.2. Previous Works and Present Outlook

The shortcomings of the present design method for wood-stud walls are due to its failure to account for the load sharing between studs, composite action of covering materials, and the nonlinear behavior of studs.

#### 1.2.1. Load Sharing

Past studies have demonstrated that the present design method is too conservative. Johnson (28) and Snodgrass (50), investigated Construction and Standard grades of Douglas-fir 2- by 4-inch dimension lumber. They independently concluded that the average bending and compression stresses for pieces in groups of three were consistently higher than the stresses of pieces taken singly at one, five and ten percent exclusion limits. This conclusion is recognized by the National Forest Products Association (34) which now allows higher unit stresses for repetitive-member uses where load sharing is known to exist.

#### 1.2.2. Composite Action

Composite action between the wall covering and studs increases the strength and stiffness of walls. Polensek and Atherton (40) reported that the experimental walls with Utility grade studs deflected 30% to 60% more if the gypsum boards wall covering was removed. However, the connection between the coverings and the studs is not infinitely stiff. Slip between the studs and wall coverings must be considered. Studies conducted by Amana and Booth (1, 2) show that deflection of a composite I-beam is directly related to the amount of slip between the flanges and the web.

### 1.2.3. Nonlinear Behavior of Studs

Some studs especially those of low strength and stiffness respond nonlinearly to an increasing load. Nonlinear response of studs is the main subject of this investigation.

The complete deflection-load curve of studs is obtained by plotting on the X-Y recorder the deflection and load of a beam continuously loaded to destruction.

Many studs display linear behavior during the early stages of a test. A typical deflection-load curve of such a stud is shown in Figure 1.1. The curve is linear up to the proportional limit (PL) after which it becomes non-linear. The slope at a certain point or section of the curve is directly related to the MOE at that particular point or section. The MOE at a discrete point, such as B in Figure 1.1, is usually defined by the tangent on the deflection-load curve at B, beam cross-section and the conditions of loading. The resulting MOE is called tangent MOE. The MOE for a section such as AB in Figure 1.1 often is related to the secant connecting A and B. The resulting MOE is called secant MOE. The highest point of the curve gives the maximum load which defines the stress at the point of rupture, i. e., the MOR. An approximate procedure to numerically define an experimental deflection-load curve consists of subdividing the curve into

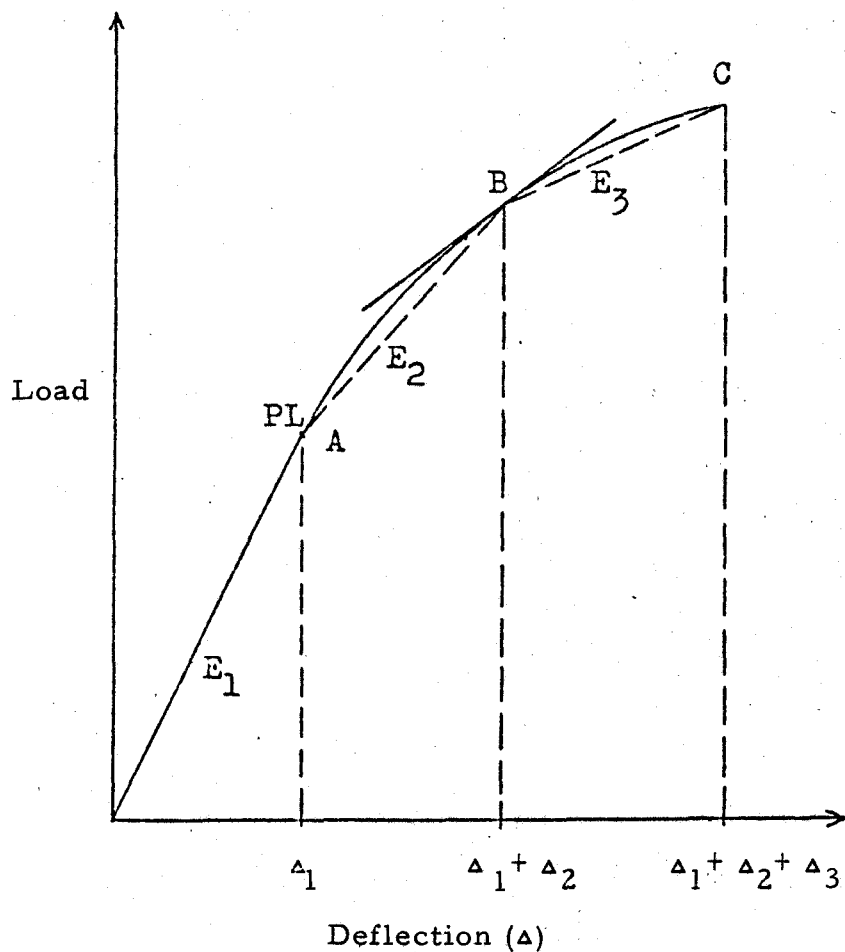


Figure 1.1. Typical deflection-load curve of lumber.

sections defined in terms of the secant MOE, such as  $E_2$  and the associated deflection  $\Delta_2$ . The whole curve may be defined by pairs of  $E_i$ 's and  $\Delta_i$ 's ( $i=1, 2, 3$ ) with surprisingly high accuracy (37).

Young's modulus ( $E_1$ ), i. e., the MOE value below the PL (36, 51) can be obtained experimentally without causing damage to the lumber. However, to obtain MOR the lumber has to be broken. In the past, experimental-statistical studies were conducted to express MOR in terms of  $E_1$  (14, 29, 46). Both moduli were obtained experimentally and regression equations were developed. The correlation coefficients for these equations varied widely. Johnson (29), in his study on Douglas-fir Select Structural, Construction, and Utility grades, obtained a correlation of 0.87. Schroeder and Atherton (46) found a correlation of 0.68 for Utility grade redwood studs. Polensek and Atherton (40) obtained correlations of 0.74 and 0.71 for Utility grade Engelmann spruce and Douglas-fir studs, respectively. Fernandez (14) investigated Douglas-fir studs of Stud grade for which a correlation of 0.66 was obtained. The results of these studies indicate that  $E_1$  does not accurately predict the MOR. Even with  $E_1$  and MOR known the total deflection-load curve is not defined. Either the deflection at the MOR or the nonlinear part of the curve is necessary to estimate the deflection-load curve.

The deflection-load curve can be more precisely defined in

terms of the PL and MOR. Recent studies (14, 46) have shown that the stress at proportional limit (SPL) is a better predictor of MOR, as indicated by a correlation of 0.90. However, the SPL can only be determined by loading the lumber beyond the PL, which probably causes some damage to the wood fibers. There currently is no satisfactorily accurate procedure for obtaining MOR without damaging the lumber.

#### 1.2.4. Finite Element Method

With the advent of high-speed computers, the finite element method (8, 11, 62) was developed. The finite element method has been described as a physical idealization of a material continuum into an assemblage of a finite number of elements which interconnect at certain points called nodal points. A piece of lumber can be represented as an assembly of a discrete number of elements. Next, a stiffness matrix and force vector are generated for each element. The element stiffness matrix and force vector represent the element elastic properties, and loads, respectively. The element matrices and force vectors are combined into an overall stiffness matrix and force vector, respectively, representing the continuum. The element stresses and nodal deflection are obtained by operating on the overall matrices and vectors, using mathematical operations, derived from equilibrium and compatibility conditions. Finite element idealization

permits accounting for changes in elastic properties within the piece and nonelastic changes at loads above the PL.

As an alternative to actual testing, a finite element model can be developed for the stud. The nonlinear behavior may be included in the model. Imposing test loads on this model and analyzing it should result in a complete deflection-load trace. Then studs representing a certain grade and species can be simulated and analyzed by the finite element method. Such a simulation requires the establishment of a mathematical-logical model of a system and the experimental manipulation of it on a digital computer (41). A simulator is an artificial laboratory or testing machine. Once a system is modeled and programmed, experiments can be performed using the model.

The finite element method has been used successfully in the analyses of wood-joist floors (39), wood-stud walls (37), plates and shells (17, 20, 33, 57), and compression tests on nonlinear materials (18). Its application to deflection-load curves of lumber is expected to yield accurate results.

### 1.3. Future Outlook

Analysis procedures for improved design of wood-stud walls are available. To apply these procedures, accurate information on the elasticity properties of wall components such as studs is necessary. Better methods of analysis (37, 38) and improved information

on the properties of wall components should result in less conservative designs of wood-stud walls than those produced by the present method.

Wood-stud walls can be made more economical by using lumber of lower grades like Utility grade, by reducing the stud cross-section, and by increasing the stud spacings. Cross-sections such as 1- by 6-inch may allow more insulation. The conventional 16-inch stud spacing in walls could be increased. The Uniform Building Code (26) presently allows 24 in. stud spacing for single-story dwellings and top stories of multi-story dwellings. The above improvements may be extended to other constructions if an improved design method demonstrates that the safety of the structure is not jeopardized.

The development of the finite element method that would simulate stud testings could lead to a new method of determining allowable design properties for studs of any grade and species. Stud probability distribution of a certain grade can be simulated from probability distributions for clear MOE and for grade defects which are already available to most wood species and grades.

#### 1.4. Justification and Objectives

The development of an improved design method for wood-stud walls requires an accurate information on the properties of studs, the principal structural component of the wall. Traditionally, such

an information has been obtained only by testing, which is expensive and time-consuming. An efficient and more economical alternative calls for developing a theoretical procedure to determine the strength and stiffness of studs. Once the theoretical model and computer program are developed and verified, studs of the commonly-used grades and species can be simulated, modeled, and then theoretically tested to determine the probability distributions for their strengths and stiffnesses. Such a procedure should make not only wall design more economical, but also could be applied to other lumber such as floor joists and components for roof trusses. The development of such a procedure is the main objective of this investigation. The specific objectives are:

1. To develop a theoretical procedure and computer program for determination of elasticity properties of studs.
2. To verify the method and computer program by physical testing.
3. To develop a simulation procedure for generation of probability distribution of elasticity properties for studs.
4. To investigate how the parameters such as grain and ring angles, MOE and MOR for clear wood, modulus of rigidity and Poisson's ratio affect the stud stiffness and strength.

## II. METHOD OF ANALYSIS

The finite element method was used to evaluate the strength and stiffness of the studs. The method is ideal for systems with complex boundary conditions and material properties.

The specific task was the development of a model and method that would simulate a stud testing procedure according to Standard D 198 (3) of the American Society for Testing and Materials (ASTM). The ASTM test requires the symmetrical loading of the stud at points one-third of the span (Figure 3.2). The load is increased continuously until the stud fails. A deflection-load curve, such as that of Figure 1.1, is obtained by plotting the load against the midspan deflection.

The chosen stud model will simulate the ASTM test. The load  $Q$ , will be increased by small increments until the stud fails. The stresses and deflections at certain points in the stud will be calculated after each increment. A computer program will be prepared for this model and test procedure.

### 2.1. Finite Element Method

The finite element method represents a study by an assembly of small stud sections, that is, subdivisions called finite elements. These elements are connected at joints which are called nodes or nodal points. The chosen displacement functions will secure the

compatibility of deflections along the boundary lines of adjacent elements. Loads simulating the test conditions are applied at the nodal points at 1/3 and 2/3 of the span. The final solution yields the displacements at the nodes including the node at L/2. The applied forces and nodal displacements are related by the overall stud stiffness matrix which is defined by the local elasticity properties and internal material geometry of the stud. The overall stiffness matrix is formed by combining the individual stiffness matrices of all the elements of the stud. The overall stiffness matrix accounts for the boundary conditions, that is, for zero displacements at point A and the vertical displacements at point B (Figure 3.2).

The nodal displacements may be obtained by (8, 11, 62)

$$\{D\} = [K]^{-1} \{Q\} \quad (2.1)$$

where

$\{D\}$  = nodal displacement vector

$[K]$  = stud stiffness matrix

$\{Q\}$  = defined external loads acting on stud

The element stresses and strains are determined by (8, 11, 62)

$$\{\epsilon_e\} = \begin{Bmatrix} \epsilon_x \\ \epsilon_y \\ \gamma_{xy} \end{Bmatrix} = [A] \{d\} \quad (2.2)$$

and

$$\{\sigma_e\} = \begin{Bmatrix} \sigma_x \\ \sigma_y \\ \tau_{xy} \end{Bmatrix} = [S] [A] \{d\} = [B] \{d\} \quad (2.3)$$

where

$\{\varepsilon_e\}$  - element strain vector

[A] - element strain displacement matrix

$\varepsilon_x, \varepsilon_y$  - normal strains

$\gamma_{xy}$  - shear strain

{d} - element nodal displacement vector

x, y - local coordinates denoting the direction of strains

and stresses

$\sigma_e$  - element stress vector

$\sigma_x, \sigma_y$  - normal stresses

$\tau_{xy}$  - shear stress

[B] - element stress displacement matrix and

[S] - stress strain matrix

The element strain vector ( $\varepsilon_e$ ) represents the displacements in the element. It is a function of the element geometry, displacement functions and nodal deflections.

The element stress vector ( $\sigma_e$ ) represents the stresses acting within the element. It is a function of the element elastic properties and geometry, displacement functions, and nodal deflections. For chosen displacement functions, the stresses are constant throughout the element. The stress at the node can be obtained by taking the average of the stresses of the elements surrounding the node.

## 2. 2. Assumptions

The finite element method is based on general assumptions such as:

1. Structural compatibility exists along the total boundary among the adjacent elements. A proper selection of displacement functions usually prevents the violation of this assumption. When the stud starts to develop cracks, the assumption is violated, but the finite element model may still represent the actual conditions on the stud.
2. Stresses exist only in two perpendicular directions, that is, the problem is reduced to a plane stress problem. This assumption may not be entirely true because of Poisson's effects in the direction of thickness. However, the stresses because of Poisson's effects are small compared to those of the other two directions.
3. The material properties are constant in the direction of the element thickness. Therefore, there is no change of stresses within the thickness. Some violation of this assumption is expected because of the material variability of wood properties in the thickness direction.

The specific assumptions pertaining to the stud analysis are:

1. The elasticity and strength properties, and the grain and ring angles are constant within the element. Some violation of this

assumption is expected because of local variations in material properties. The errors due to this violation may be reduced by a very fine finite element mesh.

2. Knots have no resistance to tension, and have the same elastic and strength properties as the tangential direction of the wood in compression. No information is available on the strength and elastic properties of knots. A casual observation of knots suggests that the knot may resist some small tension forces.
3. The elasticity properties of the elements are linear within one load increment. This assumption is true before the PL is reached. After the PL, some violation occurs, but it may be minimized by choosing small load increments.
4. When the stress in the element reaches failure stresses, the whole element is considered broken. This assumption is violated if only a part of the element fails and the adjacent parts keep on resisting forces. The errors due to this assumption may be reduced by refining the mesh.

### 2.3. The Finite Elements and their Stiffness Matrices

Two types of plane stress elements were used to model the stud. One type was a rectangular element and the other type was a triangular element.

### 2.3.1. Rectangular Elements

The main element is Cook's modified assumed stress hybrid rectangular element (9). This element has been used successfully by White (58) in his study on the analysis of end fixity in stud wall panels. Under pure bending, this element yields exact displacements and exact stresses. Stresses within the element are given by an assumed field which satisfies the differential equations of equilibrium. Figure 2.1 shows the element with its local coordinate system and differential element. The nodal points i, j, k and l are oriented counter-clockwise. The size and location of the element are defined in terms of the global Cartesian coordinates  $x$  and  $y$ . The components of the nodal displacements are  $u$  and  $v$ .

The element stiffness matrix is defined by (9)

$$[K_e] = [T]^T [H]^{-1} [T] \quad (2.4)$$

The size of  $[T]$  is five by eight, and its 24 nonzero elements are obtained from (10):

$$\left. \begin{aligned} T_{1,2g-1} &= T_{5,2g} = (y_h - y_f)/2 \\ T_{5,2g-1} &= T_{3,2g} = (x_f - x_h)/2 \\ T_{2,2g-1} &= [y_h(y_h + y_g) - y_f(y_f + y_g)]/6 \\ T_{4,2g} &= [x_f(x_f + x_g) - x_n(x_n + x_g)]/6 \end{aligned} \right\} \quad (2.5)$$

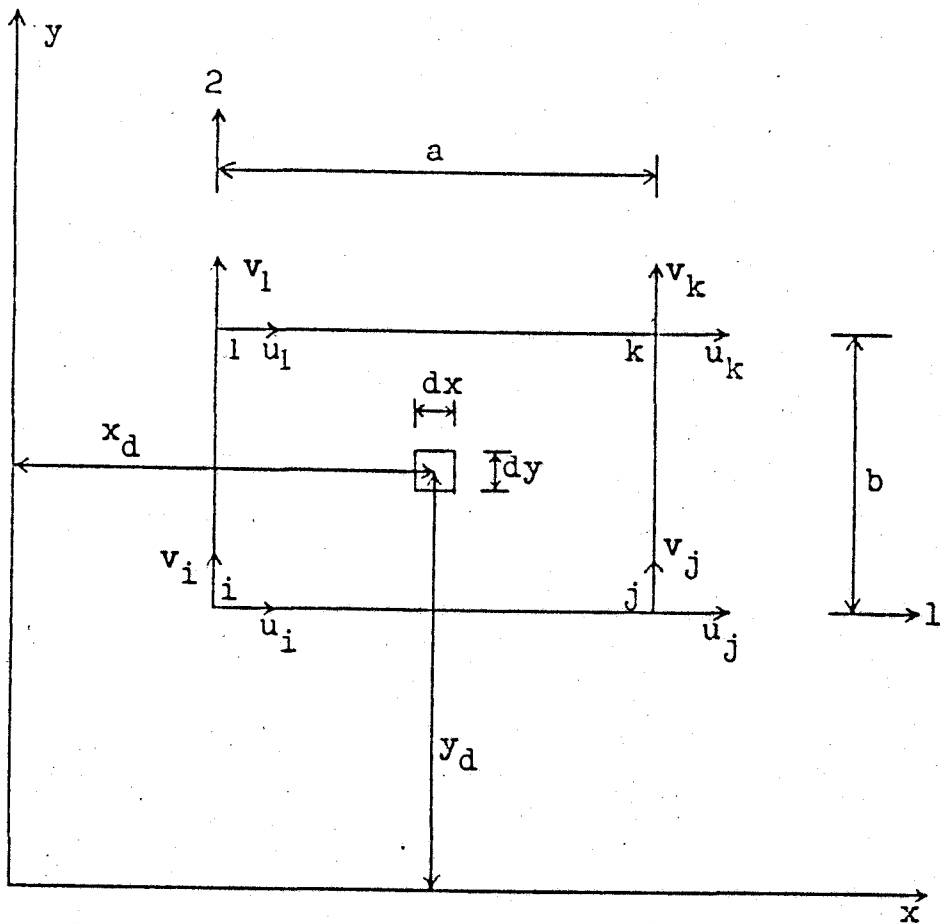


Figure 2.1. Rectangular plane stress element.

in which  $g = 1, 2, 3, 4$  and  $f, g, h$  are cyclically permuted from one to four with  $f = g-1$ , and  $h = g+1$ . For example,  $T_{11} = (y_2 - y_4)/2$ ,  $T_{12} = 0$ ,  $T_{13} = (y_3 - y_1)/2$ . The subscripts 1, 2, 3 and 4 correspond to the nodes  $i, j, k$  and 1, respectively. Using equation (2.5), the non-zero elements of matrix  $[T]$ , expressed in terms of the nodal coordinates, are (58):

$$T_{11} = T_{52} = -T_{15} = -T_{56} = (y_j - y_1)/2 \quad (2.6)$$

$$T_{13} = T_{54} = -T_{17} = -T_{58} = (y_k - y_i)/2 \quad (2.7)$$

$$T_{34} = T_{53} = -T_{38} = -T_{57} = (x_i - x_k)/2 \quad (2.8)$$

$$T_{36} = T_{55} = -T_{32} = -T_{51} = (x_j - x_1)/2 \quad (2.9)$$

$$T_{21} = [y_j(y_j + y_i) - y_1(y_1 + y_i)]/6 \quad (2.10)$$

$$T_{23} = [y_k(y_k + y_j) - y_i(y_i + y_j)]/6 \quad (2.11)$$

$$T_{25} = [y_1(y_1 + y_k) - y_j(y_j + y_k)]/6 \quad (2.12)$$

$$T_{27} = [y_i(y_i + y_1) - y_1(y_1 + y_k)]/6 \quad (2.13)$$

$$T_{42} = [x_1(x_1 + x_i) - x_j(x_j + x_i)]/6 \quad (2.14)$$

$$T_{44} = [x_i(x_i + x_j) - x_k(x_k + x_j)]/6 \quad (2.15)$$

$$T_{46} = [x_j(x_j + x_k) - x_1(x_1 + x_k)]/6 \quad (2.16)$$

and

$$T_{48} = [x_k(x_k + x_1) - x_i(x_i + x_1)]/6 \quad (2.17)$$

The five by five matrix  $[H]$  of equation (2.4) equals (9)

$$[H] = \iint_t \frac{1}{t} [P]^T [C] [P] dx dy \quad (2.18)$$

in which integration is performed over the entire element area.

The symbols in equation (2.18) are defined as follows (9):

$t$  = element thickness

$$[P] = \begin{bmatrix} 1 & y_d & 0 & 0 & 0 \\ 0 & 0 & 1 & x_d & 0 \\ 0 & 0 & 0 & 0 & 1 \end{bmatrix} \quad (2.19)$$

and

$$[C] = \begin{bmatrix} \frac{1}{E_x} - \frac{\nu_{xy}}{E_x} & 0 \\ \frac{-\nu_{yx}}{E_y} \frac{1}{E_y} & 0 \\ 0 & \frac{1}{G_{xy}} \end{bmatrix} \quad (2.20)$$

where

$E_x, E_y$  - modulus of elasticity in direction indicated by subscript

$\nu_{xy}, \nu_{yx}$  - Poisson's ratio, i. e., the ratio of the strain in the direction of the second subscript to the strain in the direction of the first subscript with the stress applied in the direction of the first subscript.

$G_{xy}$  - shear modulus in the x-y plane.

Equations (2.4) through (2.19) are valid for any quadrilateral element. White (58) first modified  $[H]$  for rectangles and then inverted it to obtain matrix  $[F]$  which was valid only for rectangles. Further simplification was made by applying

$$E_x \nu_{yx} = E_y \nu_{xy} \quad (2.21)$$

The non-zero elements of matrix [F] are (58)

$$F_{11} = \frac{4E_x^2 E_y - 3E_x(E_y^\nu xy)^2}{[E_x E_y - (E_y^\nu xy)^2]abt} \quad (2.22)$$

$$F_{21} = F_{12} = \frac{-6E_x}{ab^2 t} \quad (2.23)$$

$$F_{22} = \frac{12E_x}{ab^3 t} \quad (2.24)$$

$$F_{31} = F_{13} = \frac{E_x E_y (E_y^\nu xy)}{[E_x E_y - (E_y^\nu xy)^2]abt} \quad (2.25)$$

$$F_{33} = \frac{4E_x^2 E_y^2 - 3E_y(E_y^\nu xy)^2}{[E_x E_y - (E_y^\nu xy)^2]abt} \quad (2.26)$$

$$F_{34} = F_{43} = \frac{-6E_y}{a^2 bt} \quad (2.27)$$

$$F_{44} = \frac{12E_y}{a^3 bt} \quad (2.28)$$

and

$$F_{55} = \frac{G_{xy}}{abt} \quad (2.29)$$

The stresses of the differential element are calculated by equation (2.3) with

$$[B] = \frac{1}{t} [P][F][T] \quad (2.30)$$

The stress variation within the element in one direction is linear with respect to the perpendicular direction.

### 2.3.2. Triangular Elements

The triangular element was used for locations on the stud where the rectangular element could not easily be applied such as around knots and transition locations between two different sizes of elements. The displacements within the triangular elements are linear and have a polynomial form. It is expressed in terms of generalized coordinates and hence referred to as generalized coordinate displacement model. The element, shown in Figure 2.2, has its nodal points, i, j, and k oriented counterclockwise. The displacement functions of this element are linear and equal to (11, 62)

$$\left. \begin{aligned} u &= \alpha_1 + \alpha_2 X + \alpha_3 Y \\ v &= \alpha_4 + \alpha_5 X + \alpha_6 Y \end{aligned} \right\} \quad (2.31)$$

where

$u, v$  - displacements in the  $x$  and  $y$  directions, respectively,

of a certain point within the element

$\alpha_1, \alpha_2, \alpha_3, \alpha_4, \alpha_5, \alpha_6$  - generalized coordinates

$x, y$  - Cartesian coordinates of certain points within the element.

The triangular element stiffness matrix is defined by

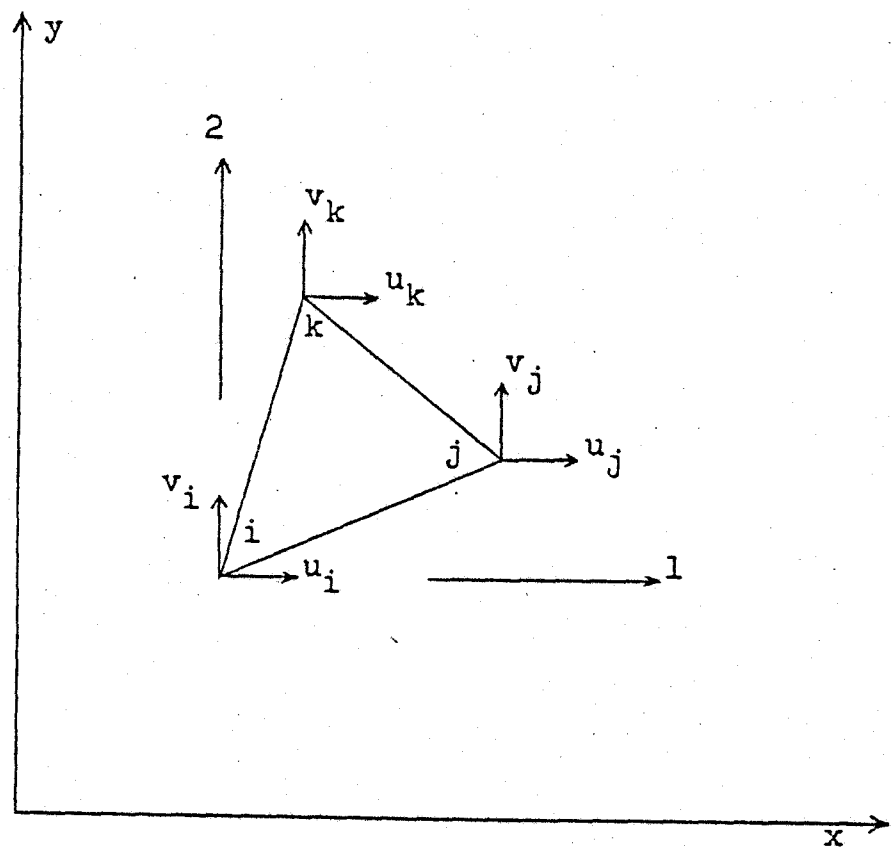


Figure 2.2. Triangular plane stress element.

$$[K_e] = \int_A [A]^T [S] [A] t dA \quad (2.32)$$

where

$A$  - area of triangle

$[A]$ ,  $[S]$  - defined in equation (2.3)

The strain-displacement matrix, defined in terms of the nodal coordinates  $x$  and  $y$ , equals (62)

$$[A] = \frac{1}{2A} \begin{bmatrix} -y_{kj} & 0 & y_{ki} & 0 & -y_{ji} & 0 \\ 0 & x_{kj} & 0 & -x_{ki} & 0 & x_{ji} \\ x_{kj} & -y_{kj} & -x_{ki} & y_{ki} & x_{ji} & -y_{ji} \end{bmatrix} \quad (2.33)$$

where

$$y_{ij} = y_i - y_j \quad (2.34)$$

$$x_{ij} = x_i - x_j \quad (2.35)$$

The stress-strain matrix is (11, 62)

$$[S] = \frac{1}{(1-\nu)xy} \begin{bmatrix} E_x & E_y \nu xy & 0 \\ E_x \nu yz & E_y & 0 \\ 0 & 0 & (1-\nu) \frac{\nu}{xy} G_{xy} \end{bmatrix} \quad (2.36)$$

The area of the triangular element is given by

$$A = (x_{ji}y_{ki} - x_{ki}y_{ji})/2 \quad (2.37)$$

Because of the linear displacement functions the stresses are constant throughout the element.

## 2.4. Elasticity Parameters

The parameters used to define the stud elasticity are:

1. Three moduli of elasticity denoted by  $E_L$ ,  $E_T$  and  $E_R$ . The subscripts L, T and R denote the longitudinal, tangential and radial directions in the wood, respectively.
  2. Three moduli of rigidity denoted by  $G_{LT}$ ,  $G_{LR}$  and  $G_{TR}$ . The subscripts LT, LR and TR are the three planes of elastic symmetry. For example,  $G_{LT}$  is the modulus of rigidity based on the shear strain in the LT (longitudinal-tangential) plane and shear stresses in the LR (longitudinal-radial) and TR (tangential-radial) planes.
  3. Six Poisson's ratios denoted by  $\nu_{LR}$ ,  $\nu_{RL}$ ,  $\nu_{LT}$ ,  $\nu_{TL}$ ,  $\nu_{RT}$  and  $\nu_{TR}$ . The first symbol of the subscript refers to the direction of applied stress and the second symbol refers to the direction of lateral deformation.
- The  $E_L$  for each of the studs may be obtained experimentally by tension and compression tests of small, clear specimens according to ASTM Standard D 143-52 (3). The approximate values for Poisson's ratios are available in the Wood Handbook (54). Estimates of the remaining moduli may be calculated from the Wood Handbook regression relations (54) as follows

$$E_T = 0.050 E_L \quad (2.38)$$

$$E_R = 0.068 E_L \quad (2.39)$$

$$G_{LT} = 0.078 E_L \quad (2.40)$$

$$G_{LR} = 0.064 E_L \quad (2.41)$$

$$G_{TR} = 0.007 E_L \quad (2.42)$$

The Wood Handbook elasticity values and equations were determined from test results accumulated over the years (54). They have their own inherent variability and are affected by specific gravity, moisture content, temperature, and strain rate (4, 6, 30, 31, 32, 35, 48, 49, 52, 54, 61).

Elasticity values are also available from other sources such as the studies conducted by Hearmon (21), and Bodig and Goodman (4).

The finite element model uses the elastic properties in the direction of the geometric stud axes x, y, and z as shown in Figure 2.3. If the axis of elastic symmetry does not coincide with the geometric axis, the affected property should be modified.

#### 2.4.1. Modification of Elastic Properties by Axial Transformation

Wood is often quoted as a typical example of an orthotropically elastic material (12, 21, 22, 27, 42, 44, 45, 55), i.e., it is elastically symmetric about three mutually perpendicular planes. It has nine independent compliance parameters expressed by the

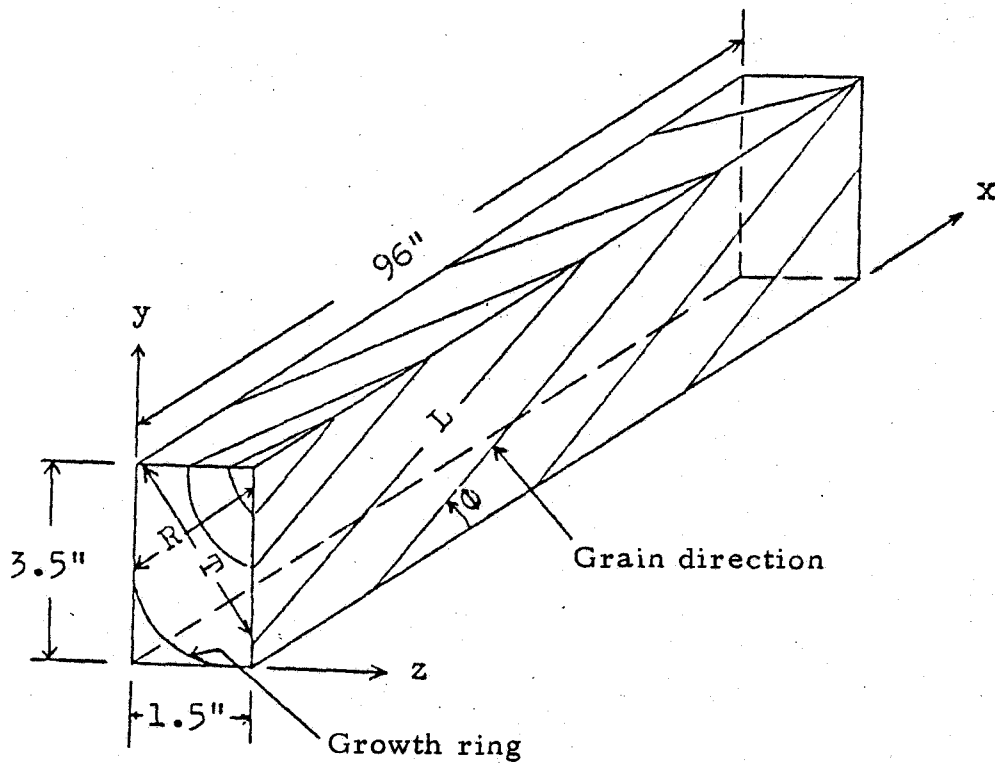


Figure 2.3. Geometry and elasticity of studs: the geometric axes  $x$ ,  $y$  and  $z$ , and the elastic axes  $L$ ,  $T$  and  $R$  do not coincide.  $\phi$  is the grain angle.

corresponding elastic parameters:  $E_L$ ,  $E_R$ ,  $E_T$ ,  $G_{LR}$ ,  $G_{LT}$ ,  $G_{TR}$ ,  $\nu_{RL}$ ,  $\nu_{LT}$  and  $\nu_{TR}$ . Its strain-stress relationship can be expressed in matrix form as (19, 23)

$$\{\varepsilon\} = [s] \{\sigma\} \quad (2.43)$$

or

$$\left\{ \begin{array}{l} \varepsilon_L \\ \varepsilon_T \\ \varepsilon_R \\ 2\varepsilon_{TR} \\ 2\varepsilon_{LR} \\ 2\varepsilon_{LT} \end{array} \right\} = \left[ \begin{array}{cccccc} \frac{1}{E_L} & -\frac{\nu_{LT}}{E_L} & -\frac{\nu_{LR}}{E_L} & 0 & 0 & 0 \\ -\frac{\nu_{TL}}{E_T} & \frac{1}{E_T} & -\frac{\nu_{TR}}{E_T} & 0 & 0 & 0 \\ -\frac{\nu_{RL}}{E_R} & -\frac{\nu_{RT}}{E_R} & \frac{1}{E_R} & 0 & 0 & 0 \\ 0 & 0 & 0 & \frac{1}{G_{TR}} & 0 & 0 \\ 0 & 0 & 0 & 0 & \frac{1}{G_{LR}} & 0 \\ 0 & 0 & 0 & 0 & 0 & \frac{1}{G_{LT}} \end{array} \right] \left\{ \begin{array}{l} \sigma_L \\ \sigma_T \\ \sigma_R \\ \sigma_{TR} \\ \sigma_{LR} \\ \sigma_{LT} \end{array} \right\} \quad (2.44)$$

in which  $\{\varepsilon\}$  = strain vector

$[s]$  = flexibility matrix

$\{\sigma\}$  = stress vector

and other symbols have been defined earlier in the text.

The strain-stress relation in wood can also be expressed in tensor form as (19, 23)

$$\epsilon_{ij} = s_{ijkl} T_{kl} \quad (2.45)$$

in which

$\epsilon_{ij}$  = strain tensor

$s_{ijkl}$  = elastic compliance tensor and

$T_{kl}$  = stress tensor

Axial transformation of the elasticity parameters was accomplished by the tensor transformation law (19):

$$s'_{ijkl} = a_{im} a_{jn} a_{ko} a_{lp} s_{mnop} \quad (2.46)$$

in which  $s'_{ijkl}$  = transformed  $s_{ijkl}$ ;  $a_{im}$ ,  $a_{jn}$ ,  $a_{ko}$ , and  $a_{lp}$  are the direction cosines of the angles of rotation of the x-, y- and z-system to L-, T- and R-system. The subscripts i, j, k, l, m, n, o, and p are equal to 1, 2, or 3. Figure 2.4 defines the rotation of the coordinate axes and Table 2.1 identifies the direction cosines.

Table 2.1. Direction cosines of the angles of rotation.

	x(L)	z(T)	y(R)
x'	$a_{11} = \cos\phi$	$a_{12} = 0$	$a_{13} = \sin\phi$
z'	$a_{21} = \sin\phi\sin\theta$	$a_{22} = \cos\theta$	$a_{23} = -\cos\phi\sin\theta$
y'	$a_{31} = -\sin\phi\cos\theta$	$a_{32} = \sin\theta$	$a_{33} = \cos\theta\cos\phi$

Equation 2.46 was used to obtain the effective values of the

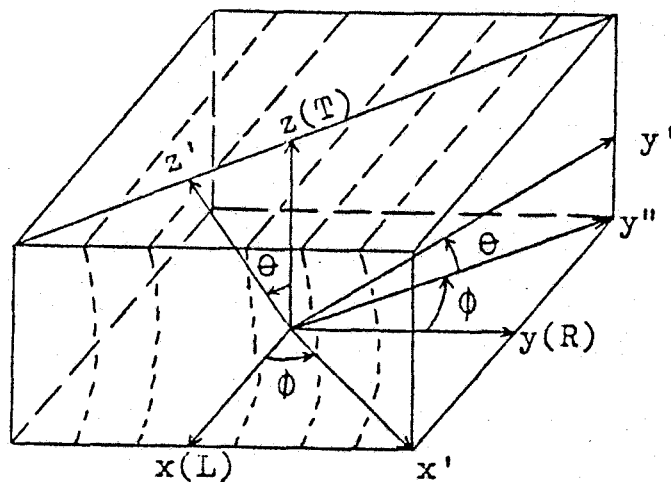


Figure 2.4. Rotation of axes. The rotation was first done along axis  $z$  at a grain angle  $\phi$  to positions  $x'$  and  $y''$ . The second rotation was along  $x'$  axis at a ring angle  $\theta$  to positions  $x''$  and  $y'''$ .

elasticity parameters for various grain angles,  $\phi$ . The following transformation equations were obtained:

$$s'_{11} = \frac{\cos^4 \phi}{E_L} + \frac{\sin^4 \phi}{E_R} + \cos^2 \phi \sin^2 \phi \left[ \frac{1}{G_{RL}} - \frac{2\nu_{LR}}{E_L} \right] \quad (2.47)$$

$$\begin{aligned} s'_{13} = & \sin^2 \phi \cos^2 \theta \left[ \frac{\cos^2 \phi}{E_L} - \frac{\nu_{RL} \sin^2 \phi - \cos^2 \phi}{E_R} - \frac{\cos^2 \phi}{G_{RL}} \right] \\ & - \frac{\cos^2 \phi}{E_L} \left[ \nu_{LT} \sin^2 \theta + \nu_{LR} \cos^2 \phi \cos^2 \theta \right] \\ & - \frac{\nu_{RT} \sin^2 \phi \sin^2 \theta}{E_R} \end{aligned} \quad (2.48)$$

$$\begin{aligned} s'_{33} = & \frac{\sin^4 \phi \cos^4 \theta}{E_L} + \frac{\sin^4 \theta}{E_T} + \sin^2 \theta \sin^2 \phi \cos^2 \theta \\ & \left[ \frac{1}{G_{LT}} - \frac{2\nu_{LT}}{E_L} \right] + \cos^2 \theta \cos^2 \phi \left[ \frac{\cos^2 \theta \cos^2 \phi}{E_R} \right. \\ & \left. - \frac{2\nu_{LR} \cos^2 \theta \sin^2 \phi}{E_L} - \frac{2\nu_{TR} \sin^2 \theta}{E_T} + \frac{\sin^2 \theta}{G_{TR}} \right. \\ & \left. + \frac{\sin^2 \phi}{G_{RL}} \right] \end{aligned} \quad (2.49)$$

$$\begin{aligned} s'_{55} = & 4 \cos^2 \phi \cos^2 \theta \sin^2 \phi \left[ \frac{1 + 2\nu_{LR}}{E_L} + \frac{1}{E_R} \right] \\ & + \sin^2 \theta \left[ \frac{\sin^2 \phi}{G_{TR}} + \frac{\cos^2 \phi}{G_{LT}} \right] + \frac{\cos^2 \theta}{G_{RL}} \\ & \left[ \cos^2 \phi - \sin^2 \phi \right]^2 \end{aligned} \quad (2.50)$$

in which  $\phi$  and  $\theta$  are defined in Figure 2.3 and the other symbols

have been defined earlier in the text. The transformed strain-stress relation can now be written as

$$\{\varepsilon'\} = [s'] \{\sigma'\} \quad (2.51)$$

in which  $\{\varepsilon'\}$  and  $\{\sigma'\}$  are the strains and stresses, respectively, along the stud geometric axes; and  $[s']$  is defined earlier in the text.

## 2.5. Nonlinear Analysis

Three main techniques are available for the solution of nonlinear problems by the finite element method (11): incremental or stepwise procedure (linear step-by-step analysis), iterative or Newton method, and step-iterative or mixed procedure.

The incremental procedure was used in this study because of the following reasons:

- a. it is relatively simple and applicable to nearly all types of nonlinear behavior,
- b. it provides a relatively completely description of the deformation-load behavior, and
- c. it provides the results at intermediate stages of the analysis.

It consumes, however, more computer time than the iterative technique.

The iterative method is faster and easier to use than the incremental method. It is useful in the case in which the materials have

different elastic properties in tension and compression (59). Its principal disadvantage is that there is no assurance that it will converge to the exact solution (13). Furthermore, the displacements, stresses, and strains are determined for only the total load; hence, no information concerning the behavior at intermediate loads is obtained.

The mixed method combines the incremental and iterative procedures. It was not used in this study because there is no assurance that it will converge to the exact solution.

#### 2.5.1. Linear Step-by-step Analysis

As previously mentioned, the theoretical model and procedure simulate the ASTM (3) flexure test depicted in Figure 3.2. The stud was modeled by rectangular and triangular elements described in Sections 2.3.1 and 2.3.2. The flow diagram in Figure 2.5 shows the most important steps in the linear step-by-step analysis. The corresponding computer program is listed in Appendix A.

Load  $Q$  was applied gradually at increments of  $\Delta Q$  and represented by  $\{\Delta Q\}$ . The incremental displacements and stresses were calculated by

$$\{\Delta D\} = [K_i]^{-1} \{\Delta Q\} \quad (2.52)$$

$$\{\Delta \sigma_e\} = [B] \{\Delta d\} \quad (2.53)$$

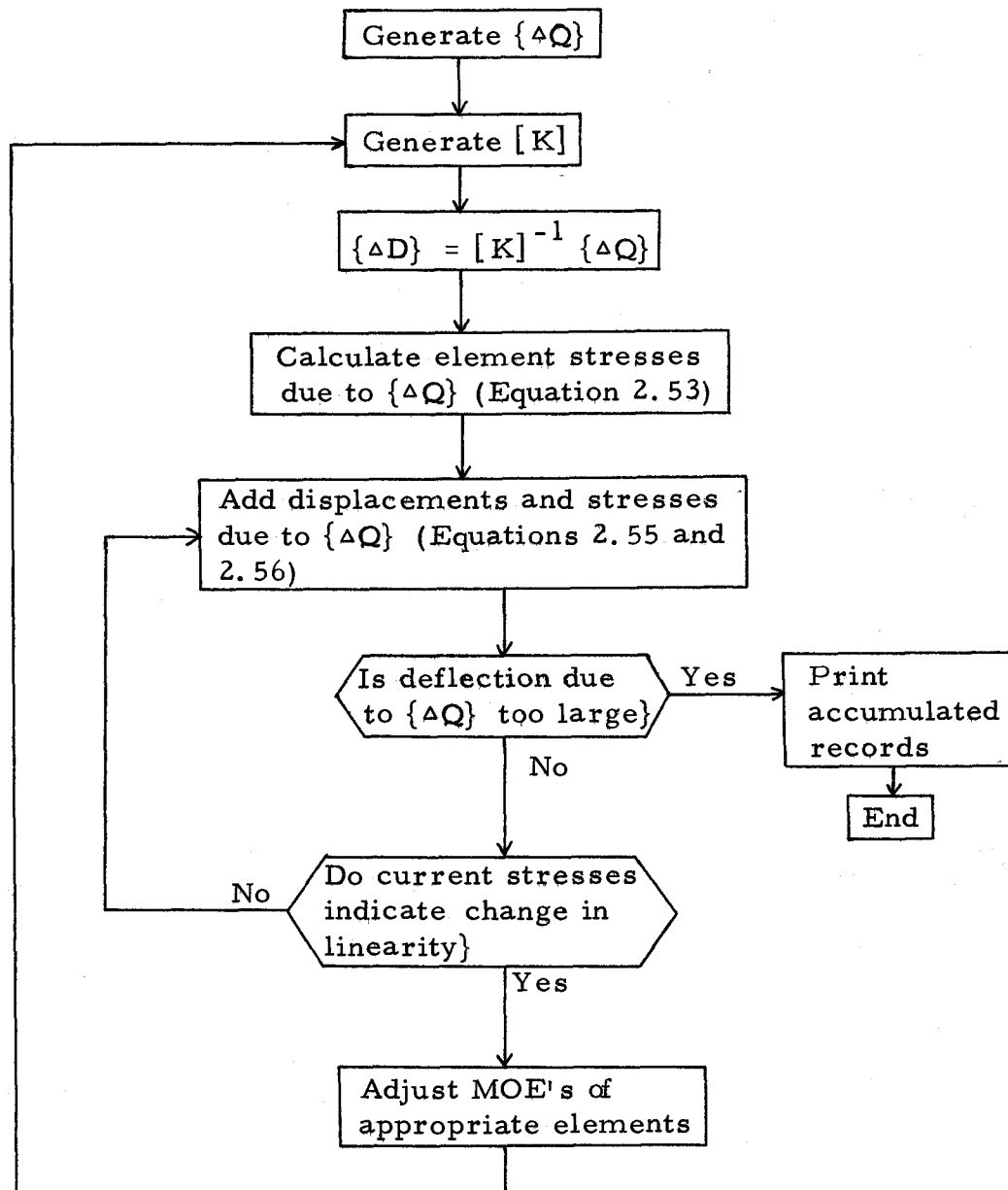


Figure 2.5. Flow diagram for linear step-by-step analysis.

in which

$\{\Delta D\}$  = displacements due to  $\{\Delta Q\}$

$[K_i]$  = stud stiffness matrix. The subscript  $i$  is associated with changes in linearity at any point in the stud.

$\{\Delta \sigma_e\}$  = element stresses due to  $\{\Delta Q\}$

$\{\Delta d\}$  = element nodal displacements due to  $\{\Delta Q\}$

$\{\Delta Q\}$  and  $[B]$  are defined earlier in the text. After the  $n$ th increment, the accumulated loads, displacements, and stresses are the sum of the corresponding incremental values:

$$\{Q_n\} = \sum_{j=1}^n \{\Delta Q_j\} \quad (2.54)$$

$$\{D_n\} = \sum_{j=1}^n \{\Delta D_j\} \quad (2.55)$$

$$\{\sigma_{e(n)}\} = \sum_{j=1}^n \{\Delta \sigma_{e(j)}\} \quad (2.56)$$

in which  $\{Q_n\}$ ,  $\{D_n\}$  and  $\{\sigma_{e(n)}\}$  are the accumulated load, displacement, and stress vector, respectively, and  $j$  is a dummy index of summation.

The accumulated stresses along the grain,  $\bar{\sigma}_L$ , were compared with clear wood stresses  $\sigma_L$ , associated with the actual elasticity properties of each finite element. A typical example of the  $\sigma_L$  to  $\epsilon_L$  diagram is shown in Figure 2.6. For example, the MOE of an element changes from  $E_1$  to  $E_2$  after the element stress  $\sigma_L$  reaches its actual PL-value. When  $\sigma_L$  reaches the clear-wood failure stress,

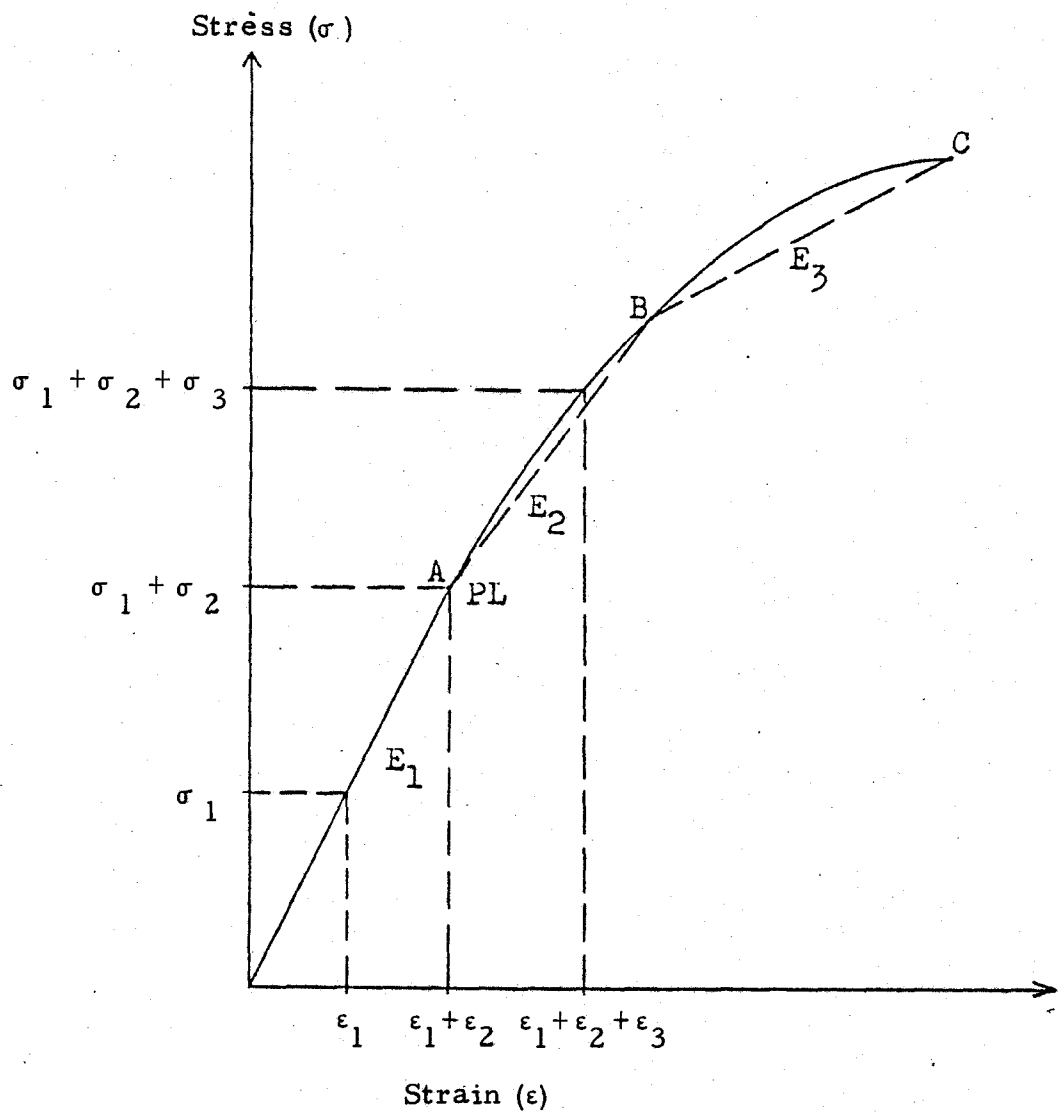


Figure 2.6. A strain-stress curve of an element. Such relations should be obtained experimentally for each representative location of the stud.

the element is considered broken and its elastic properties were reduced close to zero.

When the MOE of one or more of the elements changed, a new stud stiffness matrix is generated to account for such changes. The analysis procedure continues as shown in the flow diagram in Figure 2.5.

The analysis is terminated when the change in midspan deflection due to  $\Delta Q$  is greater than four times the corresponding deflection during the initial load increment. This criterion was selected after comparing the deflection-load curves of the experimental beams with their corresponding theoretical solutions.

In cases where the geometric longitudinal axis of the stud does not coincide with the grain direction,  $\sigma_L$  was evaluated by the Mohr's circle (7, 43, 47, 53) according to

$$\sigma_\phi = \frac{\sigma_x - \sigma_y}{2} \cos 2\phi - \tau_{xy} \sin 2\phi + \frac{\sigma_x + \sigma_y}{2} \quad (2.57)$$

in which the subscripts x, y and  $\phi$  are defined in Figure 2.3 and  $\tau_{xy}$  is the shear stress in the x-y plane.

The midspan deflection,  $y_n$  was obtained after each increment from the accumulated vertical displacement of an element node at midspan (equation 2.55). The corresponding load equals to  $Q_n = n \Delta Q_j$ . The relation of  $y_n$  to  $Q_n$  is the desired deflection-load curve of the stud.

### III. VERIFICATION

The verification of the procedure and computer program was accomplished by comparing the experimental results with the corresponding theoretical results.

The experimental results were obtained by testing in flexure five 96 inches long Douglas-fir studs of nominal size 2- by 4-inches in accordance with the ASTM Standard D198 (3). The studs were then theoretically analyzed by the developed finite element procedure using the experimentally obtained elasticity properties for the representative locations on each stud.

#### 3.1. Selection, Preparation and Characterization of Specimens

Douglas-fir studs were chosen regardless of grade with the prime consideration that they can be easily characterized. Studs with clustered knots, warps and splits were avoided. Those with smaller grain angles were preferred.

The specimens were obtained from the sawmill unseasoned. They were dried and equalized to about 8% moisture content in the dry kiln of the Forest Research Laboratory, Oregon State University. Five specimens, three of which were clear of knots, were chosen out of about 150 studs selected at the mill.

Each of the five chosen specimens was carefully inspected and

mapped for strength-reducing characteristics. The diameter and location of knots were recorded. The grain angles were measured every 12 inches or less depending on whether there were local grain disturbances between the 12-inch intervals. The ring angles were measured, after the test, every 18 inches. Figure 3.1 shows the characteristics of specimen number 5. The moisture content and specific gravity were also determined and are shown in Appendix I.

### 3.2. Flexure Test

The specimens were tested in flexure to failure in accordance with ASTM Standard D198 (3) on a Tinius Olsen testing machine with a maximum load capacity of 60,000 pounds. The undamaged parts of broken studs were saved for elasticity evaluation. The beam span was 90 inches. Strains were measured by Linear Variable Differential Transformers (LVDT) at the tension and compression sides of the specimen as shown in Figure 3.2. Figure 3.3 shows a direct-current LVDT used in this study.

Generally the LVDTs measured elongations or contractions at certain spans. They produce electrical outputs proportional to the displacements of a separate movable core (24). In this investigation the electrical signals were sent to a data acquisition system where they were converted into linear displacements in inches and plotted by an X-Y recorder.

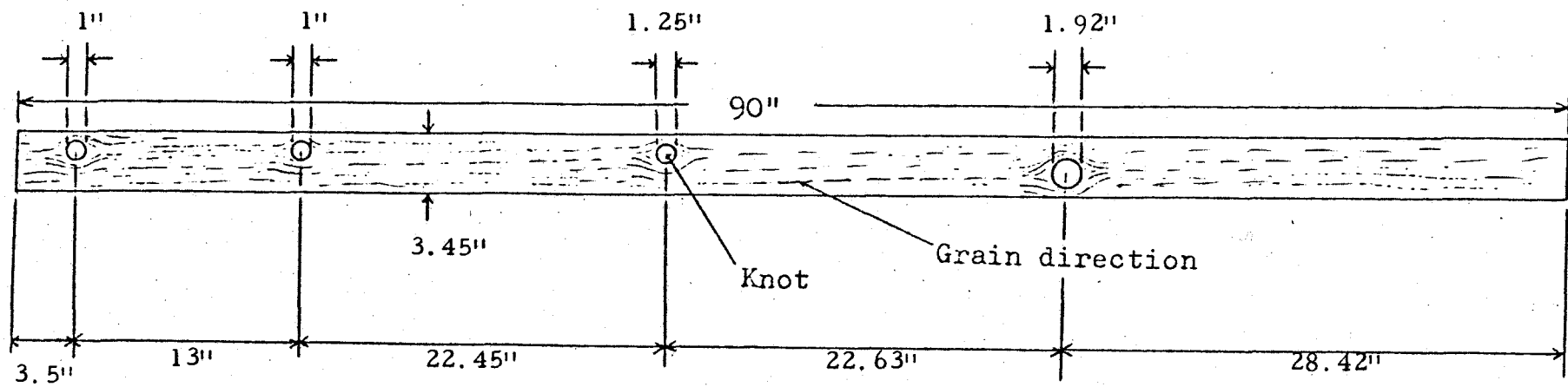


Figure 3.1. Characteristics of stud No. 5.

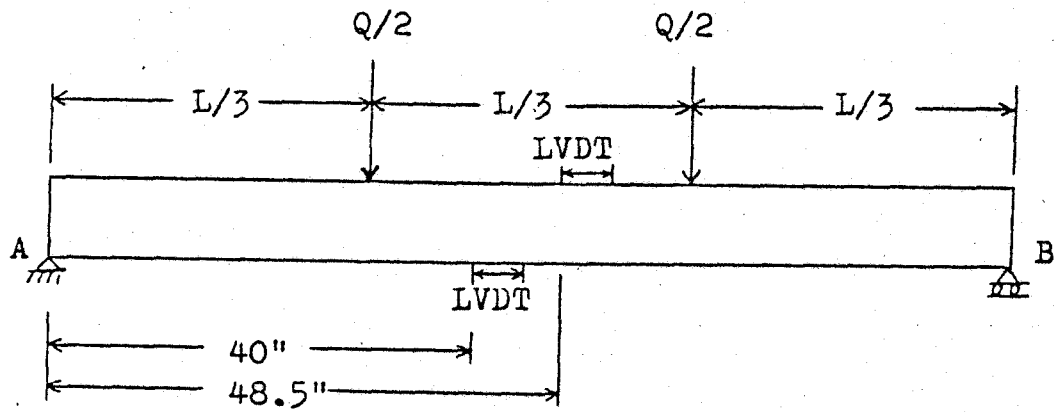


Figure 3.2. Stud loading condition and location of LVDT's.  
Q is the load and L is the beam span. The  
LVDT span was about four inches.

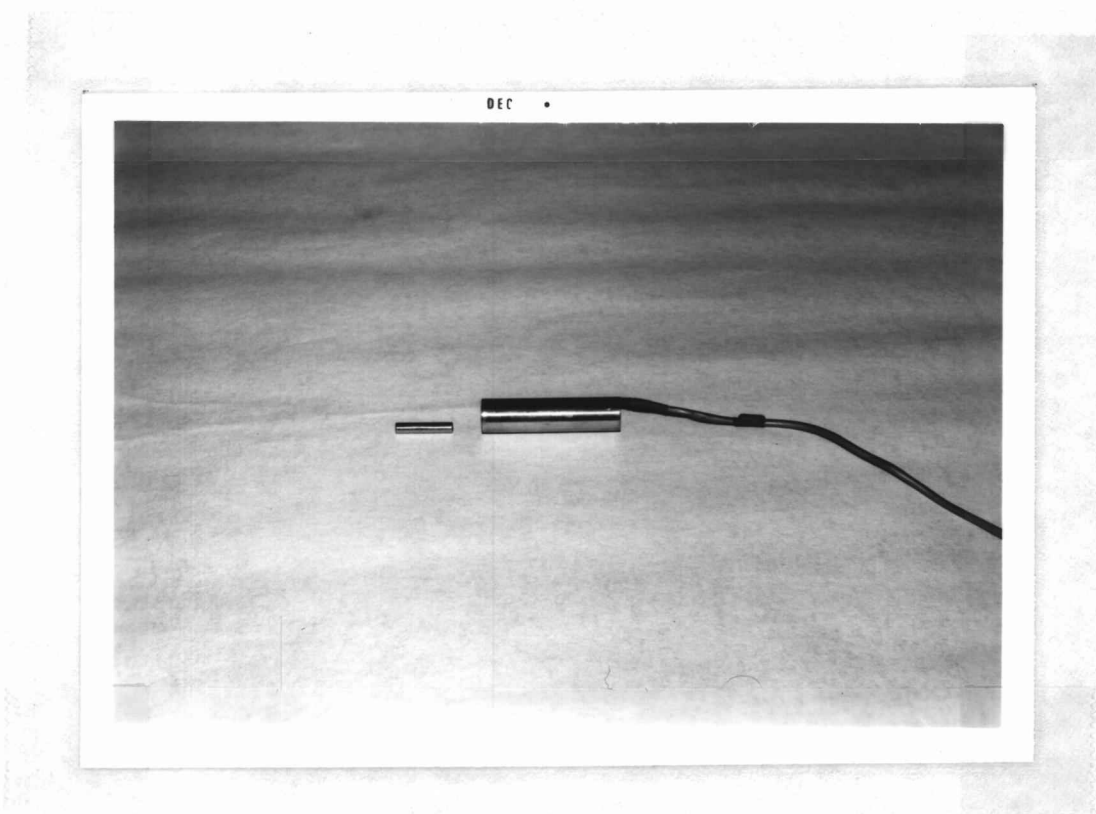


Figure 3.3. A photograph of an LVDT with the movable core at left. The LVDT is about 3.25 inches long and the core is about 1.31 inches long. The resolution of the LVDT was 0.0001 inch.

Continuous graphs of the load to the midspan deflection, also recorded for the specimens, are shown in Figures 3.11 and 3.12. From these deflection-load graphs, subdivided in three linear sections, the secant moduli of elasticity were calculated by:

$$E_1 = \frac{23 Q_1 L^3}{1296 y_1 I} \quad (3.1)$$

$$E_2 = \frac{23(Q_2 - Q_1)L^3}{1296(y_2 - y_1)I} \quad (3.2)$$

$$E_3 = \frac{23(Q_3 - Q_2)L^3}{1296(y_3 - y_2)I} \quad (3.3)$$

in which

$E_1, E_2, E_3$  = moduli of elasticity at the three sections of the deflection-load curve (psi)

$Q_1, Q_2, Q_3$  = total stud loads at points A, B, and C, respectively, in Figures 3.11 and 3.12 (pounds)

$L$  = beam span (inches)

$y_1, y_2, y_3$  = midspan deflections (inches) due to loads  $Q_1, Q_2$ , and  $Q_3$ , respectively,

and

$I$  = moment of inertia of the beam (inches<sup>4</sup>)

The stresses associated with loads  $Q_1, Q_2$  and  $Q_3$  were calculated from

$$S_1 = \frac{Q_1 L}{bh^2} \quad (3.4)$$

$$S_2 = \frac{Q_2 L}{bh^2} \quad (3.5)$$

$$S_3 = \frac{Q_3 L}{bh^2} \quad (3.6)$$

in which

$b$  = breadth of beam and

$h$  = depth of beam

The calculated experimental moduli of elasticity and stresses in bending for the experimental studs are shown in column three of Table 3.1. The load at  $PL$  ( $Q_1$ ) was obtained by determining where the deflection-load curve starts to deviate from a straight line.  $Q_3$  is the load at the maximum point of the curve.  $Q_2$  is the load at a point about midway between  $Q_1$  and  $Q_3$ . The three section moduli ( $E_1$ ,  $E_2$  and  $E_3$ ) were calculated considering the points where  $Q_1$ ,  $Q_2$  and  $Q_3$  were located.

### 3.3. Compression and Tension Tests of Small, Clear Specimens

The elasticity properties of the representative locations for each of the five experimental studs were obtained by testing small, clear specimens cut from the undamaged parts of each of the broken

studs. The specimens obtained from the lower half of the beam depth were tested in tension and those from the upper half were tested in compression.

The dimensions of the tension and compression specimens are shown in Figure 3.4.

The tension specimens were tested by the Instron testing machine (Figure 3.5). The compression specimens were tested on the Tinius Olsen testing machine (Figure 3.6) which has much higher load capacity than that of the Instron. The test speed was chosen to correspond to the stud-beam test; strain rate of 0.001 in./in. min. corresponded to the ASTM Standard D198 (3) and was the same for both kinds of test. LVDT's were used to measure deformations. Specimens were tested to failure. Continuous curves were recorded for each point monitored. Elongation-load curves were determined for tension specimens and shrinkage-load curves for compression specimens.

The experimental deflection-load curves were subdivided into three sections as shown in Figure 1.1. The moduli of elasticity and the corresponding stresses were calculated for each specimen by:

$$E_1 = \frac{Q_1 L}{y_1 A} \quad (3.7)$$

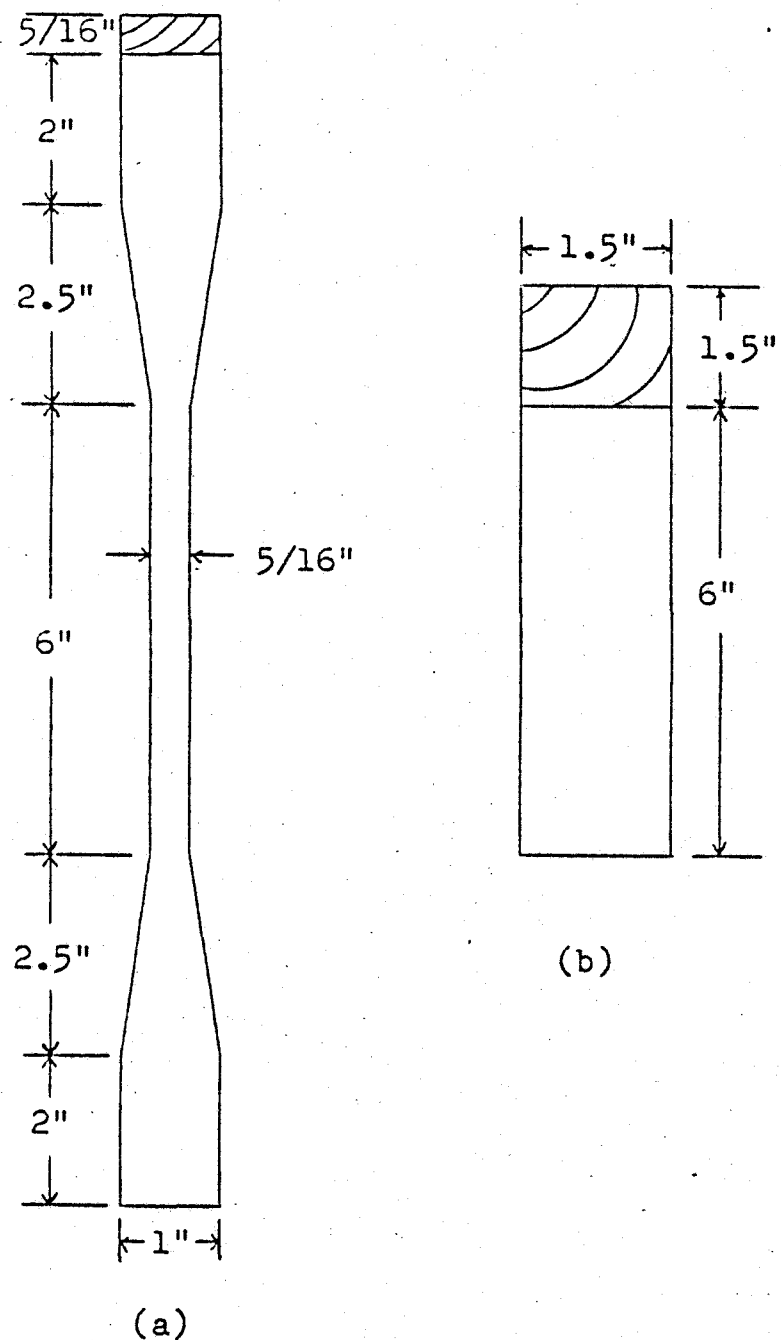


Figure 3.4. Dimensions of the tension (a) and compression (b) specimens.

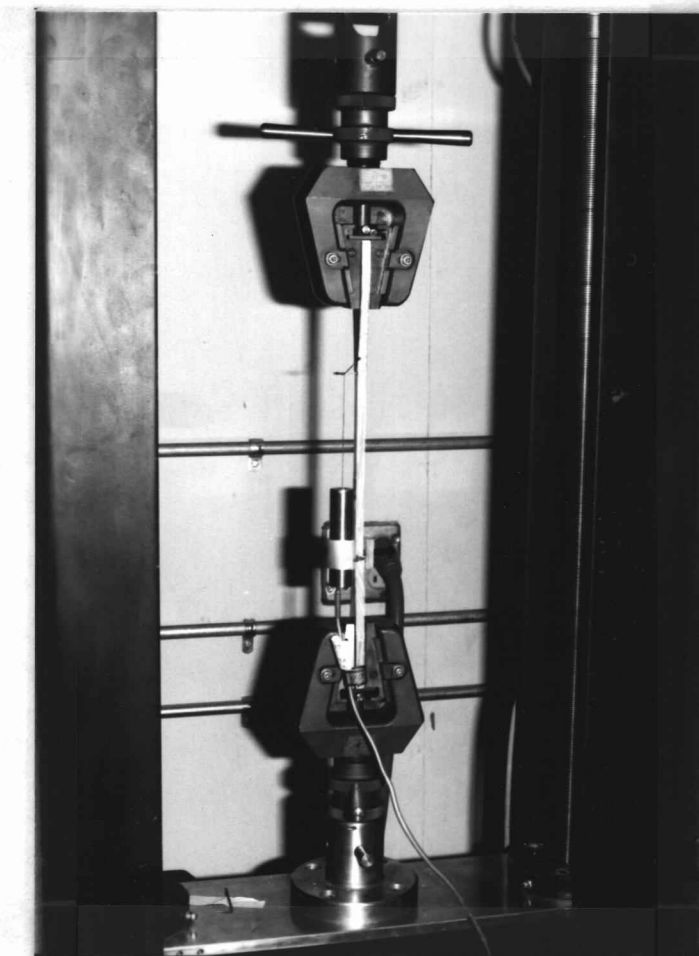


Figure 3.5. The arrangement for tension tests in the Instron testing machine. The LVDT was adjusted to a span of about six inches.

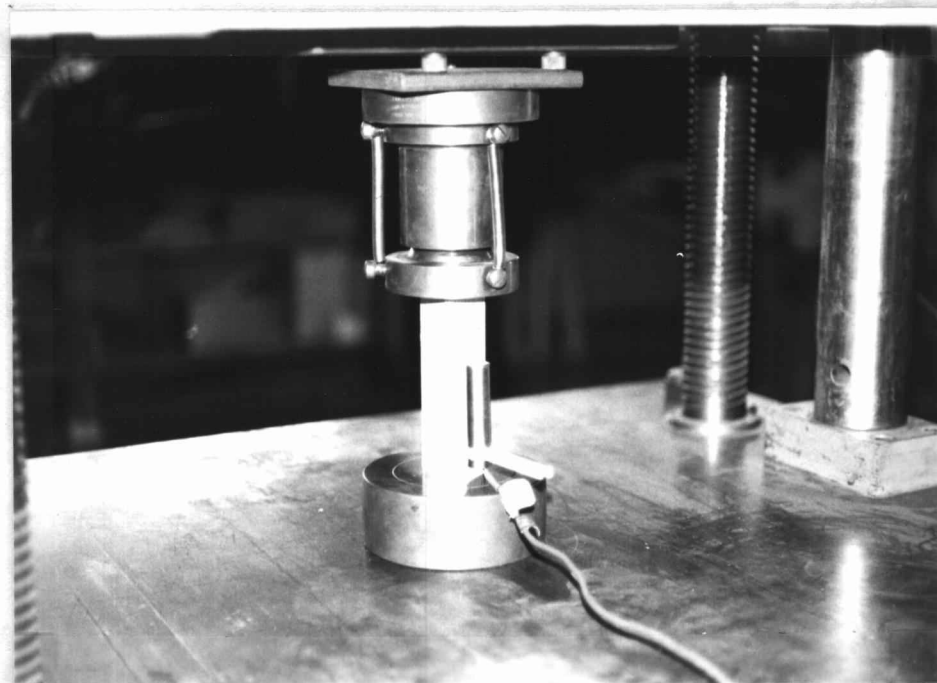


Figure 3.6. The arrangement for compression tests in the Tinius Olsen testing machine. The LVDT span was about four inches.

$$E_2 = \frac{(Q_2 - Q_1)L}{(y_2 - y_1)A} \quad (3.8)$$

$$E_3 = \frac{(Q_3 - Q_2)L}{(y_3 - y_2)A} \quad (3.9)$$

$$S_1 = \frac{Q_1}{A} \quad (3.10)$$

$$S_2 = \frac{Q_2}{A} \quad (3.11)$$

$$S_3 = \frac{Q_3}{A} \quad (3.12)$$

in which:

$A$  = cross sectional area of specimen (inches<sup>2</sup>)

$L$  = span length within which deflections were measured  
(inches) and

$y_1$ ,  $y_2$ ,  $y_3$  = deflections within span  $L$  due to loads  $Q_1$ ,  $Q_2$   
and  $Q_3$ , respectively.

All other symbols have been defined earlier in the text. The results, listed in Appendix J, were used to represent the elasticity and strength properties of the locations on the stud from which the corresponding specimens were cut.

The properties of the broken sections of the studs are the most important elements in the analysis. However, no clear specimens can be obtained from these sections. Therefore, the average elasticity and strength values of the undamaged sections were used to

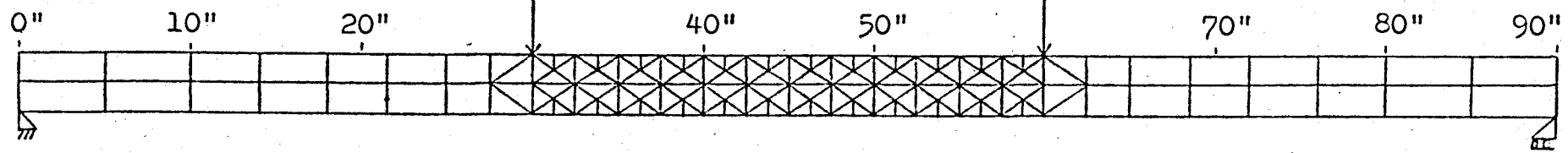
approximate the properties of the broken sections of the stud.

### 3.4. Finite Element Mesh

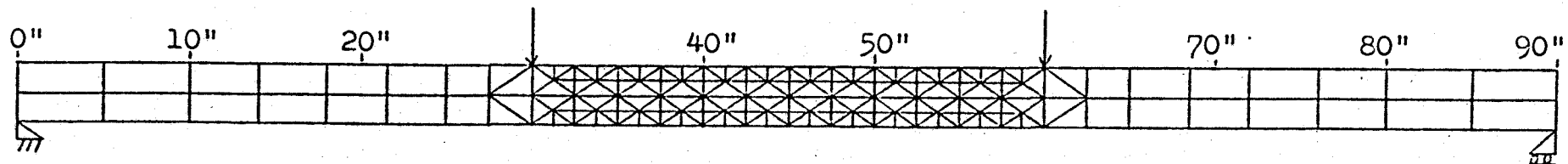
The mesh refinement for the experimental studs was limited by the capacity of the computer system used. For the Cyber 73, the computer system of the Oregon State University, the limit was the mesh with 170 elements and 190 nodes. The mesh refinement is important because the finer the mesh the closer the results to the true solution (8, 11).

The three experimental studs of clear wood are denoted as stud No. 1, 2 and 3. These studs had no other defects except for the grain orientation. The final finite element mesh for these studs was chosen after analyzing stud No. 2 with two kinds of mesh and examining the results. The first mesh had 156 elements and 135 nodes (Figure 3.7a). The second mesh, with 200 elements and 157 nodes (Figure 3.7b), had finer elements than the first mesh in the middle third of the stud. The results shown in Figure 3.8 indicate that the deflection-load curve obtained by using the finer mesh (Figure 3.7b) is not very different from that obtained using the coarser mesh (Figure 3.7a). Since it is less expensive to analyze the mesh with fewer elements, the mesh in Figure 3.7a was adopted to analyze studs Nos. 1, 2 and 3.

The mesh for the two studs containing knots, stud No. 4 with



(a)



(b)

Figure 3.7. The two mesh refinements studied to determine the sizes and number of elements used in the analyses of the three clear wood studs.

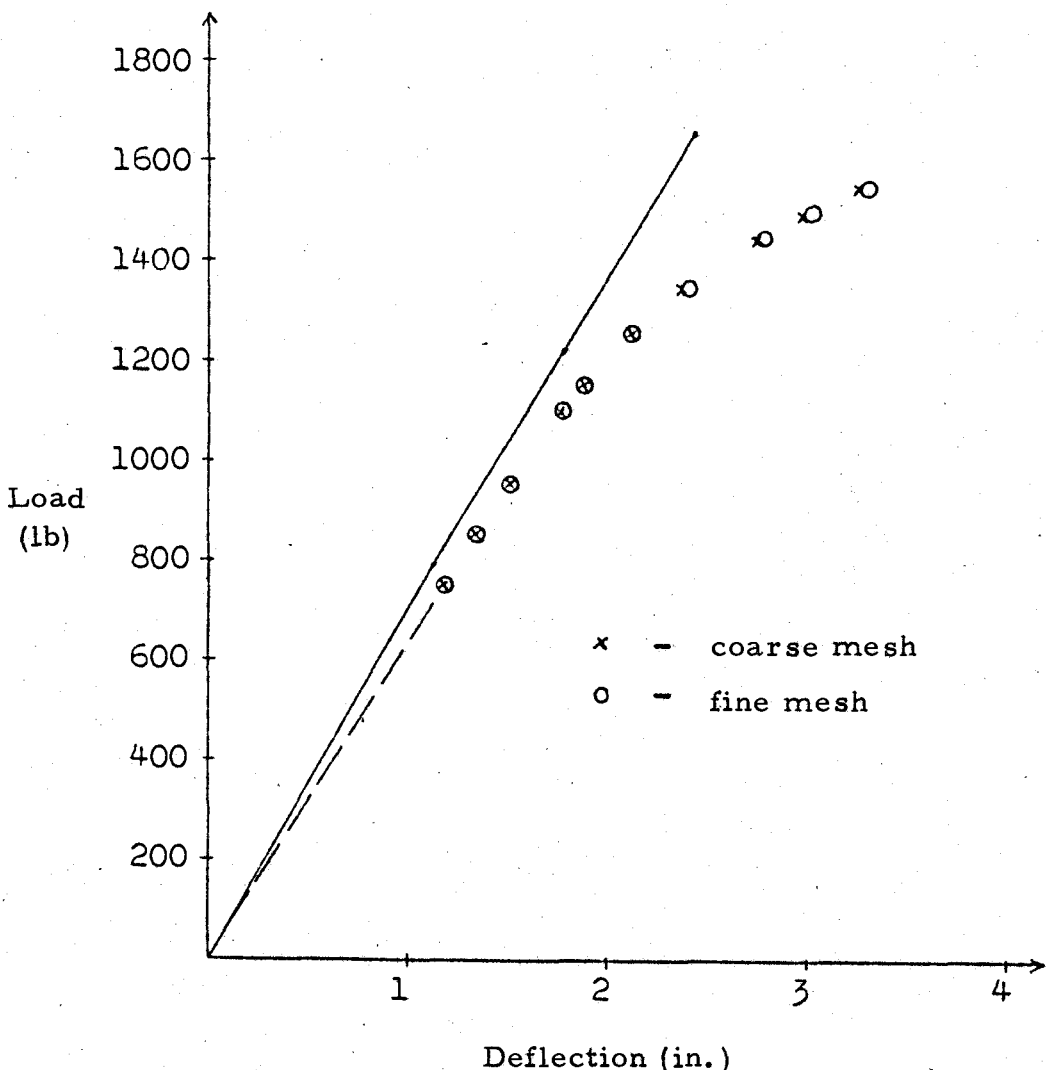


Figure 3.8. Deflection-load curves of stud No. 2 obtained experimentally (solid line), and theoretically using two finite element models. The coarse mesh contains 156 elements while the fine mesh has 200 elements.

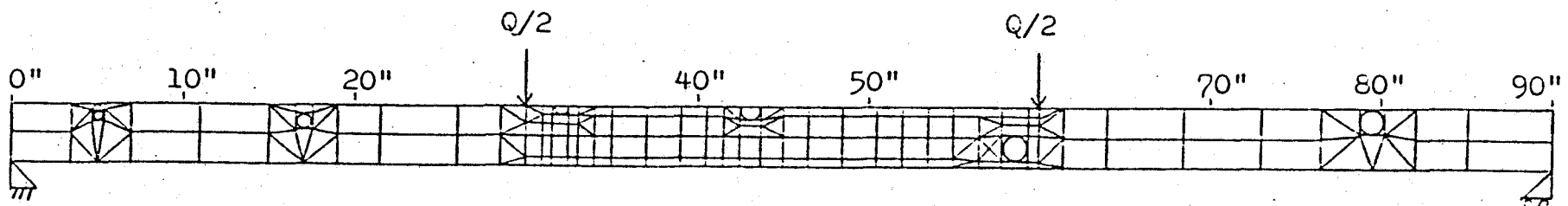
189 elements and 199 nodes and stud No. 5 with 173 elements with 184 nodes are shown in Figures 3.9a and 3.9b, respectively. The material properties of stud Nos. 1, 2, 3, 4, and 5 are listed under the input data in Appendices B, C, D, E, and F, respectively. The data may be identified from the commentaries of the computer program (Appendix A).

Figures 3.7 and 3.9 also depict the boundary and loading conditions. The left bottom corner of the stud is fixed against horizontal translation and the right bottom corner is free. Two equal loads are applied at a distance of 30 and 60 inches from the supports.

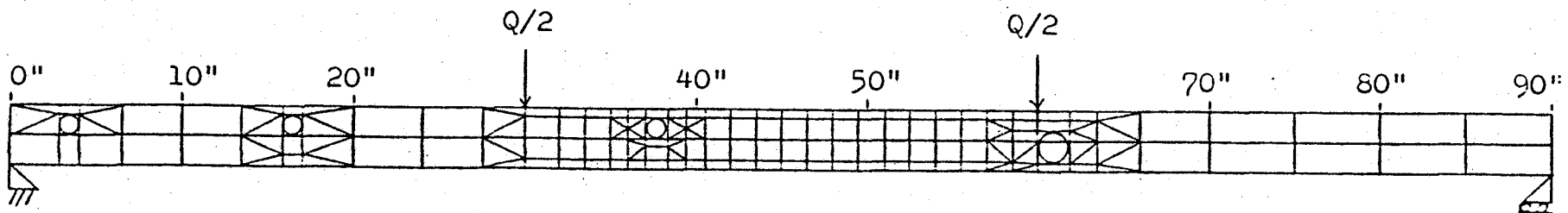
In the analysis the load is continuously being increased by small increments. The smaller the increment the closer the approximation to the solution. Therefore, stud No. 2 was analyzed three times using the increments of total load,  $\Delta Q$ , of 30, 50 and 200 pounds. Figure 3.10 shows the results. The deflection-load curves for  $\Delta Q$  equalling 30 pounds and 50 pounds are almost identical. The curve with  $\Delta Q$  equalling 200 pounds is somewhat stiffer than the first two.

Small load increments require more loading cycles which requires more computer time. Large load increments require less computer time, but the analysis is less sensitive to changes in load and deflection. To optimize between computer time needed and the analysis sensitivity,  $\Delta Q$  was selected as 50 pounds.

Knots are assumed to have negligible resistance to tensile



(a)



(b)

Figure 3.9. Finite element models used to analyze stud numbers four (a) and five (b). The circles enclosed by squares are the areas occupied by knots.

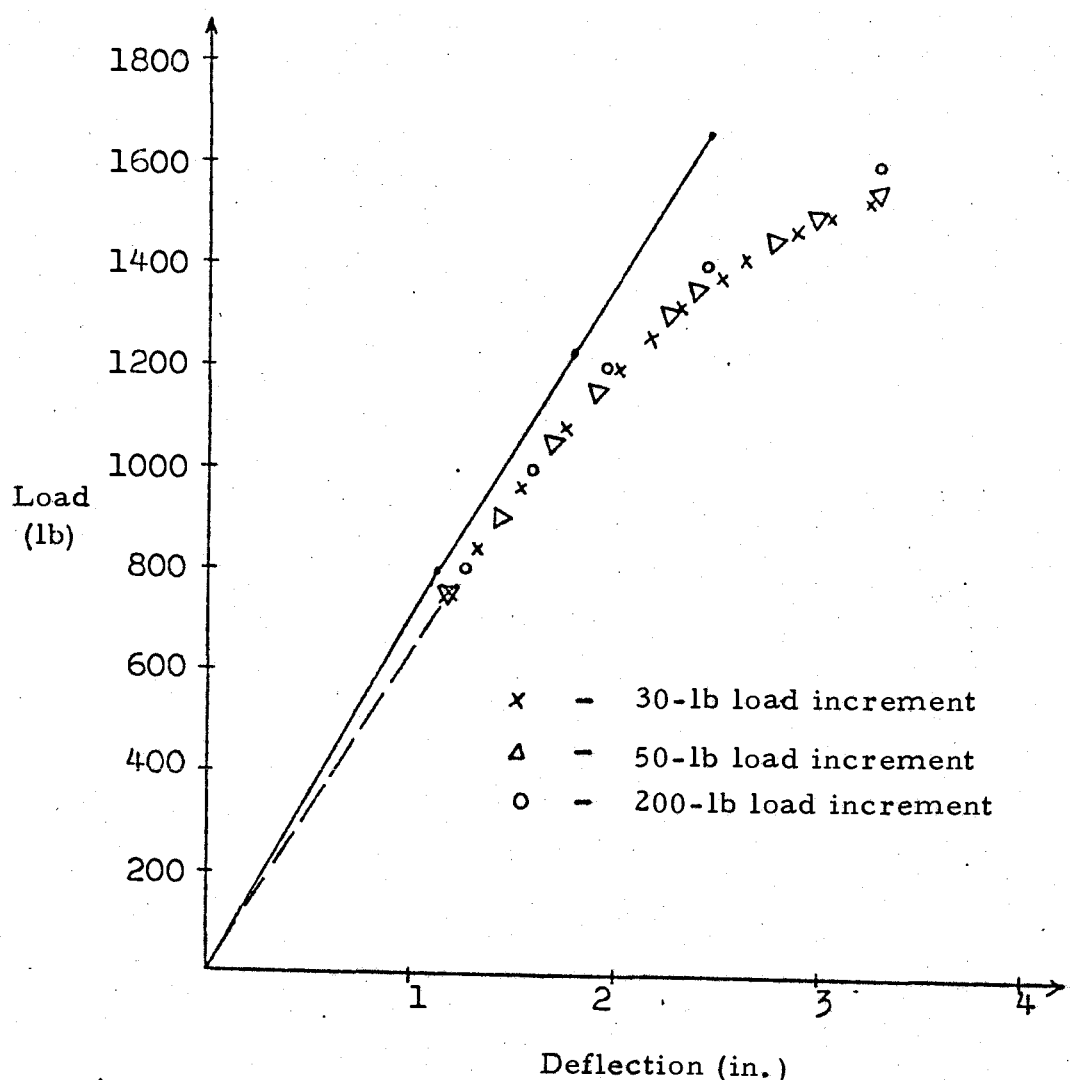


Figure 3.10. Deflection-load curves of stud No. 2 showing the experimental solution (solid line) and three theoretical solutions using three different load increments (30-, 50-, and 200 lb).

stresses. In compression, they are assumed to resist higher loads than normal clear wood. The elastic properties of elements containing knots on the tension half of the specimen were assigned values close to zero. Elements containing knots in the compression side were assigned values equal to those of the normal clear wood in tangential direction, that is, the weakest orthotropic direction in wood.

### 3.5. Comparison of Experimental and Theoretical Results

The deflection-load curves obtained theoretically and experimentally for the experimental studs are shown in Figures 3.11 and 3.12. The moduli of Elasticity  $E_1$ ,  $E_2$  and  $E_3$  and the maximum stress ( $S_3$ ) were calculated using equations 3.1, 3.2, 3.3, and 3.6, respectively. The deflections  $y_1$  and  $y_2$  were the same as those of the experimental curves. The percentage difference between the theoretical and experimental values were calculated by:

$$\% \text{ difference} = \frac{\text{Experimental} - \text{Theoretical}}{\text{Experimental}} \times 100\% \quad (3.13)$$

The results are shown in Table 3.1.

The differences between the experimental and theoretical results for the MOR range from 10.1% to 25.3%.

This can be considered as a significant improvement over the current method for allowable stresses, that develops the allowable stress from the values for the clear wood MOR, which is reduced for

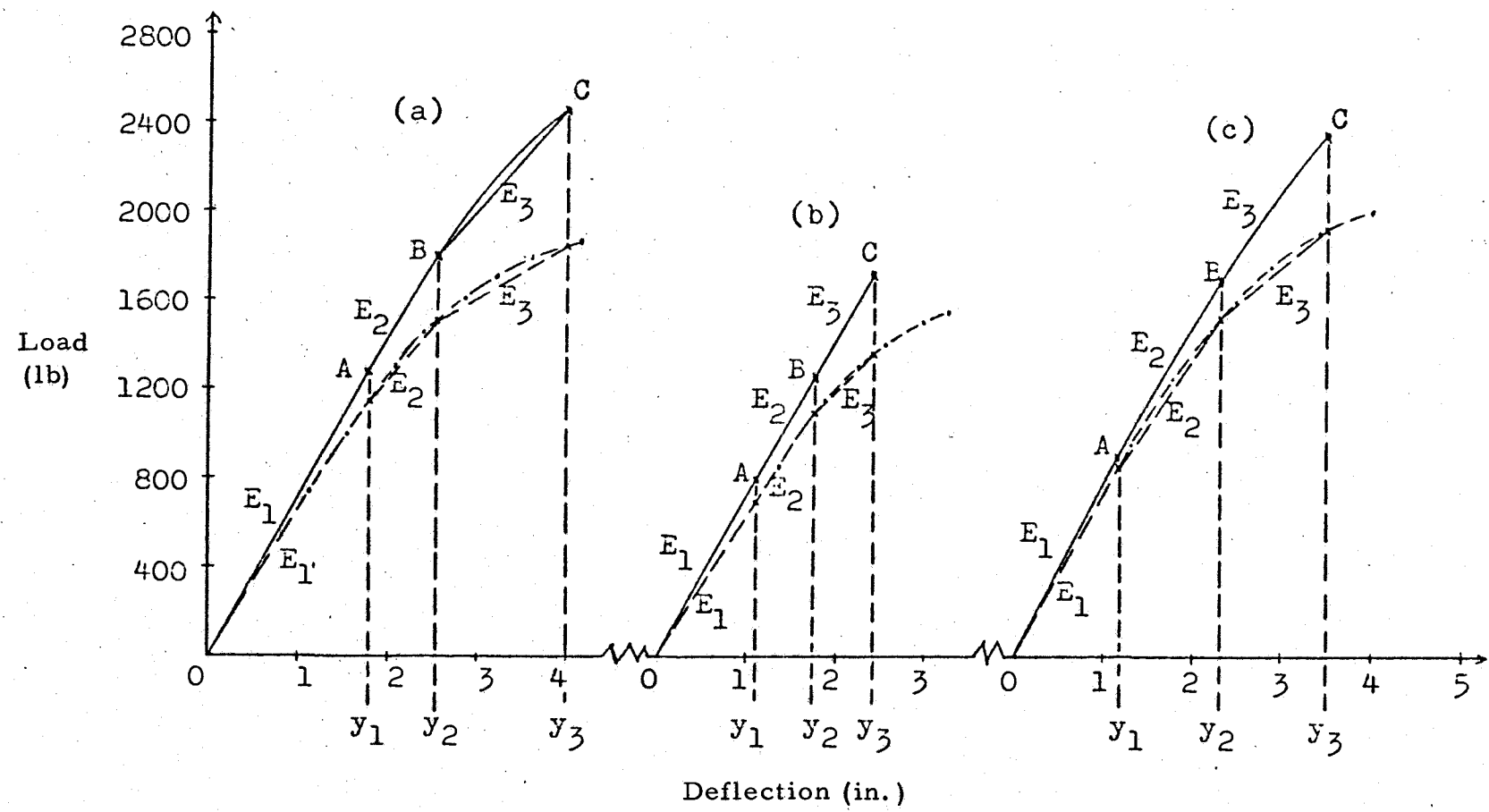


Figure 3.11. Deflection-load curves obtained experimentally (solid lines) and theoretically (broken lines) for stud numbers 1 (a), 2 (b), and 3 (c).

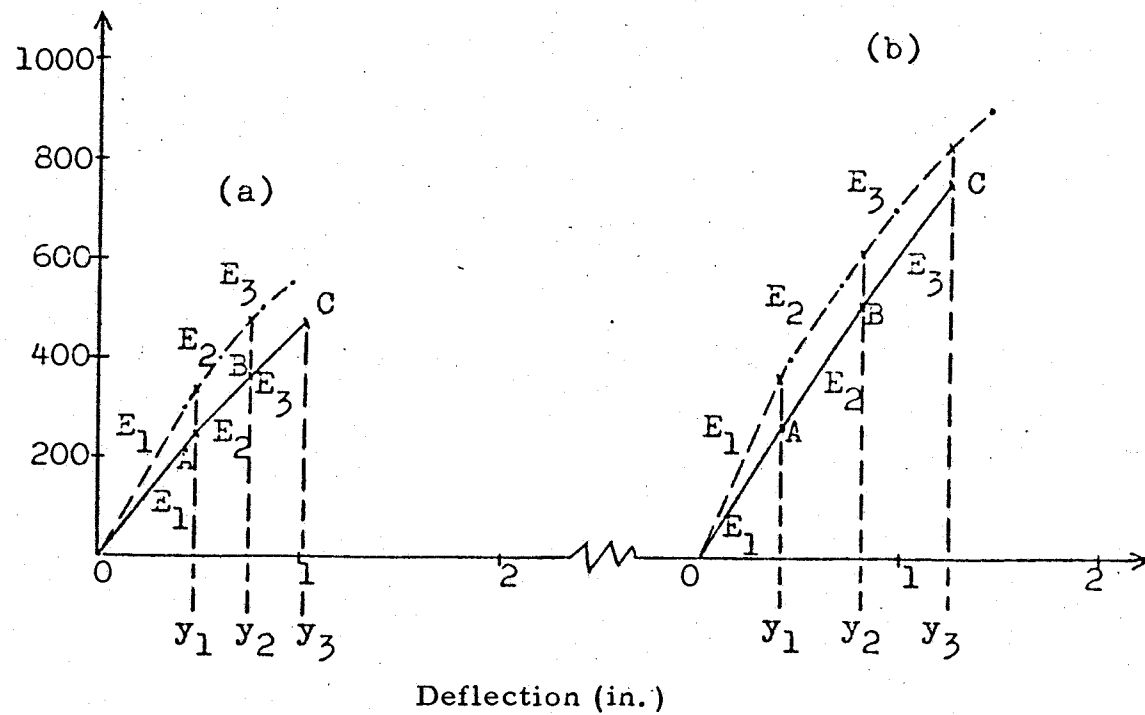


Figure 3.12. Deflection-load curves obtained experimentally (solid lines) and theoretically (broken lines) for stud numbers four (a) and five (b).

Table 3.1. Experimental and theoretical values of load, MOE and MOR. The percentage difference between the experimental and theoretical values of MOE and MOR are given.

Stud No. 1	Property 2	Experimental value 3	Theoretical value 4	Percentage difference 5
1	$Q_1$ (lb)	1,284	1,140	
	$Q_2$ (lb)	1,800	1,500	
	$Q_3$ (lb)	2,465	1,840	
	$E_1$ (psi)	1,856,000	1,647,800	11.2
	$E_2$ (psi)	1,733,900	1,209,700	30.2
	$E_3$ (psi)	1,203,200	615,200	48.8
	MOR (psi)	12,640	9,440	25.3
2	$Q_1$	797	700	
	$Q_2$	1,231	1,090	
	$Q_3$	1,661	1,350	
	$E_1$	1,801,700	1,582,500	12.2
	$E_2$	1,732,300	1,556,700	10.1
	$E_3$	1,689,900	1,021,800	39.5
	MOR	8,490	6,900	18.7
3	$Q_1$	888	850	
	$Q_2$	1,690	1,520	
	$Q_3$	2,352	1,920	
	$E_1$	1,953,700	1,870,100	4.3
	$E_2$	1,890,600	1,579,400	16.5
	$E_3$	1,481,200	895,000	39.5
	MOR	12,310	10,050	18.3
4	$Q_1$	247	330	
	$Q_2$	360	470	
	$Q_3$	472	550	
	$E_1$	1,336,300	1,785,400	-33.6
	$E_2$	1,152,200	1,427,500	-23.9
	$E_3$	1,060,400	1,009,900	4.8
	MOR	2,470	2,870	-16.2
5	$Q_1$	264	360	
	$Q_2$	511	610	
	$Q_3$	748	825	
	$E_1$	1,612,200	2,198,400	-36.4
	$E_2$	1,508,400	1,526,700	-1.2
	$E_3$	1,412,900	1,281,700	9.3
	MOR	3,750	4,130	-10.1

defects and safety. The current method was reported to produce a working stress which is 400% lower than the actual stress (38).

The difference range for  $E_1$  is 4.3% to 36.4%, for  $E_2$ , 1.2% to 30.2%, and for  $E_3$ , 4.8% to 48.8%.

The effects of the stud properties used in the analysis on the accuracy of the theoretical deflection-load curves are discussed in section VI.

#### IV. PARAMETER STUDY

A parameter study was conducted to determine the effect of six parameters on the deflection-load curves. The parameters are: moduli of elasticity  $E_L$ ,  $E_R$  and  $E_T$ , clear-wood stresses  $S_1$ ,  $S_2$  and  $S_3$ , moduli of rigidity  $G_{LT}$ ,  $G_{LR}$  and  $G_{TR}$ , Poisson's ratios  $\nu_{LT}$ ,  $\nu_{TL}$ ,  $\nu_{LR}$ ,  $\nu_{RL}$ ,  $\nu_{TR}$ ,  $\nu_{RT}$ , grain angle, and ring angle.

##### 4.1. Procedure

Experimental stud No. 2 was selected for the parameter study. Only one parameter was increased at a time leaving the others unchanged. Table 4.1 depicts the parameter changes. The magnitude of the parameter change was determined on the basis of the author's opinion as to a possible margin of error in experimentally determined parameter values. For each parameter change, the stud was analyzed by the procedure developed to obtain the deflection-load curve. The curves were divided into same three sections as the curves for control model with no parameter change (Figures 4.1 and 4.2). The moduli of elasticity  $E_1$ ,  $E_2$ ,  $E_3$ , and modulus of rupture  $S_3$  were calculated by equations 3.1, 3.2, 3.3 and 3.6, respectively, and compared to the corresponding values computed for the control model. The percentage differences between the results for the actual and changed properties were calculated by equation 3.13.

Table 4.1. Magnitude of parameter increases used in parameter study.

Parameter	Magnitude of Increase
Moduli of elasticity	25%
Moduli of rigidity	25%
Poisson's ratios	100%
Clear wood stresses	50%
Grain angle	5°
Ring angle	20°

#### 4.2. Results

Figures 4.1 and 4.2 show the results of the parameter study. Table 4.2 gives for each parameter change the stud moduli and the percentage differences between the results from the control and changed values.

The  $E_1$  of the stud increased by 20% when the MOE used for the elements was increased by 25%.  $E_3$  increased by 13%.  $E_2$  and MOR did not change much.

If the grain angle of the stud is increased by 5°, the  $E_1$  decreased by 12.9%,  $E_2$  decreased by 5.7%, whereas  $E_3$  and MOR did not change much.

When the clear wood stresses used for the elements were increased by 50%, the stud MOR increased by 48.4%. However,

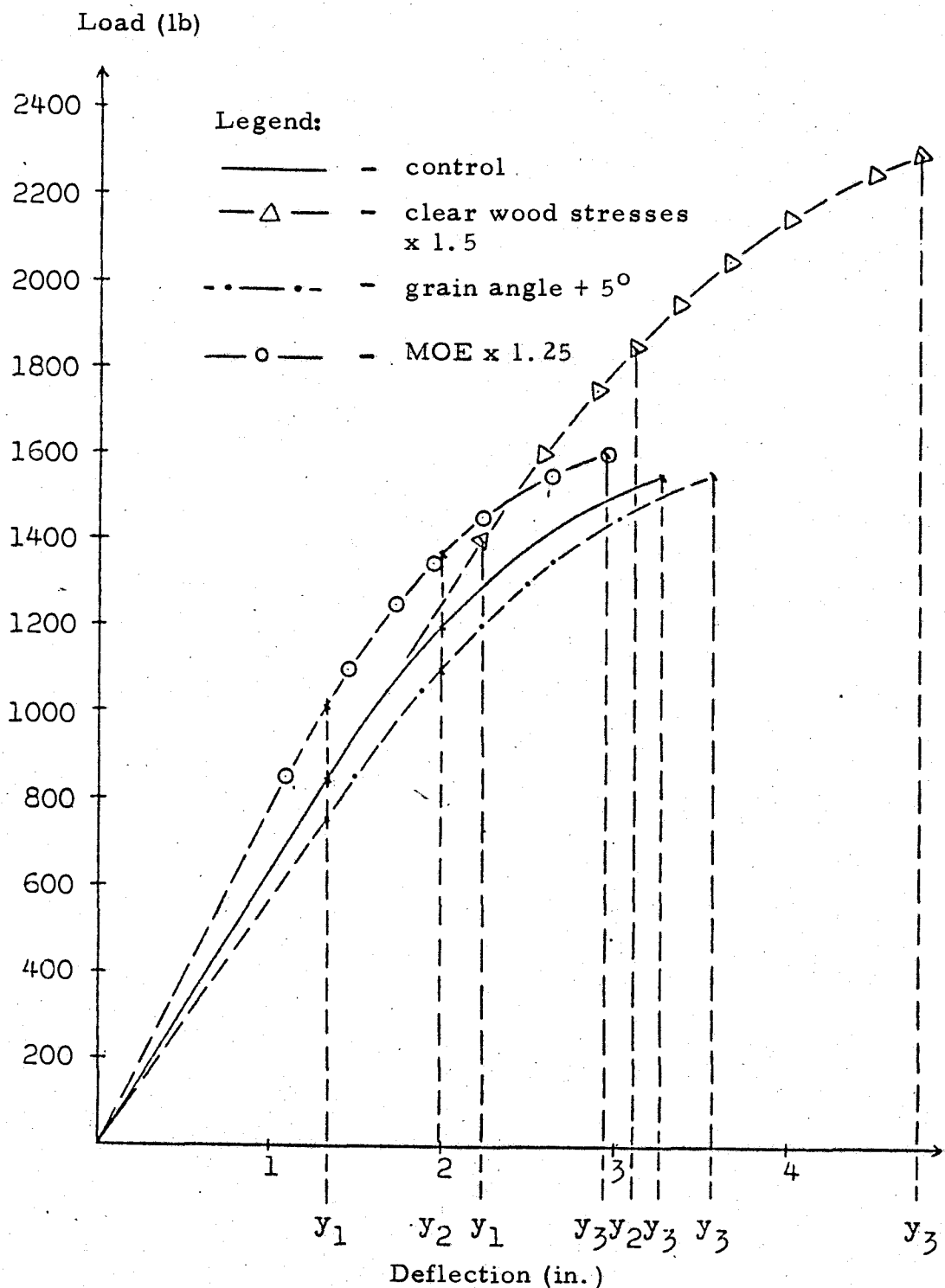


Figure 4.1. Deflection-load curves for the control model, and for the model with increased MOE's, grain angle and clear wood stresses.

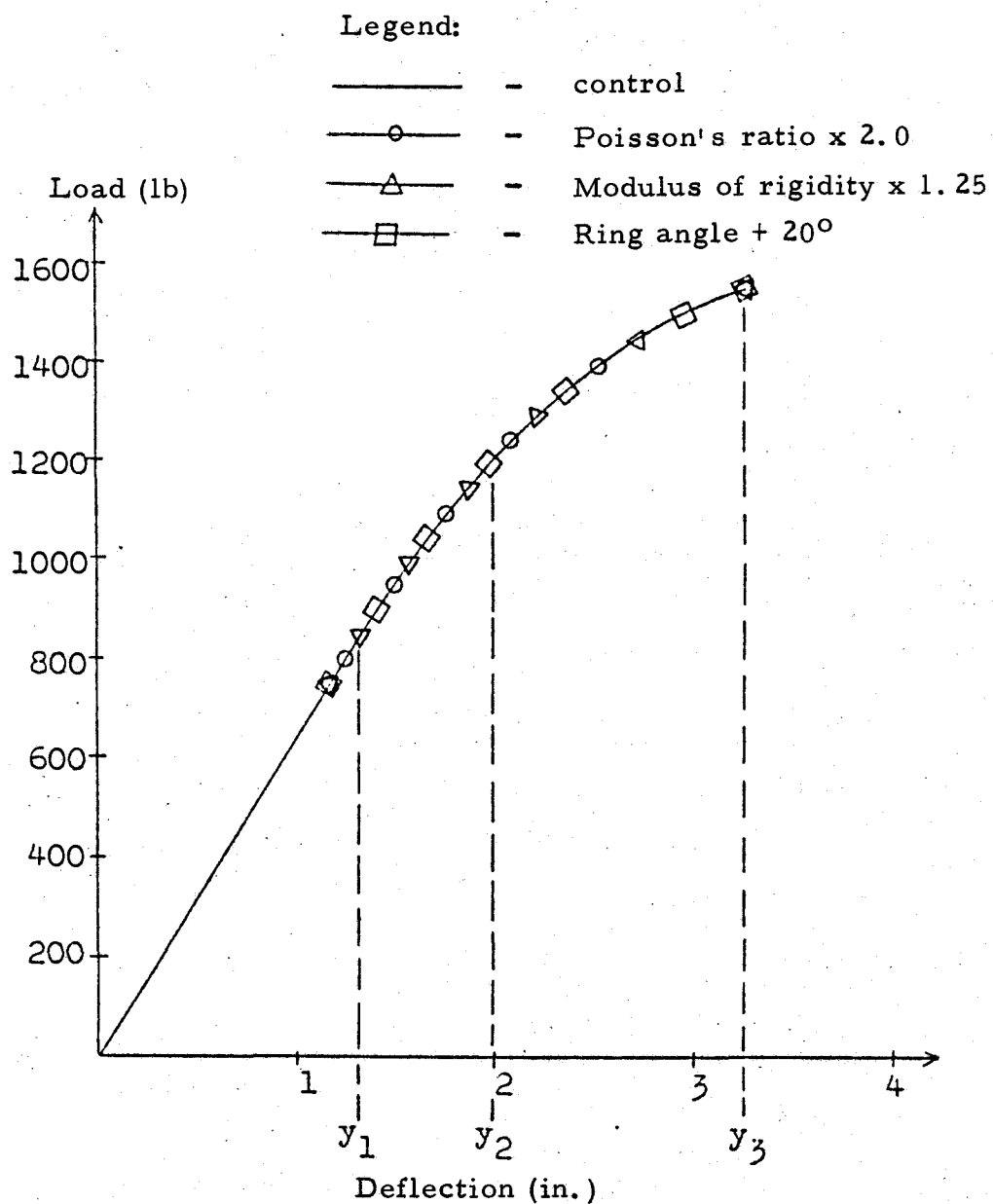


Figure 4.2. Deflection-load curves for the control model, and for the model with increased Poisson's ratio, modulus of rigidity, and ring angle.

Table 4.2. Moduli of elasticity and rigidity for deflection-load traces of control model and models with changed elasticity property.

Parameter value changed	$E_1$ (psi)	$E_2$ (psi)	$E_3$ (psi)	MOR (psi)
Control	1,620,400	1,354,700	704,000	7,920
MOE x 1.25	1,944,500	1,316,000	795,700	8,170
% difference	-20.0	2.9	-13.0	-3.2
Grain angle + 5°	1,410,700	1,432,100	725,200	7,920
% difference	12.9	5.7	-3.0	0.0
<b>Clear wood</b>				
stresses x 1.5	1,611,000	1,291,600	692,500	11,750
% difference	0.6	4.7	1.6	-48.4
Poisson's ratio x 2.0	1,620,400	1,354,700	726,900	7,920
% difference	0.0	0.0	-3.3	0.0
<b>Modulus of</b>				
rigidity x 1.25	1,632,600	1,334,500	682,500	7,920
% difference	-0.8	1.5	3.1	0.0
Ring angle + 20°	1,620,400	1,334,500	715,300	7,920
% difference	0.0	1.5	-1.6	0.0

$E_1$ ,  $E_2$  and  $E_3$  did not change much.

Changes in Poisson's ratio, shear modulus and ring angle values had a negligible effect on  $E_1$ ,  $E_2$ ,  $E_3$  and MOR.

## V. SIMULATION PROCEDURE

The finite element method for wood stud analysis may be applied to model study populations. Studs may have any of the commonly found wood defects such as ring angles, grain angles and knots.

Figure 5.1 depicts a flow diagram of the procedure. The most important steps are the generation of stud properties, formulation of a finite element model, axial transformation of elasticity properties, and application of the linear step-by-step analysis. These steps were individually discussed earlier in the text.

A computer program prepared for the simulation procedure is explained and listed in Appendix A.

### 5.1. Generation of Material Properties

The procedure generates a stud model with diameter and location of knots, grain and ring angles, and elastic and strength properties from their corresponding probability distribution.

#### 5.1.1. Diameter and Location of Knots

The knot diameter, determined by assuming that its probability distribution is uniform (60), was obtained from:

$$\text{DIAM} = 10 [\text{RANF(A)}] - 2.5 \times \quad (5.1)$$

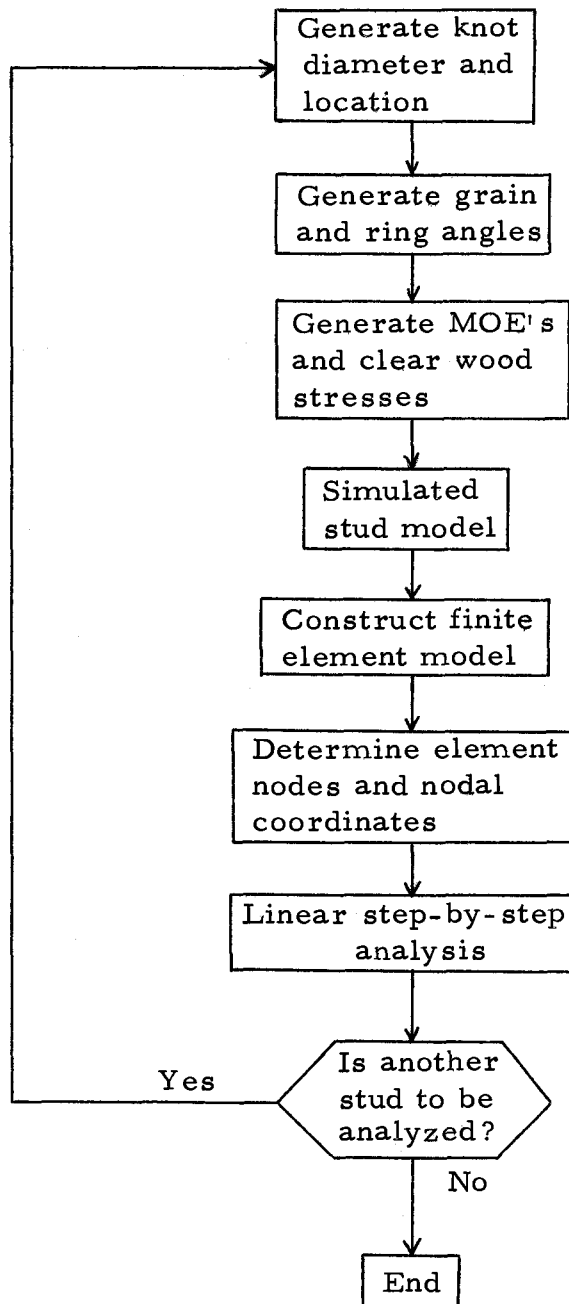


Figure 5.1. Flow diagram for simulation procedure.

where

RANF(A) = random number generator on OSU Cyber 73. It generates numbers from a uniform distribution with a range from 0 to 1.

DIAM= knot diameter with a range from 0 to 2.5 inches.

X = multiple of 2.5 which would reduce the knot diameter within the desired range.

The knots were assumed to be solid and formed continuous parts of the stud. However, they have material properties different from those of clear wood. The area they occupy are, therefore, designated by separate elements. Because knot diameters follow a continuous distribution, it would be impossible to develop a finite element mesh that could account for knot sizes with very small size increments. Therefore, for convenience in modeling knots, an increment of 0.5 in. in the range from 0.0 to 2.5 in. was chosen to classify knot diameters. Table 5.1 gives the knot diameter corresponding to the generated diameter values. Two and one-half inches is the maximum diameter allowed under the Stud grade (56). The computer program allows to reduce the range of knot diameters, if desired. Table 5.2 gives the range of knot diameters chosen in examples of this study. Some of the knot diameter ranges were chosen to account for the requirements of Stud, Construction, Standard and Utility grades (56). The Stud grade was used in this

study. The other diameter ranges were included for an eventual future use.

Table 5.1. Generated value and the corresponding knot diameter used in simulating the stud model.

Generated value	Knot diameter (in.)
0.00 to 0.25	0.0
0.26 to 0.75	0.5
0.76 to 1.25	1.0
1.26 to 1.75	1.5
1.76 to 2.25	2.0
2.26 to 2.75	2.5

Table 5.2. Values of variable IP and the corresponding knot diameter ranges considered by the model.

IP*	Knot diameter range (in.)
1	1.0-2.5
2	1.5-2.5
3	2.0-2.5
4	0.0-2.5
5	0.0-1.5
6	0.0-1.0
7	1.0-2.0
8	0.0-2.0

\*IP is the variable in the computer program which controls the range of knot diameters.

The knot location was assigned by dividing the stud into 1260 sections of size 0.5- by 0.5-inch. One section, designated as the center of the knot, was picked at random by the equation

$$\text{LOC} = 10,000 [\text{RANF(A)}] - 1,260 \times \quad (5.2)$$

where

LOC = number of part where the center of the knot is located

X = multiple of 1, 260 which would reduce the location  
number within the desired range

RANF(A) = defined earlier in the text.

#### 5.1.2. Grain and Ring Angles

The grain and ring angles were obtained in the same manner as that of the knot diameter and location. The range of the ring angles is from  $0^{\circ}$  to  $90^{\circ}$ , and that of the grain angles is from  $0^{\circ}$  to  $14^{\circ}$ . Fourteen degrees is the maximum grain angle allowed under the Stud grade (56).

The generated values for grain angles were used for elements not disturbed by knots. For elements around knots, the grain angles are distorted and are, therefore, increased according to their location around the knot as shown in Figure 5.2. If the diameter of the knot is larger, the area of the affected elements is increased proportionately.

#### 5.1.3. Elastic and Strength Properties

The MOE's and stresses of clear wood were based on the assumption that their frequency distributions are normal (60). The following equation (15) was used:

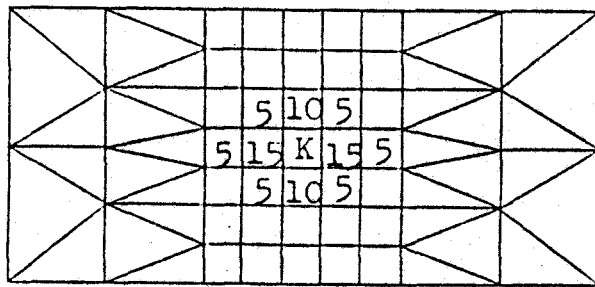


**Figure 5.2.** Elements disturbed by knots. The square containing letter K is the area occupied by the knot. A knot can be located in any of the square elements. The numbers in elements around the knot are the magnitude in which the grain angles are increased over the actual local orientation in these elements. The magnitude of the grain angle increment around knots was determined by inspecting the grain angle distortions around knots in lumber.

$$X = \mu + (-2\sigma^2 \ln U_1)^{\frac{1}{2}} \cos 2\pi U_2 \quad (5.3)$$

in which

$X$  = generated value of the property

$\mu$  = average value of the property

$\sigma^2$  = variance of the property, and

$U_1, U_2$  = random numbers ranging from 0.0 to 1.0 generated from a uniform distribution.

The frequency distributions of MOE's and stresses of clear wood were obtained from the results (unpublished) of a recent bending test of small, clear Douglas-fir specimens conducted at the Forest Research Laboratory, Oregon State University.

### 5.2. Finite Element Mesh

Figure 5.3 shows the stud model. It could be applied to studs generated in the simulation procedure. This model was chosen because of its efficiency in modeling knots. The stud was divided into 36 sections along its length with each section 2.5 inches long. Each section was designated by letters A through F. For clear wood stud, the mesh in Figure 5.3a is used. Knots may be modeled by substituting sections of the clear-wood mesh with the appropriate mesh defined in Figure 5.3b through 5.3g. Any one of Figures 5.3b through 5.3g may be substituted with a section of a stud in Figure 5.3a depending

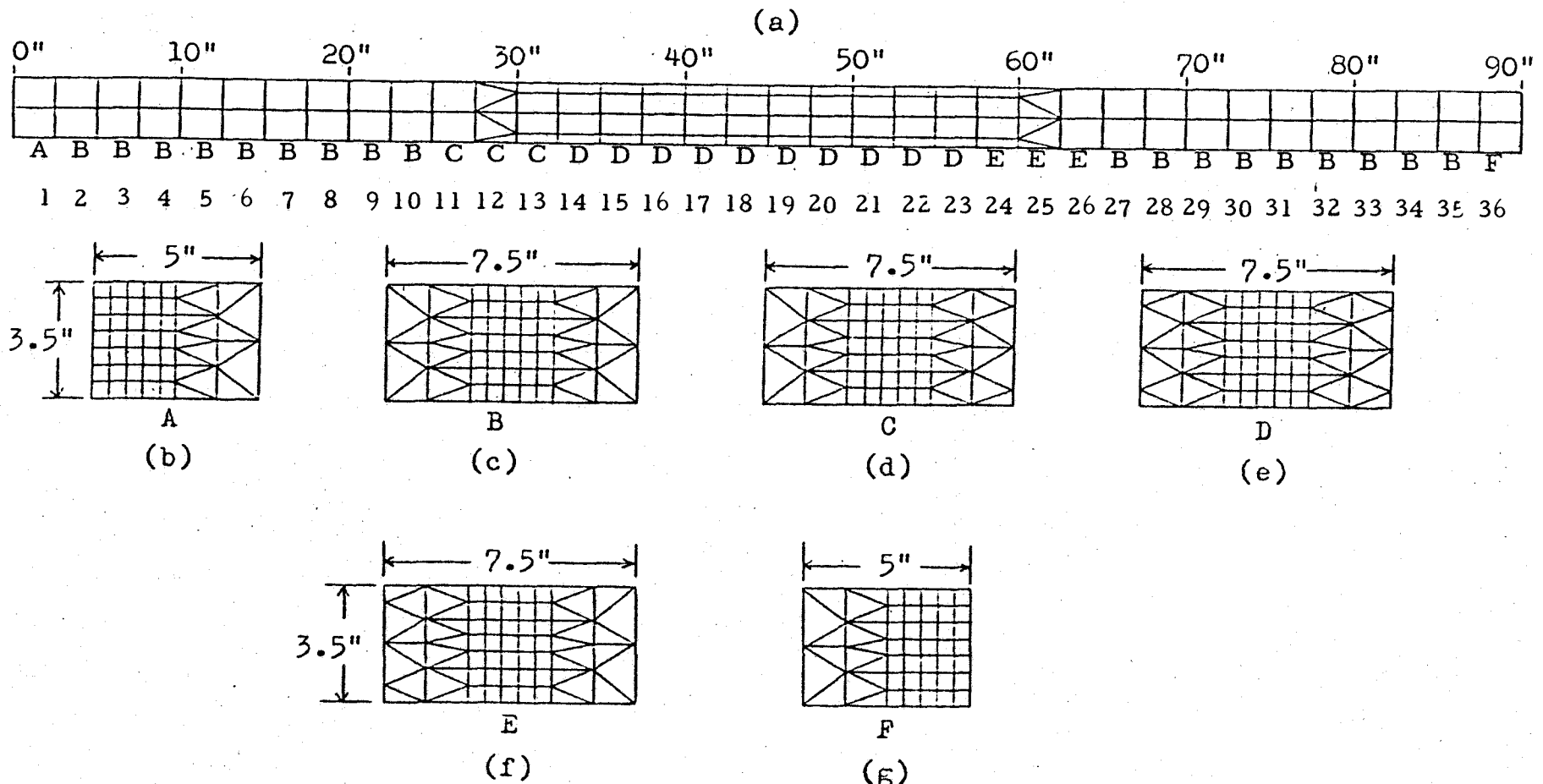


Figure 5.3. Finite element mesh used in the analyses of wood studs. Figure 5.3a is the unmodified mesh associated with clear wood. Figures 5.3b through 5.3g are the replacements for sections affected by knots. The letters A through F in Figure 5.3a designate the position of the mesh defined in Figures 2.7b through 2.7g.

on the location of the knot. The letter designating a section in Figure 5.3a corresponds to the letter in one of Figures 5.3b through 5.3g to be substituted where the critical knot is located in the stud. The knot is located in one of the square elements in Figures 5.3b through 5.3g. For example, if the knot is located in section 15 of Figure 5.3a, sections 14, 15 and 16 are replaced by Figure 5.3e. The elements and nodes are re-numbered and nodal coordinates determined.

One limitation of the method is that edge knots can not be modeled. However, this could easily be added to the procedure by assigning a certain area in the wide face of the stud to a knot with the same strength-reducing effect as that of the edge knot.

## VI. DISCUSSION

This chapter deals with the finite element model and simulation procedure, accuracy of stud properties for verification and its effect on the theoretical results, and with the applications of the finite element model and simulation procedure.

### 6.1. Finite Element Model and Simulation Procedure

The finite element method used in this study is able to predict the deflection-load curves of studs with sufficient accuracy. However, the method has some limitations. The material properties are assumed to be constant within the element, which usually is not true in case of wood. The number of elements, which has an effect on the accuracy of the results, is limited by the memory capacity of the computer being used. Finally, the actual three-dimensional stud is described by a two-dimensional finite element model.

The simulation procedure has also its limitation. The material properties of studs follow certain probability distributions which can not be exactly defined. These distributions are approximated by known probability distributions.

### 6.2. Accuracy of Stud Properties for Verification and Effect on the Theoretical Results

The stud properties for the analysis are obtained by testing,

from previous studies, and methodical mapping and inspection of stud defects.

#### 6.2.1. Moduli of Elasticity

The  $E_L$ 's used in the verification of the finite element method were obtained from tension and compression tests of the undamaged parts of the stud after testing. The broken parts, the most important sections of the studs used for the verification, were only approximated by the average  $E_L$ 's of the undamaged parts. Considering the high variability of wood even in the same piece of lumber, the average  $E_L$ 's of the undamaged sections could be different from those of the broken parts. The  $E_T$  and  $E_R$  values were determined by using regression relations developed in previous studies. The regression relations were based on a specific sample of small clear specimens. Therefore, it is highly possible the properties of studs used for verification deviated from the actual values. Such deviations or errors in the determination of the true MOE's of the stud could significantly alter the computed deflection-load curve of the stud. Because, as shown in the parameter study, an increase of the MOE values used in the analysis by 25% caused an increase in the stud  $E_1$  value by 20%.

### 6.2.2. Shear Moduli and Poisson's Ratio

The shear moduli were determined using regression relations from previous studies, and Poisson's ratio values were taken from previous research. These values and relations could be different from those of the stud. However, this is not very important because, as shown in the parameter study, these factors did not affect the deflection-load curve of the stud. The results of the parameter study on Poisson's ratio agrees with the works of Brodeau (5), Fung (16) and Walker (55) who concluded that accurate determination of Poisson's ratio does not seem very critical in solving plane stress problems.

### 6.2.3. Grain and Ring Angles

The grain and ring angles were obtained by measurement. They were measured at a certain interval along the stud length. Due to the natural variability in the grain and ring directions, it is virtually impossible to obtain the exact angles for the elements. Only the grain angles at the stud surface can be measured. It can not be ascertained if the grains are twisted or changed directions inside the wood. The grain angles of elements around knots are also difficult to obtain because they are not constant. Errors in the angle determination should lead to errors in the theoretical deflection-load curve of the stud. From the parameter study discussed in an earlier section of

the text, the ring angle was not a significant factor in the analysis.

However, an increase in the grain angle by  $5^{\circ}$  caused a decrease in the  $E_1$  value of the stud by 12.9%, or about 2.6% change in  $E_1$  per degree error in grain angle.

#### 6.2.4. Clear Wood Stresses

The clear wood stresses ( $S_1$ ,  $S_2$ ,  $S_3$ ) associated with the MOE's ( $E_1$ ,  $E_2$ ,  $E_3$ ) like the  $E_L$ 's were obtained from tests of small clear specimens. They are, therefore, subject to the same type of error as those of the  $E_L$ 's. The clear wood stresses of the broken sections of the stud were approximated by the average stresses obtained from the undamaged parts. From the parameter study earlier in the text, the clear wood stresses are critical in the determination of MOR. An increase in clear wood stresses by 50% caused an increase in MOR of the stud by 48.4%.

#### 6.2.5. Knots

The elastic properties used for the knots could also have affected the theoretical deflection-load curve of the stud. The negligible value assigned to the elasticity properties of knots in the tension side of the stud could have decreased the MOE of the stud. The elasticity properties assigned to knots in the compression side, i.e., properties of clear wood in the tangential direction, could be too low

thus decreasing the MOE of the stud. These suggest that studies on the properties of knots are necessary.

### 6.3. Applications of the Finite Element Model and Simulation Procedure

The finite element model and simulation procedure developed in this study could be used to determine the stiffness and strength of studs used in walls. This will make it possible to obtain a more precise information on the behavior of walls under certain loading conditions.

The theoretical method could also be used as a substitute for an actual bending test. The allowable design stresses and MOE of different lumber grades and species could be determined theoretically. This is possible for wood species in which clear wood values are available. This procedure is less expensive than the current method of actual tests.

## VII. CONCLUSIONS AND RECOMMENDATIONS

The most important conclusions of this study are:

1. The finite element method is an excellent procedure to employ in the analysis of wood studs.
2. The finite element model and simulation procedure developed in this study can be used to approximate the deflection-load curves of studs.
3. An increase in the accuracy of stud properties will increase the precision of the computed deflection-load curves.
4. An increase in the MOE values alone by 25% increased the stud  $E_1$  value by 20%; an increase in grain angles alone by 5° decreased the stud  $E_1$  value by 12.9%; and an increase in clear wood stresses alone by 50% increased the stud MOR value by 48.4%.
5. Poisson's ratio, shear modulus and ring angle, taken singly, are not important properties affecting the accuracy of the deflection-load curve of the stud.

The recommendations of the study are:

1. Studies on the elasticity properties of knots should be done.
2. The probability distributions of wood properties should be defined.
3. Further studies should be conducted on the application of the

- developed model and procedure on the determination of allowable design properties of different lumber grades and species.
4. A study should be conducted to determine the effects of combinations involving any of MOE, MOR, grain and ring angles, Poisson's ratio and shear modulus on the theoretical deflection-load curve.

## BIBLIOGRAPHY

1. Amana, E. J. and L. G. Booth. Theoretical and experimental studies on nailed and glued plywood stress-skin components: Part I. Theoretical study. London. Journal of the Institute of Wood Science 4(1):43-69. 1967.
2. \_\_\_\_\_\_. Theoretical and experimental studies on nailed and glued plywood stress-skin components: Part II. London. Journal of the Institute of Wood Science 4(20): 19. 1968.
3. American Society for Testing and Materials. Annual book of ASTM standards, part 22. Philadelphia, Pa. 1975.
4. Bodig, J. and J. R. Goodman. Prediction of elastic parameters for wood. Wood Science, Vol. 5, No. 4. April, 1973.
5. Brodeau, A. Theoretical study of the flexure of prismatic wooden beams when the wood fiber is not parallel to the beam axis. Centre Technique du Bois, Paris. 1966.
6. Brown, H. P., Panshin, A. J., and C. C. Forsaith. Textbook of wood technology, Vol. II. The physical, mechanical and chemical properties of the commercial woods of the United States. McGraw-Hill, New York. 783 p. 1952.
7. Byars, E. E. and R. D. Snyder. Engineering mechanics of deformable bodies. Third Edition. Intext Educational Publishers, New York. 1975.
8. Cook, R. D. Concepts and applications of finite element analysis. John Wiley and Sons, Inc. New York. 1974.
9. \_\_\_\_\_. Improved two-dimensional finite element. Journal of the Structural Division, American Society of Civil Engineers. September, 1974.
10. Cook, R. D. and J. K. Al-Abdulla. Some plane quadrilateral 'hybrid' finite elements. American Institute of Aeronautics Journal, Vol. 7, no. 11, Nov., 1969, pp. 2184-2185.
11. Desai, C. S. and J. F. Abel. Introduction to the finite element method. Van Nostrand Reinhold Co., New York. 1972.

12. Ethington, R. L. and H. C. Hilbrand. Anisotropy in wood. American Society for Testing and Materials, Spec. Publ. No. 405, p. 21-38. 1965.
13. Felippa, C. A. Refined finite element analysis of linear and nonlinear two-dimensional structures. Ph. D. Dissertation, Department of Civil Engineering, University of California, Berkeley, 1966.
14. Fernandez, V. A. A method for approximating distributions of mechanical properties for structural lumber. M. S. thesis. Dept. of Forest Products, Oregon State University, Corvallis, June, 1975.
15. Fishman, G. S. Concepts and methods in discrete event digital simulation. John Wiley and Sons. New York. 1973.
16. Fung, Y. C. Foundations of solid mechanics. Prentice Hall, Engelwood Cliffs, N.J. 1965.
17. Gallagher, R. H. Analysis of plate and shell structures. Proceedings of the symposium on application of finite element methods in Civil Engineering. School of Engineering, Vanderbilt University, ASCE, 1969.
18. Girijavallabhan, C. V. and K. C. Mehta. Stress-strain relationship from compression tests on nonlinear materials. Proceedings of the symposium on application of finite element methods in Civil Engineering. School of Engineering, Vanderbilt University, ASCE, 1969.
19. Goodman, J. R. and J. Bodig. Orthotropic elastic properties of wood. Proceedings of National Structural Engineering Meeting, ASCE, Portland, Oregon. Journal of the Structural Division, Nov., 1970.
20. Harris, H. G. and A. B. Pifko. Elastic-plastic buckling of stiffened rectangular plates. Proceedings of the symposium on application of finite element methods in Civil Engineering. School of Engineering, Vanderbilt University, ASCE, 1969.
21. Hearmon, R. F. S. The elasticity of wood and plywood. Forest Products Research, Department of Scientific and Industrial Research, London. Special Report No. 7, 1948.

22. Hearmon, R. F. S. The theory of elasticity of orthotropic materials. Proceedings of the Conference on the Mechanical Behavior of Wood. University Extension, University of California, pp. 84-95, 1962.
23. \_\_\_\_\_ . An introduction to applied anisotropic elasticity. Oxford University Press. 1961.
24. Herceg, E. E. Handbook of measurement and control. Schaevitz Engineering, Pennsauken, N.J. 1972.
25. Hyle, R. J., Jr. Wood technology in the design of structures. Mountain Press Publishing Company. Missoula, Montana. Oct., 1973.
26. International Conference of Building Officials. Uniform building code. Whittier, California. 1973.
27. Jayne, B. A. and S. K. Suddarth. Mechanics of fibrous orthotropic materials. Paper presented at the Fifth Pacific Area National Meeting of the American Society for Testing and Materials, Seattle, Wash., 1965.
28. Johnson, J. W. Random products method to set stresses for lumber. Report No. T-20. Oregon Forest Research Center. Feb., 1961.
29. \_\_\_\_\_ . Relationships among moduli of elasticity and rupture: seasoned and unseasoned coast-type Douglas-fir and seasoned western hemlock. Proceedings of the second symposium on Nondestructive Testing of Wood. Spokane, Wash., April, 1965.
30. Kollmann, F. The influence of temperature on some mechanical properties of wood. C.S.I.R.O., Transl. No. 2017, Melbourne, Australia. 1953.
31. Kollman, F. and W. A. Cote, Jr. Principles of wood science and technology. Vol. I. Solid wood. Springer-Verlag, New York. 592 p. 1968.
32. Liska, J. A. Research progress on the relationships between density and strength. Proc. Symp. Density, U.S. Forest Prod. Lab., Madison, Wis., p. 89-97. 1965.

33. McNeice, G. M. An elastic-plastic finite element analysis for plates with edge beams. Proceedings of the symposium on application of finite element methods in Civil Engineering. School of Engineering, Vanderbilt University, ASCE, 1969.
34. National Forest Products Association. National design specification for stressed-graded lumber and its fastenings. Washington, D.C., 1973.
35. Palka, L. C. Predicting the effect of specific gravity, moisture content, temperature and strain rate on the elastic properties of softwoods. Wood Science and Technology, Vol. 7, p. 127-141. 1973.
36. Pearson, C. E. Theoretical elasticity. Harvard University Press. Cambridge, Massachusetts. 1959.
37. Polensek, A. Finite element analysis of wood-stud walls. J. of the Structural Division (American Society of Civil Engineers) 102 (ST 7):1317-1335. 1976.
38. \_\_\_\_\_ . Rational design procedure for wood-stud walls under bending and compression loads. Wood Science 9(1):8-20. 1976.
39. \_\_\_\_\_ . Static and dynamic analysis of wood-joist floors by the finite element method. Ph. D. thesis. Dept. of Civil Engineering, Oregon State University, Corvallis. June, 1972.
40. Polensek, A. and G. H. Atherton. Compression-bending strength and stiffness of walls with Utility grade studs. Forest Products Journal, Vol. 26, No. 11, November, 1976.
41. Pritsker, A. A. B. The GASP IV simulation language. Wiley-Interscience, New York. 1974.
42. Radcliffe, B. M. A theoretical evaluation of Hankinson's formula for modulus of elasticity of wood at an angle to the grain. Quart. Bull. Mich. Agr. Exp. Sta. 48(2):286-295. 1965.
43. Rogers, G. L. Mechanics of solids. J. Wiley and Sons, Inc. New York. 1964.

44. Schniewind, A. P. Transverse anisotropy of wood. Forest Products Journal, Vol. 9, No. 10, 1959.
45. \_\_\_\_\_ . The mechanical behavior of wood. Proceedings of a conference held at the University of California, Berkeley, Aug. 27-Sept. 1, University Extension, University of California, 1962.
46. Schroeder, G. A. and G. H. Atherton. Mechanical properties of utility grade redwood two-by-four studs. Dept. of Forest Products, Oregon State University, Corvallis, May, 1973.
47. Seely, F. B. and J. O. Smith. Advanced mechanics of materials. Second Edition. J. Wiley and Sons, Inc., New York. 1952.
48. Siimes, F. E. Effect of specific gravity, moisture content, temperature and heating time on the tension and compression strength and elasticity properties perpendicular to the grain of Finnish pine, spruce and birch wood and the significance of these factors on the checking of timber at kiln drying. Finnish State Inst. Tech. Res., Publ. No. 84, Helsinki. 86 p. 1967.
49. Sliker, A. Young's modulus parallel to the grain in wood as a function of strain rate, stress level and mode of loading. Wood and Fiber, Vol. 4, no. 4, 1973.
50. Snodgrass, J. D. Statistical approach to working stresses for lumber. Journal of the Structural Division. Proceedings of the American Society of Civil Engineers. Feb, 1959.
51. Sokolnikoff, I. S. Mathematical theory of elasticity. Second Edition. McGraw-Hill Book Company, Inc., New York. 1956.
52. Sulzberger, P. H. The effect of temperature on the strength of wood, plywood and glued joints. Aeron. Res. Cons. Comm., Australia, Rep. ACA-46. 44 p. 1953.
53. Timoshenko, S. and J. M. Lessells. Applied elasticity. First Edition. Westinghouse Technical Night School Press, East Pittsburgh, Pa., 1925.
54. U. S. Forest Products Laboratory. Wood handbook: wood as an engineering material. Washington, D. C., U. S. Department of Agriculture. 1974.

55. Walker, J. Interpretation and measurement of strains in wood. Ph. D. thesis, Purdue Univ., Lafayette, Ind., 150 p. 1961.
56. West Coast Lumber Inspection Bureau. Standard grading rules for west coast lumber. 1975.
57. Whang, B. Elasto-plastic orthotropic plates and shells. Proceedings of the symposium on application of finite element methods in Civil Engineering. School of Engineering. Vanderbilt University, ASCE. 1969.
58. White, R. H. Finite element analysis of end fixity in stud wall panels. M.S. thesis, Oregon State University. 1975.
59. Wilson, E. L. Finite element analysis of two-dimensional structures. Ph.D. Dissertation, University of California, Berkeley, 1963.
60. Wood, L. W. The factor of safety in design of timber structures. Proceedings of the American Society of Civil Engineers, Paper No. 1838. Journal of the Structural Division, Vol. 84, No. ST7. Nov., 1958.
61. Ylinen, A. Comparative investigation on the influence of loading and deformation rate on the ultimate strength of wood. U.S. Forest Prod. Lab., Transl. FPL-562, Madison, Wis., 11 p. 1962.
62. Zienkiewicz, O. C. The finite element method in engineering science. London, McGraw-Hill, 1971.

## **APPENDICES**

## APPENDIX A: COMPUTER PROGRAM

A computer program written in Fortran IV language was prepared for the model and procedure described in Sections II and V. It is based on the programs reported by Zienkiewicz (62) and White (58). The program is listed at the end of this appendix. Subroutines were added to

1. Check element stresses and change, if necessary, elasticity properties of the elements,
2. Generate material properties of a hypothetical stud, and
3. Determine the finite element mesh used in the analysis.

One subroutine was modified to account for changes in elasticity properties due to grain and ring angles.

The computer program was adapted for the Oregon State University Control Data Corporation Cyber 73 computer system which has enough storage for 170 elements, 190 nodes, 10 nodal boundary conditions and 170 different materials. The maximum half-band width of the stiffness matrix is 20. It takes about 85 seconds of computer time to analyze the problem given in Appendix C and 280 seconds for the problem in Appendix G.

The program consists of the main program and 11 subroutines. More information about the program and

**PLEASE NOTE:**

Computer print-out on pages  
89-142 is small and indistinct.  
Best available copy. Filmed  
as received.

**UNIVERSITY MICROFILMS.**

subroutines is shown in the numerous commentaries of the program. The program is listed as follows:

```

PROGRAM FERN(INPUT=180,OUTPUT,TAPES=INPUT
2,TAPE15,TAPE21=OUTPUT)

C
C      PLANE STRESS FINITE ELEMENT PROGRAM
C      PART OF THE PROGRAM WAS TAKEN FROM THE FINITE ELEMENT
C      METHOD IN ENGINEERING SCIENCE(971) BY ZIENKIEWICZ, AND
C      R. WHITE'S M.S. THESIS. IT WAS MODIFIED AND EXPANDED
C      TO HANDLE STUD TESTS
C
COMMON/DATA/TITLE(8),NP,NE,NB,NDF,NMAT,NSZF,NLD,IP
1,CD,PINC,NMP,DMAX,NLNP,IV,I6,JSIM,NSIM
2,ISTD,IENDD,JSTS,JENDS,EAV,ESD,AMOR,SDMOR
3,AST2,ASPL,E:2,E13,RING,ADEF,ISEED
COMMON CORD(190,2),NCP(170,4),IMAT(170),ORT(170,7)
1,NBC(10),NFIIX(10),R1(380),SK(380,20),NODES(170)
2,KPC(170),LD(170),IK(170),EST(170,36),BOATA(170,24)
3,R(3),ESTIFM(12,12),A(8,6),B(3,8),RS(8),SMAX(170)
4,NQ(10),LB(170),RR(10,2),SMIN(170),ANG(170)
5,ERAT(12,2),SPL(12),STR2(12),XMOR(12),NI(170)
6,ST(170),IX(170),ORTHO(12,14),GR(170),STGRN(170)
7,FORC(170,3),DISP(2,190),RAND(5),COORD(190,2)
8,NOPP(170,4),ASMAX(170)
C
C      READ INPUT GEOMETRY AND PROP.
C
READ(5,*)NSIM,JSIM,IP,ISEED
DO 300 JN=1,NSIM
CALL QDATA(JN)
NSZF=NP*NDF
C
C      NSIM=NO. OF SPECIMENS TO BE THEORETICALLY TESTED
C      JSIM=1 IF SPECS. ARE TO BE THEORETICALLY OBTAINED
C      IP=4 IF RANGE OF KNOT DIA. (RKD)=0. TO 2.5 IN.
C      =1 IF RKD = 1.0 TO 2.5 IN.
C      =2 IF RKD= 1.5 TO 2.5 IN.
C      =3 IF RKD= 2.0 TO 2.5 IN.
C      =5 IF RKD= 0. TO 1.5 IN.
C      =6 IF RKD= 0. TO 1.0 IN.
C      =7 IF RKD= 1.0 TO 2.0 IN.
C      =8 IF RKD= 0. TO 2.0 IN.
C      IF ISEED=1, THE STARTING SEED IS RANDOM NO.
C      GENERATION IS THE SAME.
C      NSZF=NUMBER OF EQUATIONS IN THE SYSTEM
C      NLD=NUMBER OF LOAD CASES
C
DO 200 LI=1,NLD
C
C      READ LOAD
C
CALL LOAD(LI)
C
C      FORM, THEN SOLVE SIMULTANEOUS EQUATIONS
C
CALL FORMK(LI)
CALL SOLVE
C
C      CALCULATE FORCES AND STRESSES
C
CALL STRESS(LI,JN)
IF(ADEF.GT.CD)GO TO 300
CALL CHECK(LI)
200 CONTINUE
300 CONTINUE

```

```

STOP
END

C
SUBROUTINE GDATA(JN)
COMMON/DATA/TITLE(8),NP,NE,NB,NDF,NMAT,NSZF,NLD,IP
1,CD,PINC,NMP,DMAX,NLNP,IV,16,JSIM,NSIM
2,ISTD,IENDD,JSTS,JENDS,EAV,ESD,AMOR,SDMOR
3,AST2,ASPL,E12,E13,RING,ADEF,ISEED
COMMON CORD(190,2),NOP(170,4),IMAT(170),ORT(171,7)
1,NBC(10),NFIIX(10),RI(380),SK(380,28),NODES(170)
2,KP(170),LD(170),IK(170),EST(170,36),BODATA(170,24)
3,R(3),ESTIFMC(12,12),A(8,6),B(3,8),RS(8),SMAX(170)
4,NQ(10),LB(170),RR(10,2),SMIN(170),ANG(170)
5,ERAT(12,2),SPL(12),STR2(12),XMOR(12),NI(170)
6,ST(170),IX(170),OR1HD(12,14),GR(170),STGRN(170)
7,FORC(170,3),DISP(2,190),RAND(5),COORD(190,2)
8,NOPP(170,4),ASMAX(170)
REWIND 15

C
C READ TITLE AND CONTROL
C
IF(JN.GT.1)GO TO 221
READ(5,7)TITLE
7 FORMAT(8A6)
IF(JSIM.NE.1)GO TO 504
READ(5,*)EAV,ESD,AMOR,SDMOR,AST2,ASPL,E12,E13
504 READ(5,*)NP,NE,NB,NDF,NMAT,II,NMP,DMAX
2,PINC,NLNP,NLD,ISTD,IENDD,JSTS,JENDS
NPP=NP
NEE=NE
IF(JSIM.NE.1)GO TO 280
221 CALL SIMI
280 DO 200 I=1,NE
LR(I)=LD(I)=IK(I)=IX(I)=0
SMAX(I)=SMIN(I)=STGRN(I)=ST(I)=0.
DO 200 J=1,3
FORC(I,J)=0.
200 CONTINUE
DO 201 I=1,NP
DO 201 J=1,NDF
DISP(J,I)=0.
201 CONTINUE

C
C NP=NUMBER OF NODAL POINTS
C
C NE=NO. OF ELEMENTS
C
C NB=NUMBER OF RESTRAINED BOUNDARY NODES
C
C NDF=NO. OF DEGREES OF FREEDOM PER NODE
C
C NMAT=NUMBER OF ELEMENT MATERIAL TYPES

```

```

C   II=0 IF INPUT DATA ARE TO BE PRINTED
C   PINC=LOAD INCREMENT (NEGATIVE DOWNWARD)
C   DMAX=DEFLECTION AFTER THE FIRST LOAD BEYOND WHICH
C         PROGRAM STOPS (NEGATIVE DOWNWARD).
C   NMP=NODE AT POINT WHERE DMAX IS DETERMINED
C   NLNP=NO. OF LOADED NODAL POINTS
C   ISTD=NODE NO. IN WHICH PRINTING OF DISPLACEMENTS STARTS
C   IENDD=NODE NO. IN WHICH PRINTING OF DISPLACEMENTS ENDS
C   JSTS=ELEMENT NO. IN WHICH PRINTING OF STRESSES STARTS
C   JENDS=ELEMENT NO. IN WHICH PRINTING OF STRESSES ENDS
C   EAV=AVE. CLEAR WOOD MOE OF SPECIES
C   ESD=STANDARD DEVIATION(SD) OF MOE
C   AMOR=Ave. MODULUS OF RUPTURE(MOR)
C   SDMOR=SD OF MOR
C   ASPL=Ave. STRESS AT PROPORTIONAL LIMIT
C   AST2=Ave. STRESS AT POINTS BET. MOR AND SPL(DEPENDS -
C         ON WHERE SECANT E CHANGES)
C   E12=RATIO OF AVE. E2 TO EAV
C   E13=RATIO OF AVE. E3 TO EAV
C
C   READ MATERIAL PROPERTIES
C
IF(JSIM.NE.1)GO TO 808
IENDD=NP
JENDS=NE
WRITE(21,807)JN
807 FORMAT(//1X,"SIMULATION SPECIMEN NO.",14)
808 IF(II.NE.0)GO TO 28
WRITE(21,100)TITLE
100 FORMAT(//1X,BA6//)
IF(JSIM.EQ.1)GO TO 150
28 DO 30 J=1,NMAT
30 READ(5,*)N,(ORTHO(N,1),I=1,14)
GO TO 153

C
C GENERATE MATERIAL PROPERTIES
C
150 IF(ISEED.NE.1)GO TO 902
00 152 I=1,2
152 RAND(I)=RANF(A)
GO TO 904
902 XT=RANSET(TIME(A))
RAND(1)=RANF(B)
XTI=RANGE1(XT)
RAND(2)=RANF(C)
904 ORTHO(1,1)=FAV+SORT(-2.*ESD**2* ALOG(RAND(1)))*
PCOS(2.*3.1416*RAND(2))
N2=NE+
ORTHO(1,2)=ORTHO(1,1)+0.068

```

```

ORTHO(1,3)=ORTHO(2,3)=ORT(N2,3)=0.292
ORTHO(1,4)=ORTHO(2,4)=ORT(N2,4)=0.020
ORTHO(1,5)=ORTHO(1,1)*0.064
ORTHO(1,6)=ORTHO(1,1)*0.050
ORTHO(1,7)=ORTHO(1,1)*0.078
ORTHO(1,8)=ORTHO(1,1)*0.007
ORTHO(1,9)=ORTHO(2,9)=0.449
ORTHO(1,10)=ORTHO(2,10)=0.022
ORTHO(1,11)=ORTHO(2,11)=0.390
ORTHO(1,12)=ORTHO(2,12)=0.287
ORTHO(1,13)=ORTHO(1,1)*E12
ORTHO(1,14)=ORTHO(1,1)*E13
ORT(N2,1)=ORTHO(2,1)=1000.
ORT(N2,2)=ORTHO(2,2)=68.
ORT(N2,5)=ORTHO(2,5)=64.
ORTHO(2,6)=50.
ORTHO(2,7)=78.
ORTHO(2,8)=7.
ORTHO(2,13)=700.
ORTHO(2,14)=500.
GO TO 222

C N2=NE+1
C
153 READ(5,*)N2,(ORT(N2,I),I=1,5)
222 DO 61 J=1,NMAT
      ERAT(J,1)=ORTHO(J,13)/ORTHO(J,1)
      61 ERAT(J,2)=ORTHO(J,14)/ORTHO(J,1)
      IF(JSIM.EQ.1)GO TO 223

C READ STRESSES
C
31  DO 31 I=1,NMAT
      READ(5,*)N,SPL(I),STR2(I),XMOR(I)
      GO TO 260
223  IF(ISEED.NE.1)GO TO 906
      DO 224 J=1,2
      RAND(J)=RANF(A)
      GO TO 908
224  XT=RANSET(TIME(A))
      RAND(1)=RANF(B)
      XT=PANGET(XT)
      RAND(2)=RANF(C)
      908  XMOR(1)=AMOR+SQRT(-2.*SDMOR**2* ALOG(RAND(1)))+
      2COS(2.*3.1416*RAND(2))
      STR2(1)=XMOR(1)*AST2/AMOR
      SPL(1)=XMOR(1)*ASPL/AMOR
      XMOR(2)=3000.
      STR2(2)=2000.

C SPL(2)=1000.
C N=MATERIAL NUMBER
C ORTHO(N,1)=MODULUS OF ELASTICITY (MOE) IN L-DIRECTION
C ORTHO(N,2)=MOE IN R-DIRECTION
C ORTHO(N,3)=POISSON RATIO (LR)
C ORTHO(N,4)=POISSON RATIO (RL)
C ORTHO(N,5)=MODULUS OF RIGIDITY (RL)
C ORTHO(N,6)=MOE IN T-DIRECTION
C ORTHO(N,7)=MODULUS OF RIGIDITY (LT)
C ORTHO(N,8)=MODULUS OF RIGIDITY (TR)
C ORTHO(N,9)=POISSON RATIO (LT)
C ORTHO(N,10)=POISSON RATIO (TL)
C ORTHO(N,11)=POISSON RATIO (RT)
C ORTHO(N,12)=POISSON RATIO (TR)
C ORTHO(N,13)=E2
C ORTHO(N,14)=E3
C
C READ NODAL POINT DATA
C N=NODAL POINT(ND)
C COORD(N,1)=ND X-COORDINATE
C COORD(N,2)=ND Y-COORDINATE
C
260  IF(JN.GT.1)GO TO 225
      260  DO 40 J=1,NPP
      40  READ(5,*)N,(COORD(N,M),M=1,2)

C READ ELEMENT DATA
C N=ELEMENT NO.
C NOPP(N,1)=NUMBER OF THE ELEMENT NODE 1
C NOPP(N,2)=NUMBER OF THE ELEMENT NODE J
C NOPP(N,3)=NUMBER OF THE ELEMENT NODE K
C NOPP(N,4)=NUMBER OF THE ELEMENT NODE L
C IMAT(N)=ELEMENT MATERIAL TYPE. (EQUAL TO ELEMENT NO.)
C NODES(N)=NUMBER OF NODES IN ELEMENT N
C NI(N)=NUMBER OF LOCAL MATERIAL PROPERTY OF ELEMENT
C
      IF(JSIM.EQ.1)GO TO 52
      DO 50 J=1,NEE
      50  READ(5,*)N,(NOPP(N,M),M=1,4),NODES(N),IMAT(N),NI(N)
          GO TO 51
      51  DO 53 J=1,NEE
      53  READ(5,*)N,(NOPP(N,M),M=1,4)
      51  IF(JSIM.EQ.1)GO TO 225
          DO 227 K=1,NP
          DO 227 L=1,2
          227  COORD(K,L)=COORD(K,L)
          DO 270 N=1,NE
          DO 270 M=1,4

```

```

270 NOP(N,M)=NOPP(N,M)
GO TO 251
225 DO 824 I=1,NE
NI(I)=I
824 IMAT(I)=I
CALL SIM2
CALL SIM4
251 DO 252 J=1,NE
NF=NI(J)
ORT(J,6)=ORTHO(NF,13)
ORT(J,7)=ORTHO(NF,14)
252 CONTINUE
IF(II.NE.0)GO TO 41
WRITE(21,311)
311 FORMAT(//1X,"ELEMENT",5X,"GRAIN ANGLE",5X,
2"RING ANGLE"//)
41 DO 33 J=1,NE
C
C IF NSGR IS NOT EQUAL TO ZERO, IT IS THE NO.
C OF ELEMENT WITH SAME ANGLES AND MECH. PROP.
C AS THE CURRENT ELEMENT
C
45 IF(JSIM.EQ.1)GO TO 49
READ(5,*)N,NSGR
IF(NSGR.NE.0)GO TO 45
READ(5,*)GR(J),RING
45 IF(II.NE.0)GO TO 29
IF(NSGR.NE.0)GO TO 46
WRITE(21,312)N,GR(J),RING
GO TO 29
46 WRITE(21,313)N,NSGR
313 FORMAT(3X,13,1X,16)
312 FORMAT(3X,13,10X,F5.2,11X,F5.2)
29 IF(NSGR.EQ.0)GO TO 42
GR(J)=GR(NSGR)
ORT(J,1)=ORT(NSGR,1)
ORT(J,2)=ORT(NSGR,2)
ORT(J,3)=ORT(NSGR,3)
ORT(J,4)=ORT(NSGR,4)
ORT(J,5)=ORT(NSGR,5)
GO TO 33
C
C N=ELEMENT NO.
C GR=GRAIN ANGLE
C RING = RING ANGLE
C

```

```

S55=4.*CG*CR*SG+((1.+2.*ULR)/EL+1./ER)+SR*(SG/GTR+
2CG/GLT)*(CR/GRL)*(CG-SG)**2
ORT(J,1)=100000./S11
ORT(J,2)=100000./S33
ORT(J,3)=(-1)*ORT(J,1)*S13/100000.
ORT(J,4)=(-1)*ORT(J,2)*S13/100000.
ORT(J,5)=100000./S55
33 CONTINUE
C READ BOUNDARY CONDITIONS
C NBC=RESTRAINED BOUNDARY NODE NO.
C NFIX(I)=BOUNDARY CONDITION TYPE
C NFIX = 01 - FIXED IN Y-DIRECTION
C NFIX = 10 - FIXED IN X-DIRECTION
C NFIX = 11 - FIXED IN BOTH X AND Y DIRECTIONS
C
IF(JSIM.NE.1)GO TO 99
NFIIX(1)=11
NFIIX(2)=1
R(1)=0.0
R(2)=PINC
IF(16.GT.1)GO TO 91
NQ(1)=84
NQ(2)=144
NBC(1)=8
97 NBC(2)=184
GO TO 90
91 NBC(1)=3
IF(16.GT.11)GO TO 92
NQ(1)=89
NQ(2)=149
98 NBC(2)=189
GO TO 90
92 IF(16.GT.12)GO TO 93
NQ(1)=79
NQ(2)=147
96 NBC(2)=187
GO TO 90
93 IF(16.GT.13)GO TO 85
NQ(1)=42
NQ(2)=145
87 NBC(2)=185
GO TO 90
85 NQ(1)=37
IF(16.GT.23)GO TO 86
NQ(2)=145
GO TO 87
86 IF(16.GT.24)GO TO 94
NQ(2)=137
GO TO 87
94 IF(16.GT.25)GO TO 95
NQ(2)=102
GO TO 96
95 NQ(2)=97
IF(16.GT.35)GO TO 97
GO TO 98
99 READ(S,*)NBC(I),NFIIX(I),I=1,NB)
DO 209 I=1,NLNP
209 READ(S,*)NQ(I),(R(K),K=1,NDF)
90 WRITE(15)(NBC(I),NFIIX(I),I=1,NB),
IF(I1.NE.0)GO TO 500
C PRINT INPUT DATA
C
WRITE(21,108)
WRITE(21,8)(N,(ORT(N,I),I=1,5),N=1,NE)
WRITE(21,60)
80 FORMAT(//1X,"ELEMENT",3X,"SPL",5X,"STR2",4X,"MOR",
26X,"E2",8X,"E3"//)
DO 81 I=1,NE
N=NIC(I)
E1 WRITE(21,82)I,SPL(N),STR2(N),XMOR(N),ORT(I,6),
2ORT(I,7)
82 FORMAT(3X,13.2X,3(2X,F6.0),2(2X,FB.0))
WRITE(21,102)
WRITE(21,2)(N,(CORD(N,M),M=1,2),N=1,NP)
WRITE(21,103)
WRITE(21,3)(N,(NDP(N,M),M=1,4),NODES(N),IMAT(N),NI(N),
2N=1,NE)
WRITE(21,104)
WRITE(21,6)(NBC(I),NFIIX(I),I=1,NB)
500 CONTINUE
WRITE(21,100)TITLE
WRITE(21,109)
WRITE(21,110)
DO 208 I=1,NLNP
208 WRITE(21,9)NQ(I),(R(K),K=1,NDF)
9 FORMAT(15,2F10.2)
109 FORMAT(2X,"LOADS")
110 FORMAT(2X,"NODE",7X,"X",7X,"Y")
2 FORMAT(15,2F10.5)
3 FORMAT(B15)
6 FORMAT(15,18)
8 FORMAT(15,2F13.2,2F9.5,F13.2)
102 FORMAT(//," NODAL POINTS COORDINATES"//)
103 FORMAT(//," ELEMENTS"//)
104 FORMAT(//," BOUNDARY CONDITIONS"//)
108 FORMAT(//," MATERIAL PROPERTIES"//)
RETURN

```

```

C      END
C
C      SUBROUTINE SIM1
C
C      GENERATES VALUES FOR NP, NE AND NMP
C
COMMON/DATA/TITLE(8),NP,NE,NB,NDF,NMAT,NSZF,NLD,IP
1,C0,PINC,NMP,DMAX,NLNP,IV,I6,JSIM,NSIM
2,ISTD,IENDO,JSTS,JENDS,EAV,ESD,AMOR,SOMOR
3,AST2,ASPL,E12,E13,RING,ADEF,ISEED
COMMON CORD(190,2),NODP(170,4),IMAT(170),ORT(171,7)
1,NBC(10),NFX(10),R1(380),SK(380,20),NODES(170)
2,KP(170),LC(170),IK(170),EST(170,36),BODATA(170,24)
3,R(3),ESTIFM(12,12),A(8,6),B(3,8),RS(8),SMAK(170)
4,NQ(10),LB(170),RR(10,2),SMIN(170),ANG(170)
5,ERAT(12,2),SPL(12),STR2(12),XMOR(12),NI(170)
6,ST(170),X(170),ORTHO(12,14),GR(170),SIGRN(170)
7,FORC(170,3),DISP(2,190),RAND(5),COORD(190,2)
8,NOPPC(170,4),ASMAX(170)
IF(ISEED.NE.1)GO TO 201
VX=RANF(A)
GO TO 200
201 XT=RANSET(TIME(A))
VX=RANF(B)
XTI=RANGE(XT)
200 IV=VX*10000
156 IF(IV.LT.1261)GO TO 155
IV=IV-1260
GO TO 156
155 I6=(IV+34)/35
IF(16.GT.1)GO TO 157
NP=184
NE=152
NMP=114
GO TO 151
157 IF(16.GT.11)GO TO 167
NP=189
NMP=119
IF(16.GT.10)GO TO 158
NE=167
GO TO 151
158 NE=165
GO TO 151
167 IF(16.GT.12)GO TO 168
NP=187
NE=163
NMP=117
GO TO 151
168 IF(16.GT.13)GO TO 169
NP=185
NE=161
NMP=115
GO TO 151
169 IF(16.GT.19)GO TO 173
NP=185
NE=165
IF(16.GT.16)GO TO 170
NMP=115
GO TO 151
170 IF(16.GT.17)GO TO 174
NMP=115
GO TO 151
174 IF(16.GT.18)GO TO 175
NMP=107
GO TO 151
175 NMP=72
GO TO 151
173 NMP=67
IF(16.GT.24)GO TO 180
NP=185
IF(16.GT.23)GO TO 176
NE=165
GO TO 151
176 NE=161
GO TO 151
180 IF(16.GT.25)GO TO 181
NP=187
NE=163
GO TO 151
181 IF(16.GT.35)GO TO 183
NP=189
IF(16.GT.26)GO TO 182
NE=165
GO TO 151
182 NE=167
GO TO 151
183 NP=184
NE=152
151 RETURN
END

C      SUBROUTINE SIM2
C
C      GENERATES NODAL COORDINATES AND ELEMENT NODE NDS.
C
COMMON/DATA/TITLE(8),NP,NE,NB,NDF,NMAT,NSZF,NLD,IP
1,C0,PINC,NMP,DMAX,NLNP,IV,I6,JSIM,NSIM

```

```

2,ISTD,JEND0,JSTS,JENDS,EAV,ESD,AMOR,SDMOR
3,AST2,ASPL,E12,E13,RING,ADEF,ISEED
COMMON CORD(190,2),NOPC(170,4),IMAT(170),DRT(171,7)
1,NRC(10),NFIIX(10),RI(380),SK(380,23),NODES(170)
2,KPC(170),LD(170),IK(170),EST(170,36),BDATA(170,24)
3,R(3),ESTIFM(12,12),A(8,6),B(3,8),RS(8),SMAX(170)
4,NQ(10),LB(170),RR(10,2),SMIN(170),ANG(170)
5,ERAT(12,2),SPL(12),STR2(12),XMOR(12),NI(170)
6,ST(170),IX(170),ORTHO(12,14),GR(170),STGRNC(170)
7,FORC(170,3),DISP(2,190),RAND(5),COORD(190,2)
8,NOPPC(170,4),ASMAX(170)
DIMENSION COOR(5)
COOR(1)=3.5
COOR(2)=2.5
COOR(3)=1.75
COOR(4)=1.
COOR(5)=0.
IF(16.GT.1)GO TO 228
B1=-0.5
M9=M7=0
IM=6
GO TO 291
228 IF(16.GT.10)GO TO 235
IM=6
M7=3+3*(16-2)
239 DO 245 I=1,M7
CORD(I,1)=COORD(I,1)
245 CORD(I,2)=COORD(I,2)
DO 250 I=1,5
M8=M7+I
CORD(M8,1)=CORD(M7,I)+1.25
250 CORD(M8,2)=COORD(I)
M9=M7+5
B1=CORD(M8,1)+0.75
251 DO 251 I=1,6
B1=B1+0.5
B2=4.
DO 251 J=1,8
B3=B2-0.5
M9=M9+I
CORD(M9,1)=B1
251 CORD(M9,2)=B2
IF(16.EQ.36)GO TO 290
DO 252 I=1,5
N1=M9+I
CORD(N1,1)=CORD(M9,1)+1.25
252 CORD(N1,2)=COORD(I)
N2=137-M7-IM
DO 260 I=1,N2

```

```

N3=N1+I
N4=M7+IM+1
CORD(N3,1)=COORD(N4,1)
260 CORD(N3,2)=COORD(N4,2)
GO TO 290
235 IF(16.GT.13)GO TO 261
M7=30+3*(16-11)
IM=6+2*(16-11)
GO TO 239
261 IF(16.GT.23)GO TO 265
IM=10
M7=41+5*(16-14)
GO TO 239
265 IF(16.GT.26)GO TO 275
M7=91+5*(16-24)
IM=10-2*(16-24)
GO TO 239
275 IM=6
M7=104+3*(16-27)
GO TO 239
290 IX=0
IF(16.GT.1)GO TO 108
JS=0
J2=-8
GO TO 106
108 IF(16.GT.2)GO TO 112
KA=1
IG=J2=M0=MN=0
JS=IH=17
GO TO 124
112 LK=1
LC=LT=0
IF(16.GT.13)GO TO 320
M0=MN=0
LX=2+2*(16-3)
IH=JS=LX+17
IG=J2=3+3*(16-3)
GO TO 322
320 IF(16.GT.26)GO TO 324
M0=1
LX=28+4*(16-14)
IH=JS=LX+19
IG=36+5*(16-14)
J2=IG+2
GO TO 322
324 MN=M0=0
LX=82+2*(16-27)
IH=JS=LX+17
IG=J2=101+3*(16-27)

```

```

J1=J+J2
    NOP(J5,1)=J1+1
    NOP(J5,2)=J1+9
    NOP(J5,3)=J1+8
    NOP(J5,4)=J1
    NODES(J5)=4
    IX=1
    IF(16.E9+36)60 TO 700
    LX=104
    IF(16.GI+1)60 TO 400
    LT=47
    IG=40
    IH=LC=52
    LK=5
    KA=36
    MN=MQ=0
    GO TO 124
400   IF(16.GI+13)60 TO 402
    LT=52
    IF(16.GI+10)60 TO 404
    KA=53+2*(16-2)
    IH=LC=KA+6
    LK=KA-46
    1G=48+3*(16-2)
    GO TO 124
404   MN=1
    KA=71+2*(16-11)
    IH=LC=KA+18
    LK=29+4*(16-11)
    1G=75+3*(16-11)
    GO TO 124
406   IF(16.GI+26)60 TO 406
    MN=1
    KA=83+4*(16-14)
    IH=LC=KA+8
    1G=86+5*(16-14)
    IF(16.GI+23)60 TO 408
    LK=41+4*(16-14)
    GO TO 413
408   MN=MQ=0
    LK=83+2*(16-24)
    413   IF(16.GI+24)60 TO 411
    LT=48
    GO TO 124
    411   IF(16.GI+25)60 TO 412
    LT=50
    DO 104 I=1,5
    J2=J2+8
    DO 104 J=1,7
    J5=J5+
    800   DO 102 I=KA,1H
    NOP(1,4)=0
    NODES(1)=3
    102   DO 104 I=1,5
    J2=J2+8
    DO 104 J=1,7

```

406 KA=135+2\*(16-27)  
 IH=LC=KA+16  
 LI=52  
 LK=83+2\*(16-24)  
 IG=149+3\*(16-27)  
 GU TO 124  
 133 NOP(KA,1)=1+1G  
 NOP(KA,2)=NOP(KB,1)=NOP(KC,1)=2+1G  
 NOP(KA,3)=NOP(KB,3)=NOP(KL,1)=9+1G  
 NOP(KB,2)=NOP(KC,3)=NOP(KD,3)=NOP(KF,3)=NOP(KL,2)  
 2=NOP(KM,1)=NOP(KN,1)=10+1G  
 NOP(KC,2)=NOP(KD,1)=3+1G  
 NOP(KD,2)=NOP(KE,1)=NOP(KF,1)=4+1G  
 NOP(KE,2)=NOP(KF,3)=NOP(KG,3)=NOP(KN,2)=NOP(KO,1)  
 2=11+1G  
 NOP(KF,2)=NOP(KG,1)=NOP(KH,1)=5+1G  
 NOP(KG,2)=NOP(KH,3)=NOP(KI,3)=NOP(KJ,3)=NOP(KO,2)  
 2=NOP(KP,1)=NOP(KQ,1)=12+1G  
 NOP(KH,2)=NOP(KI,1)=6+1G  
 NOP(KI,2)=NOP(KJ,1)=NOP(KK,1)=7+1G  
 NOP(KJ,2)=NOP(KK,3)=NOP(KQ,2)=13+1G  
 NOP(KK,2)=8+1G  
 NOP(KL,3)=NOP(KM,3)=14+1G  
 NOP(KM,2)=NOP(KN,3)=NOP(KO,3)=NOP(KP,3)=15+1G  
 NOP(KP,2)=NOP(KW,3)=16+1G  
 DU 132 I=KA, IH  
 NOP(1,4)=0  
 132 NODES(1)=3  
 GU TO 302  
 348 NOP(KA,1)=1+1G  
 NOP(KA,2)=NOP(KP,1)=NOP(KC,1)=2+1G  
 NOP(KA,3)=NOP(KB,3)=NOP(KL,1)=NOP(KM,1)=9+1G  
 NOP(KB,2)=NOP(KC,3)=NOP(KD,3)=NOP(KF,3)=NOP(KM,2)  
 2=NOP(KN,1)=NOP(KO,1)=10+1G  
 NOP(KC,2)=NOP(KD,1)=3+1G  
 NOP(KD,2)=NOP(KF,1)=NOP(KF,1)=4+1G  
 NOP(KF,2)=NOP(KF,3)=NOP(KG,3)=NOP(KU,2)=NOP(KP,1)  
 2=11+1G  
 NOP(KF,2)=NOP(KG,1)=NOP(KH,1)=5+1G  
 NOP(KG,2)=NOP(KH,3)=NOP(KI,3)=NOP(KJ,3)=NOP(KP,2)  
 2=NOP(KG,1)=NOP(KH,1)=12+1G  
 NOP(KH,2)=NOP(Al,1)=6+1G  
 NOP(KI,2)=NOP(KD,1)=NOP(KK,1)=7+1G  
 NOP(KJ,2)=NOP(KK,3)=NOP(Kn,2)=NOP(KS,1)=13+1G  
 NOP(KK,2)=8+1G  
 NOP(KL,2)=NOP(KM,3)=NOP(KN,3)=15+1G  
 NOP(KL,3)=14+1G  
 NOP(KN,2)=NOP(KW,3)=NOP(KP,3)=16+1G  
 NOP(KW,2)=NOP(KH,3)=NOP(KS,3)=17+1G  
 DO 348 I=KA, IH  
 NOP(1,4)=0  
 348 NODES(1)=3  
 GU TO 302  
 356 NOP(KA,1)=1+1G  
 NOP(KA,2)=NOP(KP,1)=NOP(KC,1)=2+1G  
 NOP(KA,3)=NOP(KB,3)=NOP(KI,1)=NOP(KJ,1)=6+1G  
 NOP(KB,2)=NOP(KC,3)=NOP(KD,3)=NOP(KJ,2)=NOP(KK,1)  
 2=NOP(KL,1)=NOP(KM,1)=7+1G  
 NOP(KC,2)=NOP(KL,1)=NOP(KE,1)=NOP(KF,1)=3+1G  
 NOP(KD,2)=NOP(KI,3)=NOP(KM,2)=NOP(KN,1)=NOP(KP,1)  
 2=8+1G  
 NOP(KE,2)=NOP(KF,3)=NOP(KG,3)=NOP(KU,2)=NOP(KP,1)  
 2=NOP(KO,1)=NOP(KH,1)=9+1G  
 NOP(KF,2)=NOP(KG,1)=NOP(KH,1)=4+1G  
 NOP(KG,2)=NOP(KH,3)=NOP(KN,2)=NOP(KS,1)=10+1G  
 NOP(KH,2)=5+1G  
 NOP(KI,2)=NOP(KJ,3)=NOP(KK,3)=12+1G  
 NOP(KI,3)=11+1G  
 NOP(KK,2)=NOP(KL,3)=13+1G  
 NOP(KL,2)=NOP(KM,3)=NOP(KN,3)=14+1G  
 NOP(KN,2)=NOP(KU,3)=NOP(KF,3)=15+1G  
 NOP(KP,2)=NOP(KQ,3)=16+1G  
 NOP(KQ,2)=NOP(KR,3)=NOP(KS,3)=17+1G  
 NOP(KS,2)=18+1G  
 DU 360 I=KA, IH  
 NOP(1,4)=0  
 360 NODES(1)=3  
 MQ=0  
 GU TO 106  
 382 I/O 150 I=LK, LK  
 LC=LC+1  
 NOP(1,1)=NOOP(1,1)+LI  
 NOP(LC,2)=NOOP(1,2)+LI  
 NOP(LC,3)=NOOP(1,3)+LI  
 1E(NOOP(1,4), F0, 0) GU TO 151  
 NOP(LC,4)=NOOP(1,4)+LI  
 NODES(LC)=4  
 GU TO 150  
 151 NOP(LC,4)=0  
 NODES(LC)=3  
 150 CONTINUE  
 1FCIX+F0, 0 GO TO 124  
 700 RETURN

```

END
C
C SUBROUTINE SIM4
C
C GENERATES KNOT DATA, GRAIN AND RING ANGLES FOR EACH
C ELEMENT AND DETERMINES WHAT MATERIAL PROPERTIES ARE
C TO BE USED BY EACH ELEMENT
C
COMMON/DATA/TITLE(B),NP,NE,NR,NIF,NMAT,NSZF,NLD,IP
1,COD,PINC,NMP,LMAX,NLP,IV,16,JSIM,NSIM
2,ISTD,ENID,JSTS,JENLS,FAU,FSE,AMON,SUMON
3,AST2,ASPL,F12,F13,RING,ADEF,ISEFT
COMMON CUREL(190,2),NUP(170,4),IMAT(170),OHT(171,7)
1,NPC(10),NFX(10),R1(380),SK(380,20),NULS(170)
2,RPC(170),LK(170),IK(170),EST(170,36),PDATA(170,24)
3,R(3),EST1(12,12),A(8,6),B(3,8),RS(8),SMAX(170)
4,NOC(10),LR(170),RH(10,2),SMIN(170),ANG(170)
5,ERH(12,2),SPCL(12),STR(12),XMUR(12),NI(170)
6,ST(170),IX(170),OHIO(12,14),GH(170),STGRN(170)
7,FOHC(170,3),DISP(2,190),RANI(5),CUREL(190,2)
8,NUPP(170,4),ASMAX(170)
100 IF(ISEED.NE.1)GO TO 920
DO 100 I=1,2
100 HAN(1)=RANF(A)
GO TO 921
920 XI=RANF(TIMEA))
HAN(1)=RANF(B)
XII=RANGET(XT)
HAN(2)=RANF(C)
921 DKNT=HAN(1)*10.
931 IF(DKNT.GT.2.75)GO TO 930
GO TO 932
930 DKNT=DKNT-2.75
GO TO 931
932 RING=HAN(1)*100.
IF(RING.GT.90.)GO TO 101
GO TO 102
101 RING=RING-90.
102 GRN=HAN(2)*100.
937 IF(GRN.GT.14.0)GO TO 935
GO TO 936
935 GRN=GRN-14.
GO TO 937
936 DO 110 I=1,NF
110 GR(1)=GRN
IF(DKNT.GT.0.25)GO TO 115
GO TO 3

```

```

115 IF(DKNT.GT.0.75)GO TO 120
IF(IP.LT.4.0K.IP.EQ.7)GO TO 108
JA=IV
130 IF(JA.LT.36)GO TO 125
JA=JA-35
GO TO 130
125 JR=JA
140 IF(JR.LT.8)GO TO 135
JR=JB-7
GO TO 140
135 IF(16.GT.1)GO TO 145
320 NI(IV)=2
IF(JB.GT.1)GO TO 155
160 IF(JB.EQ.7)GO TO 165
GR(IV+1)=GRN+10.
IF(JA.GT.28)GO TO 165
GR(IV+8)=GRN+5.
165 IF(JA.EQ.35)GO TO 220
IF(16.EQ.36)GO TO 185
GR(IV+7)=GRN+15.
IF(JA.EQ.28)GO TO 220
IF(JA.GT.22)GO TO 185
IF(16.EQ.36)GO TO 420
GR(IV+14)=GRN+5.
420 IF(JA.LT.8)GO TO 3
IF(JB.EQ.7)GO TO 220
185 GR(IV-6)=GRN+5.
220 GR(IV-7)=GRN+15.
IF(JA.LT.15)GO TO 3
GR(IV-14)=GRN+5.
IF(JA.EQ.29)GO TO 180
GO TO 3
180 IF(16.EQ.36)GO TO 3
GR(IV+9)=GRN+5.
GO TO 3
155 IF(IV-1)=GRN+10.
IF(JA.EQ.35.OH.16.FU.36)GO TO 255
GR(IV+6)=GRN+5.
IF(JA.LT.8)GO TO 160
255 GR(IV-8)=GRN+5.
IF(JA.LT.22.OH.16.FU.36)GO TO 160
IF(JA.GT.28)GO TO 195
IF(OH.GT.3)GO TO 190
GR(IV+15)=GRN+5.
GO TO 160
190 IF(OH.GT.4)GO TO 200
IF(16.EQ.36)GO TO 160

```

$GR(IV+16)=GRN+5.$   
 GO TO 160  
 200 IF(JB.EQ.7)GO TO 215  
 IF(JB.EQ.36)GO TO 160  
 $GR(IV+17)=GRN+5.$   
 GO TO 160  
 195 IF(JB.GT.3)GO TO 205  
 IF(16.EQ.36)GO TO 160  
 $GR(IV+8)=GRN+10.$   
 GO TO 160  
 205 IF(JB.GT.4)GO TO 210  
 IF(16.EQ.36)GO TO 160  
 $GR(IV+9)=GRN+10.$   
 GO TO 160  
 210 IF(16.EQ.35)GO TO 160  
 $GR(IV+10)=GRN+10.$   
 IF(JA.EQ.35)GO TO 250  
 GO TO 160  
 250  $GR(IV+11)=GRN+15.$   
 GO TO 160  
 215 IF(16.EQ.36)GO TO 160  
 $GR(IV+18)=GRN+5.$   
 GO TO 160  
 145 IF(16.GT.13)GO TO 300  
 $IV=(16-2)*2+JA+17$   
 445 IF(JA.GT.7)GO TO 370  
 IF(JB.EQ.4)GO TO 305  
 $GR(IV-9)=GRN+5.$   
 GO TO 345  
 305  $GR(IV-9)=GRN+15.$   
 345 IF(JB.GT.1)GO TO 310  
 $GR(IV-11)=GRN+15.$   
 $GR(IV-10)=GRN+5.$   
 GO TO 320  
 310 IF(JB.GT.3)GO TO 315  
 $GR(IV-10)=GRN+15.$   
 IF(JB.EQ.3)GO TO 350  
 $GR(IV-12)=GRN+5.$   
 350  $GR(IV-11)=GRN+5.$   
 IF(JB.EQ.2)GO TO 320  
 360  $GR(IV-8)=GRN+5.$   
 GO TO 320  
 315 IF(JB.GT.5)GO TO 325  
 $GR(IV-7)=GR(IV-10)=GRN+5.$   
 IF(JB.EQ.5)GO TO 330  
 $GR(IV-11)=GRN+5.$   
 IF(JB.GT.4)GO TO 330

GO TO 360  
 325 IF(JB.EQ.6)GO TO 335  
 $GR(IV-7)=GR(IV-6)=GRN+5.$   
 330  $GR(IV-8)=GRN+15.$   
 GO TO 320  
 335  $GR(IV-7)=GRN+15.$   
 GO TO 360  
 370 IF(JA.GT.14)GO TO 320  
 IF(JB.GT.1)GO TO 375  
 $GR(IV-18)=GRN+5.$   
 GO TO 320  
 375 IF(JB.GT.3)GO TO 380  
 $GR(IV-17)=GRN+5.$   
 GO TO 320  
 380 IF(JB.EQ.4)GO TO 385  
 $GR(IV-16)=GRN+5.$   
 GO TO 320  
 385 IF(JB.GT.6)GO TO 390  
 $GR(IV-15)=GRN+5.$   
 GO TO 320  
 390  $GR(IV-14)=GRN+5.$   
 GO TO 320  
 300 IF(16.GT.26)GO TO 400  
 $IV=(16-12)*4+JA+47$   
 GO TO 405  
 400  $IV=(16-27)*2+JA+99$   
 GO TO 405  
 120 IF(DKNT.GT.1.25)GO TO 450  
 IF(IP.LT.4)GO TO 108  
 IF(IP.GT.1)GO TO 108  
 IF(16.GT.1)GO TO 455  
 IF(JB.GT.2)GO TO 474  
 IF(JA.GT.9)GO TO 475  
 $IV=JA+1$   
 460  $NI(IV)=NI(IV+1)=NI(IV+7)=NI(IV+8)=2$   
 IF(DKNT.GT.1.25)GO TO 793  
 IF(JA.GT.25)GO TO 3  
 $GR(IV+15)=15.*GRN$   
 IF(JB.EQ.24)GO TO 463  
 $GR(IV+14)=15.*GRN$   
 IF(JA.EQ.20)GO TO 3  
 IF(JA.GT.16)GO TO 463  
 $GR(IV+21)=GR(IV+22)=GRN+15.$   
 IF(JA.EQ.15)GO TO 463  
 $GR(IV+28)=GR(IV+29)=GRN+5.$   
 IF(JA.EQ.6)GO TO 3  
 463  $GR(IV+2)=GR(IV+3)=GRN+10.$

IFC(JA.EQ.26)GO TO 460  
 IFC(JA.EQ.19)GO TO 464  
 IFC(JA.GT.14)GO TO 467  
 464 GR(IV+16)=GR(IV+23)=GHN+5.  
 IFC(JA.GT.4)GO TO 3  
 GR(IV+17)=GR(IV+24)=GHN+5.  
 467 GR(IV+3)=GR(IV+10)=GHN+10.  
 GO TO 3  
 475 IFC(JA.GT.23)GO TO 478  
 IV=JA=15  
 503 GR(IV+14)=GR(IV+13)=GR(IV-7)=GR(IV-6)=GHN+15.  
 IFC(JA.EQ.20..OR..JA.EQ.27)GO TO 476  
 GR(IV-5)=GR(IV-12)=GHN+5.  
 IFC(JA.EQ.22)GO TO 535  
 IFC(JA.EQ.24)GO TO 537  
 GR(IV+16)=GHN+5.  
 IFC(JA.GT.18)GO TO 476  
 535 GR(IV+17)=GHN+5.  
 537 GR(IV-4)=GR(IV-11)=GHN+5.  
 IFC(JA.EQ.22)GO TO 460  
 IFC(JA.EQ.24)GO TO 476  
 GR(IV+23)=GHN+15.  
 IFC(JA.EQ.17)GO TO 476  
 GO TO 460  
 476 IV=JA=22  
 482 GR(IV+16)=GHN+15.  
 GR(IV+18)=GR(IV+19)=GHN+5.  
 IFC(JA.EQ.24)GO TO 549  
 GR(IV-23)=GR(IV-21)=GHN+5.  
 GO TO 533  
 474 IFC(JB.GT.4)GO TO 477  
 IFC(JA.GT.11)GO TO 520  
 IV=JA=3  
 476 GR(IV-1)=GR(IV-2)=GR(IV+5)=GR(IV+6)=GHN+10.  
 IFC(JA.EQ.26)GO TO 487  
 IFC(JA.EQ.27)GO TO 460  
 GR(IV+12)=GR(IV+13)=GHN+5.  
 IFC(JA.EQ.24)GO TO 487  
 IFC(JA.GT.18)GO TO 469  
 487 GR(IV+19)=GR(IV+20)=GHN+5.  
 IFC(JA.EQ.26)GO TO 463  
 GO TO 460  
 520 IFC(JA.GT.25)GO TO 590  
 IV=JA=17  
 597 GR(IV+24)=GHN+15.  
 549 GR(IV-6)=GR(IV-9)=GR(IV-15)=GR(IV-16)=GHN+5.  
 IFC(JA.GT.19)GO TO 533

GR(IV+21)=GR(IV+22)=GR(IV+26)=GHN+5.  
 IFC(JA.EQ.19)GO TO 533  
 GR(IV+25)=GHN+5.  
 GO TO 533  
 598 IV=JA=24  
 607 GR(IV+17)=GHN+15.  
 GR(IV+14)=GHN+5.  
 IFC(JA.GT.25)GO TO 549  
 GO TO 602  
 477 IFC(JB.GT.6)GO TO 480  
 IFC(JA.GT.13)GO TO 525  
 IV=JA=5  
 GO TO 476  
 525 IFC(JA.GT.27)GO TO 595  
 IV=JA=19  
 514 GR(IV+25)=GHN+15.  
 GR(IV+27)=GHN+5.  
 GO TO 547  
 595 IV=JA=26  
 596 GR(IV+18)=GHN+15.  
 GR(IV+15)=GR(IV-20)=GR(IV-21)=GHN+5.  
 GO TO 607  
 480 IFC(JA.GT.14)GO TO 530  
 IV=JA=6  
 GO TO 476  
 530 IFC(JA.GT.28)GO TO 600  
 IV=JA=20  
 578 GR(IV+25)=GR(IV+26)=GHN+15.  
 GO TO 547  
 600 IV=JA=27  
 659 GR(IV+18)=GR(IV+19)=GHN+15.  
 GR(IV+15)=GR(IV+16)=GHN+5.  
 GO TO 607  
 455 IFC(JB.GT.2)GO TO 456  
 IFC(JA.GT.9)GO TO 625  
 JA=1  
 623 IFC(16.GT.13)GO TO 481  
 IV=(16-2)\*2+JA+17  
 GO TO 624  
 481 IFC(16.GT.26)GO TO 710  
 IV=(16-12)\*4+JA+47  
 GO TO 624  
 710 IV=(16-27)\*2+JA+99  
 624 IFC(JB.GT.2)GO TO 629  
 IFC(JA.GT.1)GO TO 649  
 GR(IV-11)=GR(IV-10)=GR(IV-9)=GHN+15.  
 GR(IV-8)=GR(IV-7)=GR(IV-6)=GHN+5.

60 TO 460  
 625 IF(JA=GT-23)GO TO 683  
 JA=15  
 GO TO 623  
 649 IF(JA=GT-15)GO TO 602  
 GR(IV-25)=GR(IV-24)=GR(IV-23)=GRN+5.  
 GO TO 533  
 613 JA=22  
 GO TO 623  
 456 IF(JB=GT-4)GO TO 526  
 IF(JA=GT-11)GO TO 642  
 JA=3  
 GO TO 623  
 629 IF(JB=GT-4)GO TO 591  
 IF(JA=GT-3)GO TO 652  
 GR(IV-10)=GR(IV-9)=GR(IV-8)=GRN+15.  
 GR(IV-13)=GR(IV-12)=GR(IV-11)=GR(IV-8)=GR(IV-7)  
 2=GR(IV-6)=GRN+5.  
 GO TO 476  
 642 IF(JA=GT-25)GO TO 689  
 JA=17  
 GO TO 623  
 652 IF(JA=GT-17)GO TO 607  
 GR(IV-24)=GR(IV-23)=GR(IV-22)=GRN+5.  
 GO TO 547  
 689 JA=24  
 GO TO 623  
 526 IF(JB=GT-6)GO TO 608  
 IF(JA=GT-13)GO TO 645  
 JA=5  
 GO TO 623  
 521 IF(JB=GT-6)GO TO 635  
 IF(JA=GT-5)GO TO 512  
 GR(IV-8)=GR(IV-7)=GRN+15.  
 GR(IV-10)=GR(IV-9)=GR(IV-6)=GR(IV-5)=GRN+5.  
 GO TO 476  
 645 IF(JA=GT-27)GO TO 516  
 JA=19  
 GO TO 623  
 512 IF(JA=GT-19)GO TO 596  
 GR(IV-22)=GR(IV-21)=GRN+5.  
 GO TO 514  
 516 JA=26  
 GO TO 623  
 648 IF(JA=GT-14)GO TO 581  
 JA=6  
 GO TO 623

635 IF(JA=GT-6)GO TO 658  
 GR(IV-8)=GR(IV-7)=GR(IV-6)=GRN+15.  
 GR(IV-9)=GR(IV-8)=GR(IV-7)=GRN+5.  
 GO TO 476  
 581 IF(JA=GT-28)GO TO 583  
 JA=20  
 GO TO 623  
 658 IF(JA=GT-29)GO TO 659  
 GR(IV-22)=GR(IV-21)=GR(IV-20)=GRN+5.  
 GO TO 578  
 583 JA=27  
 GO TO 623  
 450 IF(IP-EQ-6)GO TO 108  
 IF(DRNT-GT-1.75)GO TO 790  
 IF(CIP-EQ-3)GO TO 108  
 IF(16-GT-1)GO TO 792  
 IF(JB=GT-3)GO TO 451  
 IF(JA=GT-17)GO TO 452  
 IV=JA=1  
 GO TO 460

793 NI(IV+2)=NI(IV+9)=NI(IV+15)=NI(IV+14)=NI(IV+16)=2  
 IF(DRNT-GT-1.75)GO TO 750  
 IF(JA-EQ-18)GO TO 796  
 IF(JA-EQ-19)GO TO 3  
 GR(IV+21)=GR(IV+22)=GR(IV+23)=GRN+15.  
 IF(JA-EQ-15)GO TO 796  
 GR(IV+28)=GR(IV+29)=GR(IV+30)=GRN+15.  
 IF(JA-EQ-5)GO TO 3  
 796 GR(IV+3)=GR(IV+10)=GR(IV+17)=GRN+10.  
 IF(JA-EQ-18)GO TO 798  
 IF(JA-EQ-18)GO TO 3  
 GR(IV+24)=GR(IV+31)=GR(IV+37)=GRN+5.  
 IF(JA-EQ-4)GO TO 3  
 798 GR(IV+4)=GR(IV+11)=GR(IV+18)=GRN+10.  
 IF(JA-EQ-15)GO TO 3  
 GR(IV+25)=GR(IV+32)=GR(IV+35)=GR(IV+36)=5.+GRN  
 GO TO 3

462 IV=JA=15  
 724 GR(IV-7)=GR(IV-6)=GR(IV-5)=GR(IV-14)=GR(IV-13)  
 2=GR(IV-12)=GR(IV-24)=GRN+15.  
 IF(JA-EQ-19)GO TO 603  
 GR(IV-4)=GR(IV-11)=GR(IV-28)=GRN+5..  
 IF(JA-EQ-18)GO TO 803  
 GR(IV-3)=GR(IV-10)=GRN+5.  
 GO TO 460

451 IF(JB=GT-6)GO TO 453  
 IF(JA=GT-20)GO TO 694

603  $IV=JA=4$   
 $GR(IV-1)=GR(IV-2)=GR(IV+5)=GR(IV+6)=GR(IV+12)$ ,  
 $2=GR(IV+13)=GRN+15.$   
 IF(JA-EQ.19)GO TO 460  
 $GR(IV+27)=GR(IV+28)=GRN+5.$   
 IF(JA-EQ.18)GO TO 460  
 $GR(IV+26)=GR(IV+19)=GR(IV+39)=GRN+5.$   
 IF(JA-EQ.5)GO TO 460  
 $GR(IV+38)=GRN+5.$   
 GO TO 460  
 604  $IV=JA=18$   
 631  $GR(IV+23)=GRN+15.$   
 632  $GR(IV+25)=GR(IV+26)=GRN+15.$   
 $GR(IV-9)=GR(IV-8)=GR(IV-16)=GR(IV-15)=GR(IV+21)$   
 $2=GR(IV+22)=GRN+5.$   
 GO TO 724  
 453 IF(JA-GT.21)GO TO 461  
 $IV=JA=5$   
 738  $GR(IV+40)=GR(IV+41)=GRN+5.$   
 GO TO 833  
 461  $IV=JA=19$   
 740  $GR(IV+27)=GRN+15.$   
 $GR(IV+20)=GR(IV+23)=GRN+5.$   
 GO TO 832  
 792 IF(JB-GT.3)GO TO 462  
 IF(JA-GT.17)GO TO 846  
 $JA=1$   
 722 IF(16-EQ.13)GO TO 712  
 $IV=(16-2)*2+JA+17$   
 GO TO 714  
 712 IF(16-GT.26)GO TO 716  
 $IV=(16-12)*4+JA+47$   
 GO TO 714  
 716  $IV=(16-27)*2+JA+99$   
 714 IF(JB-GT.3)GO TO 718  
 IF(JA-GT.1)GO TO 720  
 $GR(IV-8)=GR(IV-9)=GR(IV-11)=GR(IV-10)=GRN+15.$   
 $GR(IV-5)=GR(IV-4)=GR(IV-7)=GR(IV-6)=GRN+5.$   
 GO TO 460  
 846  $JA=15$   
 GO TO 722  
 720  $GR(IV-25)=GR(IV-24)=GR(IV-23)=GR(IV-22)=GRN+5.$   
 GO TO 724  
 452 IF(JB-GT.6)GO TO 726  
 IF(JA-GT.20)GO TO 728  
 $JA=4$   
 GO TO 722

718 IF(JB-GT.6)GO TO 730  
 IF(JA-GT.4)GO TO 732  
 $GR(IV-9)=GR(IV-8)=GR(IV-7)=GR(IV-6)=GRN+15.$   
 $GR(IV-5)=GR(IV-4)=GR(IV-12)=GR(IV-11)=GR(IV-10)$   
 $2=GRN+5.$   
 GO TO 803  
 728  $JA=18$   
 GO TO 722  
 732  $GR(IV-23)=GR(IV-22)=GR(IV-21)=GR(IV-20)=GRN+5.$   
 GO TO 831  
 726 IF(JA-GT.21)GO TO 734  
 $JA=5$   
 GO TO 722  
 730 IF(JA-GT.5)GO TO 736  
 $GR(IV-8)=GR(IV-7)=GR(IV-6)=GR(IV-5)=GRN+15.$   
 $GR(IV-12)=GR(IV-11)=GR(IV-10)=GR(IV-9)=GRN+5.$   
 GO TO 738  
 734  $JA=19$   
 GO TO 722  
 736  $GR(IV-22)=GR(IV-21)=GR(IV-20)=GR(IV-19)=GRN+5.$   
 GO TO 740  
 798 IF(IP-EQ.5)GO TO 108  
 IF(DKNT.GT.2.25)GO TO 742  
 IF(16-GT.1)GO TO 744  
 IF(JB-GT.4)GO TO 746  
 IF(JA-GT.25)GO TO 748  
 $IV=JA=1$   
 GO TO 460  
 750  $NI(IV+3)=NI(IV+10)=NI(IV+17)=NI(IV+21)=NI(IV+28)$   
 $2=NI(IV+23)=NI(IV+24)=2$   
 IF(DKNT.GT.2.25)GO TO 860  
 IF(JA-EQ.11)GO TO 764  
 $GR(IV+28)=GR(IV+29)=GRN+15.$   
 $GR(IV+34)=GRN+5.$   
 764  $GR(IV+30)=GR(IV+31)=GRN+15.$   
 $GR(IV+4)=GR(IV+5)=GR(IV+6)=GR(IV+11)=GR(IV+12)$   
 $2=GR(IV+13)=GR(IV+18)=GR(IV+19)=GR(IV+20)=GRN+10.$   
 IF(JA-EQ.4)GO TO 756  
 IF(JA-EQ.8)GO TO 3  
 $GR(IV+25)=GR(IV+26)=GR(IV+27)=GRN+10.$   
 IF(JA-EQ.8)GO TO 3  
 $GR(IV+41)=GR(IV+42)=GR(IV+43)=GR(IV+44)=GR(IV+45)$   
 $2=GRN+5.$   
 $GR(IV+35)=GR(IV+36)=GRN+15.$   
 756  $GR(IV+37)=GR(IV+38)=GR(IV+39)=GR(IV+40)=GRN+15.$   
 $GR(IV+32)=GR(IV+33)=GRN+5.$   
 GO TO 3

748  $IV = JA = 8$   
 754  $GR(IV+35) = GR(IV+36) = GRN+5.$   
 1  $IF(JA+EQ.4) GO TO 460$   
 $GR(IV-3) = GR(IV-2) = GR(IV-1) = GR(IV+37) = GR(IV+38)$   
 $2 = GRN+5.$   
 762  $GR(IV-7) = GR(IV-6) = GR(IV-5) = GR(IV-4) = GR(IV+33)$   
 $2 = GR(IV+33) = GRN+5.$   
 $GO TO 460$   
 746  $IF(JA+GT.28) GO TO 752$   
 $IV = JA = 4$   
 810  $GR(IV+41) = GR(IV+42) = GRN+15.$   
 760  $GR(IV-1) = GR(IV-2) = GR(IV-3) = GRN+10.$   
 $GR(IV+25) = GR(IV+26) = GR(IV+27) = GRN+5.$   
 $IF(JA+EQ.11) GO TO 762$   
 $GO TO 754$   
 $IV = JA = 11$   
 795  $GR(IV+34) = GR(IV+35) = GRN+15.$   
 $GR(IV-8) = GR(IV-9) = GR(IV-10) = GR(IV+28) = GR(IV+29)$   
 $2 = GRN+5.$   
 $GO TO 760$   
 744  $IF(JB+GT.4) GO TO 766$   
 $IF(JB+GT.25) GO TO 768$   
 $JA = 1$   
 780  $IF(16.GT.13) GO TO 770$   
 $IV = (16-2)*2+JA+17$   
 $GO TO 772$   
 778  $IF(16.GT.26) GO TO 774$   
 $IV = (16-12)*4+JA+47$   
 $GO TO 772$   
 774  $IV = (16-27)*2+JA+99$   
 772  $IF(JB+GT.4) GO TO 776$   
 $IF(JA+GT.1) GO TO 778$   
 782  $GR(IV-6) = GR(IV-7) = GRN+15.$   
 $IF(JA+EQ.4) GO TO 788$   
 $IF(JA+EQ.11) GO TO 795$   
 $GR(IV-1) = GR(IV-2) = GR(IV-3) = GRN+5.$   
 $IF(JA+EQ.8) GO TO 754$   
 788  $GR(IV-8) = GR(IV-9) = GRN+15.$   
 $IF(JA+EQ.4) GO TO 810$   
 $GR(IV-11) = GR(IV-12) = GRN+15.$   
 $GR(IV-4) = GR(IV-5) = GRN+5.$   
 $GO TO 460$   
 768  $JA = 8$   
 $GO TO 780$   
 778  $GR(IV-5) = GR(IV-4) = GRN+15.$   
 $IF(JA+EQ.11) GO TO 815$   
 $GR(IV-12) = GR(IV-11) = GR(IV-10) = GRN+5.$

1  $IF(JA+EQ.4) GO TO 782$   
 $GR(IV-18) = GR(IV-17) = GR(IV-16) = GRN+15.$   
 815  $GR(IV-15) = GR(IV-14) = GR(IV-13) = GR(IV-12) = GRN+15.$   
 $GR(IV-9) = GR(IV-8) = GRN+5.$   
 $GO TO 782$   
 766  $IF(JA+GT.28) GO TO 784$   
 $JA = 4$   
 $GO TO 780$   
 776  $IF(JA+GT.4) GO TO 786$   
 $GR(IV-14) = GR(IV-13) = GRN+5.$   
 $GO TO 778$   
 784  $JA = 11$   
 $GO TO 780$   
 786  $GR(IV-12) = GR(IV-11) = GRN+15.$   
 $GR(IV-10) = GR(IV-9) = GR(IV-8) = GR(IV-7) = GR(IV-18)$   
 $2 = GR(IV-17) = GRN+5.$   
 $GO TO 778$   
 742  $IF(IP.GT.6) GO TO 108$   
 $IF(16.GT.1) GO TO 850$   
 $IF(JB.GT.5) GO TO 852$   
 $IV = JA = 1$   
 $GO TO 460$   
 860  $NI(IV+4) = NI(IV+11) = NI(IV+18) = NI(IV+25) = NI(IV+28)$   
 $2 = NI(IV+29) = NI(IV+30) = NI(IV+31) = NI(IV+32) = 2$   
 $GR(IV+36) = GR(IV+37) = GR(IV+38) = GR(IV+39) = GR(IV+40)$   
 $2 = GR(IV+41) = GR(IV+42) = GRN+15.$   
 $GR(IV+5) = GR(IV+6) = GR(IV+12) = GR(IV+13) = GR(IV+19)$   
 $2 = GR(IV+20) = GR(IV+26) = GR(IV+27) = GRN+10.$   
 $IF(JA+EQ.3) GO TO 3$   
 $GR(IV+35) = GRN+15.$   
 $GR(IV+33) = GR(IV+34) = GRN+10.$   
 $GR(IV+43) = GR(IV+44) = GR(IV+45) = GRN+5.$   
 $GO TO 3$   
 852  $IV = JA = 3$   
 860  $GR(IV+43) = GRN+15.$   
 $GR(IV-1) = GR(IV-2) = GRN+10.$   
 $GR(IV+33) = GR(IV+34) = GR(IV+35) = GRN+5.$   
 $GO TO 460$   
 850  $IF(JB.GT.5) GO TO 862$   
 $JA = 1$   
 875  $IF(16.GT.13) GO TO 864$   
 $IV = (16-2)*2+JA+17$   
 $GO TO 866$   
 864  $IF(16.GT.26) GO TO 868$   
 $IV = (16-12)*4+JA+47$   
 $GO TO 866$   
 868  $IV = (16-27)*2+JA+99$

```

866 GR(IV-10)=GR(IV-9)=GR(IV-8)=GR(IV-7)=GR(IV-6)
2=GR(IV-5)=GR(IV-4)=GRN+15.
1F(JA,E0,3)GO TO 870
GR(IV-11)=GRN+15.
GR(IV-3)=GR(IV-2)=GR(IV-1)=GRN+5.
GO TO 469
862 JA=3
GO TO 875
870 GR(IV-3)=GRN+15.
GR(IV-13)=GR(IV-12)=GR(IV-11)=GRN+5.
GO TO 880
3 WHILE(21,917)DKN1,16,JA
917 FORMAT(//IX,"KNOT %A-%",F5.3,SX,
2"LOCATED AT SECTION",I4,5A,"NO.",I3//)
RETURN
END

```

```

C SUBROUTINE LOAD(CL1)
COMMON/DATA/TITLE(8),NP,NE,NB,NDF,NMAT,NSZF,NLD,IP
1,CD,PINC,NMP,DMAX,NLNP,IV,16,JSIM,NSIM
2,ASTD,IENDD,JSTS,JENDS,EAV,ESD,AMOR,SDMR
3,AST2,ASPL,F12,F13,RING,ADPF,ISEED
COMMON CORL(190,2),NUP(170,4),IMAT(170),ORT(171,7)
1,NRC(10),NFI(10),RI(380),SK(380,20),NOLES(170)
2,KP(170),LI(170),IK(170),EST(170,36),BDATA(170,24)
3,R(3),ESTIFM(12,12),A(8,6),D(3,8),HS(8),SMAX(170)
4,NO(10),LR(170),HR(10,2),SMIN(170),ANG(170)
5,FRAT(12,2),SPL(12),STR2(12),XMOR(12),NI(170)
6,ST(170),IX(170),OR1HO(12,14),GR(170),STGRN(170)
7,FORC(170,3),DISP(2,190),RAND(5),COORD(190,2)
8,NUPP(170,4),ASMAX(170)

```

```

C ZERO LOAD ARRAYS
C
DO 160 J=1,NSZF
160 RI(J)=0.
1F(LI-E0,1)GO TO 200
DO 340 I=1,NLNP
1F(RR(I,1)-E0,0)GO TO 310
RI(I,1)=RR(I,1)+PINC
310 1F(RR(I,2)-E0,0)GO TO 340
RI(I,2)=RR(I,2)+PINC
340 CONTINUE
C READ, PRINT AND STORE LOAD CARD
C NO=NODAL POINT NUMBER WHERE LOAD ACTS
C RCI=HORIZONTAL LOAD COMPONENT (POSITIVE TO THE

```

```

C   RIGHT)
C   R(2)=VERTICAL LOAD COMPONENT (POSITIVE UPWARD)
C   RI=LOAD VECTOR
C
200 DO 400 I=1,NLNP
1F(LI-GT-1)GO TO 202
RR(I,1)=R(1)
RR(I,2)=R(2)
202 DO 170 K=1,NDF
IC=(NO(I)-1)*NDF+K
170 RI(IC)=R(K)+RI(IC)
400 CONTINUE
RETURN
END

SUBROUTINE FORMK(CL1)
C
C FORMS STIFFNESS MATRIX IN UPPER TRIANGULAR FORM
C
COMMON/DATA/TITLE(8),NP,NE,NB,NDF,NMAT,NSZF,NLD,IP
1,CD,PINC,NMP,DMAX,NLNP,IV,16,JSIM,NSIM
2,ASTD,IENDD,JSTS,JENDS,EAV,ESD,AMOR,SDMR
3,AST2,ASPL,F12,F13,RING,ADPF,ISEED
COMMON CORL(190,2),NUP(170,4),IMAT(170),ORT(171,7)
1,NRC(10),NFI(10),RI(380),SK(380,20),NOLES(170)
2,KP(170),LI(170),IK(170),EST(170,36),BDATA(170,24)
3,R(3),ESTIFM(12,12),A(8,6),D(3,8),HS(8),SMAX(170)
4,NO(10),LR(170),HR(10,2),SMIN(170),ANG(170)
5,FRAT(12,2),SPL(12),STR2(12),XMOR(12),NI(170)
6,ST(170),IX(170),OR1HO(12,14),GR(170),STGRN(170)
7,FORC(170,3),DISP(2,190),RAND(5),COORD(190,2)
8,NUPP(170,4),ASMAX(170)
REWIND 15

C SET BANDMAX AND NO. OF EQUATIONS
C
C NBAND = (D+1)*F WHERE
C   NBAND=HALF-BANDWIDTH
C   F=NUMBER OF DEGREES OF FREEDOM AT EACH NODE.
C   D=MAX. LARGEST DIFFERENCE OF NODAL NUMBERS
C   OCCURRING FOR ALL ELEMENTS.
C
NBAND=20

C ZERO STIFFNESS MATRIX
C
DO 300 N=1,NSZF

```

```

      DO 300 M=1,NBAND
 300  SK(N,M)=0.

C   SCAN ELEMENTS
C
      DO 400 N=1,NF
      IF(L1.EQ.1)GO TO 620
      IF(KP(N).EQ.0)GO TO 600
 620  IF(KNODES(N).EQ.4)GO TO 605
      CALL STIFT3(N)
      GO TO 650
 605  CALL STIFT4(N)
      GO TO 650
 650  IF(KNODES(N).EQ.4)GO TO 610
      M=0
      DO 770 I=1,6
      DO 770 J=1,6
      M=M+1
      ESTIFM(I,J)=EST(N,M)
      IF(I.EQ.J)GO TO 770
      ESTIFM(J,I)=ESTIFM(I,J)
 770  CONTINUE
      GO TO 650
 610  M=0
      DO 777 I=1,8
      DO 777 J=1,8
      M=M+1
      ESTIFM(I,J)=EST(N,M)
      IF(I.EQ.J)GO TO 777
      ESTIFM(J,I)=ESTIFM(I,J)
 777  CONTINUE
 650  NCN=NODFC(N)

C   RETURNS ESTIFM AS STIFFNESS MATRIX, STORE ESTIFM IN SK
C
C   FIRST ROWS
C
      DO 350 JJ=1,NCN
      NHOWR=(NODFC(N,JJ)-1)*NDF
      DO 350 J=1,NDF
      NHOWR=NHOWR+1
      I=(JJ-1)*NDF+J
 350  CONTINUE

C   THEN COLUMNS
C
      DO 330 KK=1,NCN
      NCOLP=(NODFC(N,KK)-1)*NDF

```

105

```

      DO 320 K=1,NDF
      L=(KK-1)*NDF+K
      NCOL=NCOLP+K+1-NHOWR

C   SKIP STORING IF BELOW BAND
C
      IF(NCOL>320,320,310
 310  SK(NHOWR,NCOL)=SK(NHOWR,NCOL)+ESTIFM(I,L)
 320  CONTINUE
 330  CONTINUE
 350  CONTINUE
 400  CONTINUE

C   INSERT BOUNDARY CONDITIONS
C
      READ(15)(NRC(I),NFX(I),I=1,NB)
      DO 500 N=1,NB
      NX=10*(NDF-1)
      I=NRC(N)
      NHOWB=(I-1)*NDF
      DO 490 M=1,NDF
      NHOWR=NHOWB+1
      ICON=NFX(N)/NX
      IF(ICON)450,450,420
 420  SK(NHOWB,I)=0.
      DO 430 J=2,NBAND
      SK(NHOWB,J)=0.
      NH=NHOWB+1-J
      IF(NH)430,430,425
 425  SK(NH,J)=0.
 430  CONTINUE
      NFX(N)=NFX(N)-NX*ICON
 450  NX=NX/10
 490  CONTINUE
 530  CONTINUE
      RETURN
      END

      SUBROUTINE STIFT3(N)
      C
      C   TRIANGULAR ELEMENTS - PLANE STRESS
      C
      COMMON/DATA/TITLE(8),NP,NF,NP,NDF,NKAT,NSZF,NLD,IP
      L,CD,PIHC,NEP,LMAC,NLNP,IV,T6,JSIM,NSIM

```

```

P,1STD,1ENDD,JSTS,JENDS,PAV,ESI,AMOR,SMOR
3,AST2,ASPL,E12,E13,RINGADEF,1SEFD
COMMON CORD(190,2),NOD(170,4),IMAT(170),OHT(171,7)
1,NRCC(10),NFX(10),R1(380),SK(380,20),NODES(170)
2,KPC(170),LL(170),LR(170),EST(170,36),BDATA(170,24)
3,R(3),ESTIM(12,12),A(8,6),B(3,8),RS(8),SMAX(170)
4,NOC(10),LB(170),BR(10,2),SMIN(170),ANG(170)
5,ERAT(12,2),SPL(12),STR(12),XMOR(12),NL(170)
6,ST(170),IX(170),ORTHO(12,14),GR(170),STGRN(170)
7,FORC(170,3),DISP(2,190),HARD(5),COORD(190,2)
8,NOPC(170,4),ASMAX(170)

C DETERMINE ELEMENTS CONNECTIONS
C
C I=NOPC(N,1)
C J=NOPC(N,2)
C K=NOPC(N,3)
C L=IMAT(N)

C NUMBER THE NODES COUNTER-CLOCKWISE
C
C SET UP LOCAL COORDINATE SYSTEM
C
C AJ=CORD(J,1)-CORD(I,1)
C AK=CORD(K,1)-CORD(I,1)
C FJ=CORD(J,2)-CORD(I,2)
C BK=CORD(K,2)-CORD(I,2)
C A(1,1)=AJ+BK-AK+BJ/2.
C IF(AHEA.LE.0.)GO TO 220

C FORM STRAIN DISP. MATRIX
C
C A(1,1)=0(3,2)=BJ-BK
C A(1,2)=A(1,4)=A(1,6)=A(2,1)=0.
C A(2,3)=0(2,5)=0.
C A(1,3)=A(3,4)=BK
C A(1,5)=A(3,6)=-BJ
C A(2,2)=A(3,1)=AK-AJ
C A(2,4)=A(3,3)=-AK
C A(2,6)=A(3,5)=AJ

C FORM STRESS STRAIN MATRIX FOR ORTHOTROPIC ELEMENT
C
C COMM=1./((1.-ORT(L,3)+ORT(L,4))*AREA)
C ESTIM(1,1)=COMM*ORT(L,1)
C ESTIM(1,2)=COMM*ORT(L,2)
C ESTIM(1,3)=ESTIM(3,1)=COMM*ORT(L,1)*ORT(L,4)
C ESTIM(1,3)=ESTIM(2,3)=ESTIM(3,1)=ESTIM(3,2)=0.
C ESTIM(3,3)=OHT(L,5)/AREA

C B IS THE STRESS BACKSUBSTITUTION MATRIX AND IS
C SAVED ON TAPE
C
C DO 205 I=1,3
C DO 205 J=1,6
C B(I,J)=0.
C DO 205 K=1,3
C 205 B(I,J)=B(I,J)+ESTIM(I,K)/2.*A(K,J)
C M=0
C DO 600 I=1,3
C DO 600 J=1,6
C M=M+1
C 600 BDATA(N,M)=B(I,J)

C ESTIM IS STIFFNESS MATRIX
C
C DO 210 I=1,6
C DO 210 J=1,6
C ESTIM(I,J)=0.
C DO 210 K=1,3
C 210 ESTIM(I,J)=ESTIM(I,J)+B(K,I)/2.*A(K,J)
C M=0
C DO 300 I=1,6
C DO 300 J=1,6
C M=M+1
C 300 ESTIM(N,M)=ESTIM(I,J)
C RETURN

C ERROR EXIT FOR PAD CONNECTIONS
C
C 220 WRITE(21,101)
C 101 FORMAT("ZERO OR NEGATIVE AREA ELEMENT NO.",14/
C "EXECUTION","TERMINATED")
C STOP
C END

SUBROUTINE STIFT4(ND)
C
C PENDING RECTANGULAR ELEMENT TAKEN FROM IMPROVED
C TWO-DIMENSIONAL FINITE ELEMENT BY R. D. COOK IN
C JOURNAL OF STRUCT. DIV., SEPT. 1974.
C
C COMMON/DATA/TITLE(80),NP,NF,NRHT,ENMAT,NSCF,NLD,IP,
C LCP,DPIP,NRP,DRAK,XNP,PNP,T16,USIM,NSD

```

```

2,1STD,1END,JS1S,JENDS,EAV,ESL,AMUR,SDMOR
3,AST2,ASPL,E12,E13,RING,ADFF,1SFED
COMMON CORDC(190,2),NOP(170,4),IMAT(170),ORT(171,7)
1,NRC(10),NEIX(10),RI(389),SK(389,28),NODES(170)
2,EP(170),LDC(170),IK(170),EST(170,36),BDATA(170,24)
3,R(3),ESTIFNC(12,12),A(8,6),R(3,8),RS(8),SMAX(170)
4,NJC(10),LB(170),RN(10,2),SMIN(170),ANG(170)
5,ERAT(122),SPL(12),STR(12),XMOH(12),NI(170)
6,SIC(170),IX(170),ONTHU(12,14),GR(170),SIGHN(170)
7,FORC(170,3),LISF(2,190),RAND(5),CCORI(190,2)
8,NOPP(170,4),ASMAX(170)
DIMENSION T(5,8),P(3,5),H(5,5),C(3,8)

```

BENDING RECTANGULAR ELEMENTS STIFFNESS MATRIX

DETERMINE ELEMENTS CONNECTIONS(NODES NUMBERED  
COUNTER-CLOCKWISE)

POSITIONS OF NODES:



```

I=NOP(1,1)
J=NOP(1,2)
K=NOP(1,3)
L=NOP(1,4)
N=IMAT(1)

```

FORM T MATRIX

```

DO 101 IA=1,8
DO 101 IB=1,5
101 T(IA,IB)=0.0
T(5,1)=T(1,1)=((CORDC(J,2)-CORDC(L,2))/2.)
T(5,2)=T(1,2)=((CORDC(K,2)-CORDC(L,2))/2.)
T(5,3)=T(1,3)=((CORDC(K,2)-CORDC(I,2))/2.)
T(5,4)=T(1,4)=(-1.)*T(1,1)
T(5,5)=T(1,7)=(-1.)*T(1,3)
G=CORDC(J,2)+CORDC(I,2)
D=CORDC(L,2)+CORDC(I,2)
E=CORDC(K,2)+CORDC(J,2)
F=CORDC(L,2)+CORDC(K,2)
T(2,1)=((CORDC(J,2)*G-CORDC(L,2)*D)/6.)

```

```

T(2,3)=((CORDC(K,2)*E-CORDC(I,2)*G)/6.)
T(2,5)=((CORDC(L,2)*F-CORDC(J,2)*E)/6.)
T(2,7)=((CORDC(I,2)*D-CORDC(L,2)*F)/6.)
T(5,1)=T(3,2)=((CORDC(L,1)-CORDC(J,1))/2.)
T(5,3)=T(3,4)=((CORDC(I,1)-CORDC(K,1))/2.)
T(5,5)=T(3,6)=(-1.)*T(3,2)
T(5,7)=T(3,8)=(-1.)*T(3,4)
G=CORDC(L,1)+CORDC(I,1)
D=CORDC(J,1)+CORDC(E,1)
E=CORDC(J,1)+CORDC(K,1)
F=CORDC(K,1)+CORDC(L,1)
T(4,2)=((CORDC(L,1)*G-CORDC(J,1)*D)/6.)
T(4,4)=((CORDC(I,1)*D-CORDC(K,1)*E)/6.)
T(4,6)=((CORDC(J,1)*E-CORDC(L,1)*F)/6.)
T(4,8)=((CORDC(K,1)*F-CORDC(I,1)*G)/6.)

```

C FORM P MATRIX

```

DO 100 IA=1,3
DO 100 IB=1,5
100 P(IA,IB)=0.0
X=Y=0.5
P(1,1)=P(2,3)=P(3,5)=1.
P(2,4)=((CORDC(J,1)-CORDC(I,1))*X+CORDC(I,1))
P(1,2)=((CORDC(K,2)-CORDC(J,2))*Y+CORDC(J,2))

```

C FORM H-INVERSE MATRIX

```

AB=ABS(CORDC(K,1)-CORDC(I,1))
BA=ABS(CORDC(K,2)-CORDC(I,2))
DO 102 IA=1,5
DO 102 IB=1,5
102 H(IA,IB)=0.0
CA=AB**5
CB=BA**5
COMM=144./((ORT(M,1)*ORT(M,2))-(ORT(M,3)*ORT(M,2)))
2**2)*(BA**6)+(AB**6))
H(1,1)=COMM+(((ORT(M,1)**2)*ORT(M,2)*(CB)+CA/36.))-2*(ORT(M,1)*(ORT(M,3)*ORT(M,2)))**2*CA*CB/48.-)
H(2,1)=H(1,2)=COMM+(((ORT(M,1)*(ORT(M,3)*ORT(M,2))**2)+CA*(BA**4))-(ORT(M,1)**2)*ORT(M,2)*CA*(BA**4))/324.)
H(3,1)=H(1,3)=COMM+(ORT(M,1)+ORT(M,2))*(ORT(M,3)*2ORT(M,2))*CA*CB/144.)
H(2,2)=COMM+(((ORT(M,1)**2)*ORT(M,2)*CA*(BA**3))-2*ORT(M,1)*(ORT(M,3)*ORT(M,2)))**2*CA*(BA**3))/12.
H(3,3)=COMM+((ORT(M,1)*(ORT(M,2)**2)+CA*CB/36.))-
```

```

2*(ORT(M,2)*((ORT(M,3)+ORT(M,2))+2)*CA+CB)/48.)
H(4,3)=A(3,4)=(ORT(M,2)*((ORT(M,3)+ORT(M,2))+2)*
2*(AB**4)*CB-ORT(M,1)*ORT(M,2)**2)*(AB**4)*CR)/24.**
3*COMM
H(4,4)=COMM*(ORT(M,1)*ORT(M,2)**2)*CB*(AB**3)-
2*ORT(M,2)*(ORT(M,3)+ORT(M,2))+2)*(AB**3)*CR)/12.
H(5,5)=COMM*(ORT(M,5)/144.)*(ORT(M,1)*ORT(M,2)*CA+CB-
2*(ORT(M,3)*ORT(M,2))+2)*CA+CB)

C FORM ELEMENT STIFFNESS MATRIX
C
DO 103 NA=1,8
DO 103 NC=1,5
A(NA,NC)=0.0
DO 103 JA=1,5
103 A(NA,NC)=T(JA,NA)+H(JA,NC)+A(NA,NC)
DO 104 NA=1,8
DO 104 NC=1,8
ESTIFM(NA,NC)=0.0
DO 104 JA=1,5
104 ESTIFM(NA,NC)=A(NA,JA)+T(JA,NC)+ESTIFM(NA,NC)
M=0
DO 300 I=1,8
DO 300 J=1,8
M=M+1
300 EST(N,M)=ESTIFM(I,J)

C FORM STRESS-DISPLACEMENT MATRIX AND SAVE ON BDATA
C
DO 106 NA=1,3
DO 106 NC=1,5
E(NA,NC)=0.0
DO 106 JA=1,5
106 E(NA,NC)=P(NA,JA)+H(JA,NC)+E(NA,NC)
DO 107 NA=1,3
DO 107 NC=1,8
C(NA,NC)=0.0
DO 107 JA=1,5
107 C(NA,NC)=B(NA,JA)+T(JA,NC)+C(NA,NC)
M=0
DO 600 I=1,3
DO 600 J=1,8
M=M+1
600 BDATA(M,I,J)=C(I,J)
RETURN
END

```

```

SUBROUTINE SOLVE
C DIRECT SOLUTION BY THE GAUSS ELIMINATION PROCEDURE
C AND BAND MATRIX TECHNIQUE.
C
COMMON/DATA/ITLEFC(8),NP,NE,NB,NDF,NMAT,NSZF,NLD,IP,
1,CD,PINC,NMP,LMAX,NLNF,IV,16,JSIM,NSIM
2,LS1D,LFNDD,JSTS,JNES,FAV,ESD,AMOR,SDMR
3,AST2,ASPL,E12,E13,RING,ALFF,ISFLD
COMMON CORDC(190,2),NUPC(170,4),IMAT(170),ORT(171,7)
1,NBC(10),NFI(10),R1(380),SK(380,20),NOLES(170)
2,KPC(170),LDC(170),IK(170),FST(170,36),BHATA(170,24)
3,R(3),FSTIFM(12,12),A(8,6),B(3,8),RS(8),SMAX(170)
4,NQ(10),LE(170),HR(10,2),SMIN(170),ANG(170)
5,ERAT(12,2),SPL(12),STH2(12),XMH(12),NI(170)
6,ST(170),IX(170),ORTHO(12,14),GH(170),STGRN(170)
7,FORC(170,3),DISP(2,190),HANIK(5),COORE(190,2)
8,NOPP(170,4),ASMAX(170)
NPAND=20

C REDUCE MATRIX
C
DO 300 N=1,NSZF
I=N
DO 290 L=2,NBAND
I=I+1
IF(SK(N,L))240,290,240
240 C=SK(N,L)/SK(N,1)
J=0
DO 270 K=L,NBAND
J=J+1
IF(SK(N,K))260,270,260
260 SK(I,J)=SK(I,J)-C*SK(N,K)
270 CONTINUE
SK(N,L)=C

C AND LOAD VECTOR FOR EACH EQUATION
C
R(1)=R(1)-C*R(N)
290 CONTINUE
300 R(N)=R(N)/SK(N,1)
C
C BACK-SUBSTITUTION
C
N=NSZF
350 N=N-1
IF(N)350,340,360

```

```

360 L=N
DO 400 K=2,NFAND
L=L+1
IF(SK(N,K))370,400,370
370 RIC(N)=RIC(N)-SK(N,K)*R(L)
400 CONTINUE
GO TO 350
500 RETURN
END

SUBROUTINE STRESS(CL1,JND)
COMMON/DATA/TITLE(8),NP,NE,NP,NDF,NMAT,NSZF,NLD,IP
1,CNP,PING,NMP,EMAX,NENP,IV,16,JSIM,NSIM
2,ISTD,IEEND,JOPTS,JNLS,EAV,ESD,AMOR,SMOR
3,AST2,ASPL,F12,F13,HING,ALEF,ISFD
COMMON,CORD(190,2),RUP(170,4),IMAT(170),ORT(171,7)
1,NPC(10),NFX(10),HI(380),SK(380,20),NODES(170)
2,RP(170),LD(170),IK(170),FST(170,36),BLATA(170,24)
3,n(3),ESTIFM(12,12),A(8,6),B(3,8),HS(8),SMAX(170)
4,NO(10),LB(170),RHC(10,2),SMIN(170),ANG(170)
5,ERAT(12,2),SPL(12),STR2(12),XMOK(12),NI(170)
6,ST(170),IX(170),ORTU(12,14),GR(170),STGRN(170)
7,FORCE(170,3),DISP(2,190),HAND(5),COORD(190,2)
8,NOPC(170,4),ASMAX(170)
DIMENSION DIS(2,200),FORCE(200,3)
EQUIVALENCE(DIS(1),RIC(1)),(SK(1),PURCE(1))
C
C PRINT DISPLACEMENTS
C
1F(CL1.GT.1)GO TO 50
WRITE(21,100)
WRITE(21,110)(M,(DIS(J,M),J=1,NDF),M=1STD,IEEND)
100 FORMAT(//,15X,"DISPLACEMENTS"//5X,"NODE",10X,"X",
115X,"")
110 FORMAT(1I0,2E15.5)
C
C CALCULATE RECTANGULAR ELEMENTS STRESSES
C
50 DO 200 NC=1,NE
IF(NOLF(NC).EQ.3)GO TO 222
MX=0
DO 922 I=1,3
DO 922 J=1,8
MX=MX+1
922 R(I,J)=BDATA(NC,NC)
DO 260 I=1,4
N=NOPC(NC,I)

```

```

IF(M.EQ.0)GO TO 260
K=(I-1)*2
DO 240 J=1,2
IJ=J+K
240 RSC(IJ)=DIS(J,M)
260 CONTINUE
IA=K+2
DO 300 I=1,3
FORCE(NC,I)=0.0
DO 300 J=1,IA
300 FORCE(NC,I)=FORCE(NC,I)+B(I,J)*RSC(J)
GO TO 200
C
C CALCULATE TRIANGULAR ELEMENTS STRESSES
C
222 MZ=0
DO 923 I=1,3
DO 923 J=1,6
MZ=MZ+1
923 P(I,J)=BDATA(NC,MZ)
DO 460 I=1,3
MZ=MZ+1
M=NOPC(NC,1)
IF(M.EQ.0)GO TO 460
K=(I-1)*NDF
DO 440 J=1,NDF
IJ=J+K
RSC(IJ)=DIS(J,M)
440 CONTINUE
460 CONTINUE
IA=K+NDF
DO 500 I=1,3
FORCE(NC,I)=0.
DO 500 J=1,IA
500 FORCE(NC,I)=FORCE(NC,I)+B(I,J)*RSC(J)
200 CONTINUE
DO 555 I=1,NE
DO 555 J=1,3
555 PURC(I,J)=PURC(I,J)+FORCE(I,J)
C
C CALCULATE PRINCIPAL STRESSES AND DIRECTIONS
C
DO 600 N=1,NE
C=(FORCE(N,1)+FORCE(N,2))/2.
XANG=GR(N)*2./57.29578
STV1=(FORCE(N,1)-FORCE(N,2))/2.
STG=STV1+COS(XANG)-FORCE(N,3)*SIN(XANG)+C
STGRN(N)=STGRN(N)+STG
AA=SQRT(STV1**2+FORCE(N,3)**2)

```

```

S1MAX=C+AA
S1MIN=C-AA
SMAX(N)=SMAX(N)+S1MAX
SMIN(N)=SMIN(N)+S1MIN
IF(FORCE(N,2).EQ.SMIN(N))GO TO 700
ANG(N)=57.29578*ATAN(FORCE(N,3)/(FORCE(N,2)-SMIN(N)))
GO TO 210
700 ANG(N)=90.
210 CONTINUE
600 CONTINUE
IF(LI.GT.1)GO TO 610
CD=SORT((DISP(2,NMP)*4.2**2)
C WRITE ALL STRESS COMPONENTS
C
WRITE(21,101)
WRITE(21,111)(N,(FORC(N,I),I=1,3),STGRN(N),N=JSTS
2,JENDS)
WRITE(21,790)
WRITE(21,112)(N,SMAX(N),SMIN(N),ANG(N),N=JSTS,JENDS)
610 DO 620 I=1,NP
DO 620 J=1,NDF
DISP(J,I)=DISP(J,I)+DISP(J,I)
620 CONTINUE
DEFL=DIS(2,NMP)
ADEF=AFS(DEFL)
IF(LI.EQ.1)GO TO 930
IF(CODE.LT.CD)GO TO 902
WRITE(21,811)TITLE,LI
WRITE(21,813)
WRITE(21,814)
WRITE(21,815)(N(I),CHAR(I,K),K=1,NDF),I=1,NLNP)
WHITE(21,100)
WHITE(21,110)(M,(DISP(J,M),J=1,NDF),N=1STD,1ENDD)
WHITE(21,101)
WHITE(21,111)(N,(FORC(N,I),I=1,3),STGRN(N),N=JSTS
2,JENDS)
WHITE(21,790)
WHITE(21,112)(N,SMAX(N),SMIN(N),ANG(N),N=JSTS,JENDS)
811 FORMAT(//IX,8A6,"LOAD CASE",13//)
813 FORMAT(2X,"LOAD")
814 FORMAT(2X,"NODE",7X,"X",7X,"Y")
815 FORMAT(15,2F10.2)
GO TO 931
930 IF(DEFL-DMAX)>01,931,932
932 FORMAT(//1X,"MAX-STRESS",6X,"MIN-STRESS",7X,"ANGLE")
101 FORMAT(//3X,"ELEMENT",2X,"X-STRESS",5X,"Y-STRESS",3X,

```

```

8"X-Y-STRESS",6X,"STGRN")
111 FORMAT(17.4E13.4)
112 FORMAT(10.2E17.4,F12.3)
902 RETURN
901 IF(JN.LT.NSIM)GO TO 902
STOP
END

```

#### C SUBROUTINE CHECK(LI)

C THIS SUBROUTINE DETERMINES IF ANY OF THE ELEMENTS  
C SHOULD CHANGE THEIR STIFFNESS (K) MATRIX FOR THE  
C NEXT LOAD.

```

COMMON/DATA/TITLE(8),NP,NE,NE,NDP,NMAT,NSZF,NLD,IP
1,CD,PINC,NMP,DMAX,NLNP,IV,16,JSIM,NSIM
2,1STD,1ENDD,JSTS,JENLS,EAV,ESD,AMON,SDMOR
3,AST2,ASPL,E12,E13,HING,ADEF,ISEED
COMMON CORC(190,2),NUP(170,4),IMAT(170),UR(171,7)
1,NBC(10),NFX(10),R1(380),SK(380,20),NODES(170)
2,KP(170),LC(170),IK(170),EST(170,36),BDATA(170,24)
3,R(3),EST1EM(12,12),A(8,6),B(3,8),HS(8),SMAX(170)
4,NG(10),LB(170),RH(10,2),SMIN(170),ANG(170)
5,ERAT(12,2),SPL(12),STR2(12),XNDR(12),NI(170)
6,ST(170),IX(170),URTHO(12,14),GR(170),STGRN(170)
7,FORC(170,3),DISP(2,190),RAND(5),COURD(190,2)
8,NUPP(170,4),ASMAX(170)
DIMENSION ST(200),STT(200),STD(200),STL(200),STI(200)
2,STDIF(200),STM(200),DIS(2,200),FORCE(200,3)
EQUIVALENCE(LIS(1),H(1)),(SK(1),FORC(1))
JB=0
DO 500 I=1,NE
KP(I)=0
K0=NI(I)

```

C IF LB(I)=1, ELEMENT I HAS BEEN BROKEN. CHECK  
C NEXT ELEMENT.

```

IF(LP(I).EQ.1)GO TO 500
ASMAX(I)=AFS(STGRN(I))
IF(SPL(10).GT.ASMAX(I)) GO TO 112
IF(STR2(10).GT.ASMAX(I))GO TO 201
IK(I)=IK(I)+1

```

C IF ASMAX(I) IS GREATER THAN MODULUS OF RUPTURE  
C (GR0H), ELEMENT I HAS BEEN BROKEN. CHANGE STIFFNESS  
C PROPERTIES.

```

C
C IF(XMUR(KQ))>T ASMAX(1) GO TO 114
120 IMAT(1)=NE+1
LBC(1)=1
KPC(1)=1
JR=1
GO TO 500
C
C IF IXC(1)=1, IT IS THE FIRST LOADING OF ELEMENT 1
C BEYOND THE PROPORTIONAL LIMIT (PL).
C
114 IF(IXC(1).EQ.1) GO TO 116
IF(IXC(1).GT.2) GO TO 118
STC(1)=(ASMAX(1)-ST(1))/2.
118 STC(1)=XMUR(KQ)-ASMAX(1)
IF(STC(1)<ST(1))120,120,500
116 ST(1)=ASMAX(1)
C
C IF LD(1)=1, THE K-MATRIX OF ELEMENT 1 HAVE ALREADY
C BEEN USING PROPERTIES BEYOND PL.
C
117 IF(LD(1).EQ.0) GO TO 500
GO TO 207
201 IX(1)=IXC(1)+1
IF(IX(1).EQ.1) GO TO 203
IF(IX(1).GT.2) GO TO 205
SI(1)=(ASMAX(1)-ST(1))/2.
205 STM(1)=STR2(KQ)-ASMAX(1)
IF(STM(1)<SI(1))207,207,500
207 KPC(1)=1
ORTC(1,1)=ORTC(1,1)*ERAT(KQ,2)
ORTC(1,2)=ORTC(1,1)*0.068
ORTC(1,5)=ORTC(1,1)*0.064
JR=1
LD(1)=2
GO TO 500
203 STC(1)=ASMAX(1)
IF(LD(1).EQ.1) GO TO 500
112 IF(L1.GT.2) GO TO 124
ST(1)=(ASMAX(1)-ST(1))/2.
124 STDFC(1)=SPL(KQ)-ASMAX(1)
IF(STDFC(1)<ST(1))122,122,500
122 KPC(1)=1
C
C CHANGE STIFFNESS PROPERTIES
C
C ORTC(1,1)=ORTC(1,1)*ERAT(KQ,1)
ORTC(1,2)=ORTC(1,1)*0.068
ORTC(1,5)=ORTC(1,1)*0.064
LD(1)=1
JR=1
500 CONTINUE
C
C IF JB=0, RESULTS WILL NOT BE PRINTED.
C IF JB=1, THE K-MATRIX OF ONE OR MORE OF THE
C ELEMENTS WILL CHANGE NEXT LOADING. RESULTS
C WILL BE PRINTED.
C
560 IF(JB.EQ.0) GO TO 600
IF(L1.EQ.1) GO TO 600
WRITE(21,811)TITLE,L1
WRITE(21,813)
WRITE(21,814)
WRITE(21,815)(NQ(1),CHC(1,K),K=1,NDF),I=1,NLP
WRITE(21,820)
WRITE(21,821)(M,(DISP(J,M),J=1,NDF),M=1STD,1ENDD)
WRITE(21,101)
WRITE(21,111)(N,(FORC(N,I),I=1,3),STGRN(N),N=JSTS
2,JENDS)
WRITE(21,790)
WRITE(21,793)(N,SMAX(N),SMIN(N),ANG(N),N=JSTS,JENDS)
811 FORMAT(//IX,8A6,"LOAD CASE",13//)
813 FORMAT(2X,"LOADS")
814 FORMAT(2X,"NODE",7X,"X",7X,"Y")
815 FORMAT(15.2F10.2)
820 FORMAT(//,1X,"DISPLACEMENTS"/"5X,"NODE",10X,"X",
115X,"Y")
821 FORMAT(110,2I15.5)
101 FORMAT(//3X,"ELEMENT",2X,"X-STRESS",5X,"Y-STRESS",3X,
1"X-Y-STRESS",6X,"STGRN")
111 FORMAT(17.4F13.4)
790 FORMAT(//17X,"MAX-STRESS",6X,"MIN-STRESS",7X,"ANGLE")
793 FORMAT(110,2F17.4,F12.3)
669 RETURN
END

```

APPENDIX B: INPUT FILE FOR STUD NO. 1

1	0	0	0
FINITE ELEMENT ANALYSIS (SPEC 1, MESS B)			
135	156	2	2
135	1	156	
1	1923000.	1314000.	.292 .020 1237000. 967000. 1508000.
			.13500. .449 .022 .390 .287 1484500. 723800.
2	1723300.	1172000.	.292 .020 1103000. 862000. 1344000.
			.12100. .449 .022 .390 .287 1418300. 1400600.
3	2752800.	1872000.	.292 .020 1762000. 1376000. 2147000.
			.19300. .449 .022 .390 .287 1744300. 708400.
4	1668800.	1135000.	.292 .020 1268000. 834000. 1302000.
			.11700. .449 .022 .390 .287 1438100. 1438100.
5	2341400.	1592000.	.292 .020 1498000. 1171000. 1826000.
			.16400. .449 .022 .390 .287 1638800. 1312100.
6	1890100.	1285000.	.292 .020 1210000. 945000. 1474000.
			.13200. .449 .022 .390 .287 1631000. 1485300.
7	2342300.	1593000.	.292 .020 1499000. 1171000. 1827000.
			.16400. .449 .022 .390 .287 1710600. 971500.
8	1803300.	1247000.	.292 .020 1173000. 917000. 1430000.
			.12800. .449 .022 .390 .287 1787200. 1787200.
9	2342300.	1593000.	.292 .020 1499000. 1171000. 1827000.
			.16400. .449 .022 .390 .287 1710600. 971500.
10	2223500.	1512000.	.292 .020 1423000. 1112000. 1734000.
			.15600. .449 .022 .390 .287 1924300. 1500800.
157	1000.	68.	.292 .020 64.
1	4810.	5880.	8030.
2	9470.	9870.	10350.
3	5600.	7330.	8430.
4	10620.	11160.	11700.
5	5250.	6460.	8490.
6	10340.	11160.	11920.
7	5220.	6460.	8340.
8	10240.	11050.	11870.
9	5220.	6460.	8340.
10	10160.	12480.	13640.
1	0.0	3.42	
2	0.	1.71	
3	0.	0.	
4	5.	3.42	
5	5.	1.71	
6	5.	0.	
7	10.	3.42	
8	10.	1.71	
9	10.	0.	
10	14.	3.42	
11	14.	1.71	
12	14.	0.	
13	18.	3.42	
14	18.	1.71	
15	18.	0.	
16	21.5	3.42	
17	21.5	1.71	
18	21.5	0.	
19	25.	3.42	
20	25.	1.71	
21	25.	0.	
22	27.5	3.42	
23	27.5	1.71	
24	27.5	0.	
25	30.	3.42	
26	30.	1.71	
27	30.	0.	
28	31.25	3.42	
29	31.25	2.565	
30	31.25	.855	
31	31.25	0.	
32	32.5	3.42	
33	32.5	1.71	
34	32.5	0.	
35	33.75	3.42	
36	33.75	2.565	
37	33.75	.855	
38	33.75	0.	
39	35.	3.42	
40	35.	1.71	
41	35.	0.	
42	36.25	3.42	
43	36.25	2.565	
44	36.25	.855	
45	36.25	0.	
46	37.5	3.42	
47	37.5	1.71	
48	37.5	0.	
49	38.75	3.42	
50	38.75	2.565	
51	38.75	.855	
52	38.75	0.	

53	40.	3.42
54	40.	1.71
55	40.	0.
56	41.25	3.42
57	41.25	2.565
58	41.25	.855
59	41.25	0.
60	42.5	3.42
61	42.5	1.71
62	42.5	0.
63	43.75	3.42
64	43.75	2.565
65	43.75	.855
66	43.75	0.
67	45.	3.42
68	45.	1.71
69	45.	0.
70	46.25	3.42
71	46.25	2.565
72	46.25	.855
73	46.25	0.
74	47.5	3.42
75	47.5	1.71
76	47.5	0.
77	48.75	3.42
78	48.75	2.565
79	48.75	.855
80	48.75	0.
81	50.	3.42
82	50.	1.71
83	50.	0.
84	51.25	3.42
85	51.25	2.565
86	51.25	.855
87	51.25	0.
88	52.5	3.42
89	52.5	1.71
90	52.5	0.
91	53.75	3.42
92	53.75	2.565
93	53.75	.855
94	53.75	0.
95	55.	3.42
96	55.	1.71
97	55.	0.
98	56.25	3.42
99	56.25	2.565
100	56.25	.855
101	56.25	0.
102	57.5	3.42
103	57.5	1.71
104	57.5	0.

22	28	29	32	8	3	22	3		70	60	64	63	0	3	70	5
23	29	33	32	0	3	23	3		71	61	68	64	0	3	71	5
24	26	27	30	0	3	24	4		72	63	64	67	0	3	72	5
25	26	30	33	0	3	25	4		73	64	68	67	0	3	73	5
26	27	31	32	0	3	26	4		74	61	62	65	0	3	74	6
27	30	31	34	0	3	27	4		75	61	65	68	0	3	75	6
28	30	34	33	0	3	28	4		76	62	66	65	0	3	76	6
29	32	33	36	0	3	29	3		77	65	66	69	0	3	77	6
30	32	36	35	0	3	30	3		78	65	69	68	0	3	78	6
31	33	40	36	0	3	31	3		79	67	68	71	0	3	79	5
32	35	36	39	0	3	32	3		80	67	71	70	0	3	80	5
33	36	40	39	0	3	33	3		81	68	75	71	0	3	81	5
34	33	34	37	0	3	34	4		82	70	71	74	0	3	82	5
35	33	37	40	0	3	35	4		83	71	75	74	0	3	83	5
36	34	38	37	0	3	36	4		84	68	69	72	0	3	84	6
37	37	38	41	0	3	37	4		85	68	72	75	0	3	85	6
38	37	41	40	0	3	38	4		86	69	73	72	0	3	86	6
39	39	40	43	0	3	39	3		87	72	73	76	0	3	87	6
40	39	43	42	0	3	40	3		88	72	76	75	0	3	88	6
41	40	47	43	0	3	41	5		89	74	75	78	0	3	89	5
42	42	43	46	0	3	42	5		90	74	78	77	0	3	90	5
43	43	47	46	0	3	43	5		91	75	82	78	0	3	91	5
44	40	41	44	0	3	44	4		92	77	78	81	0	3	92	5
45	40	44	47	0	3	45	6		93	78	82	81	0	3	93	5
46	41	45	44	0	3	46	4		94	75	76	79	0	3	94	6
47	44	45	48	0	3	47	6		95	75	79	82	0	3	95	6
48	44	48	47	0	3	48	6		96	76	80	79	0	3	96	6
49	46	47	50	0	3	49	5		97	79	80	83	0	3	97	6
50	46	50	49	0	3	50	5		98	79	83	82	0	3	98	6
51	47	54	50	0	3	51	5		99	81	82	85	0	3	99	5
52	49	50	53	0	3	52	5		100	81	85	84	0	3	100	5
53	50	54	53	0	3	53	5		101	82	89	85	0	3	101	5
54	47	48	51	0	3	54	6		102	84	85	88	0	3	102	5
55	47	51	54	0	3	55	6		103	85	89	88	0	3	103	5
56	48	52	51	0	3	56	6		104	82	83	86	0	3	104	6
57	51	52	55	0	3	57	6		105	82	86	89	0	3	105	6
58	51	55	54	0	3	58	6		106	83	87	86	0	3	106	6
59	53	54	57	0	3	59	5		107	86	87	90	0	3	107	6
60	53	57	56	0	3	60	5		108	86	90	89	0	3	108	6
61	54	61	57	0	3	61	5		109	88	89	92	0	3	109	5
62	56	57	60	0	3	62	5		110	88	92	91	0	3	110	5
63	57	61	60	0	3	63	5		111	89	96	92	0	3	111	5
64	54	55	58	0	3	64	6		112	91	92	95	0	3	112	7
65	54	58	61	0	3	65	6		113	92	96	95	0	3	113	7
66	55	59	58	0	3	66	6		114	89	90	93	0	3	114	6
67	58	59	62	0	3	67	6		115	89	93	96	0	3	115	6
68	58	62	61	0	3	68	6		116	90	94	93	0	3	116	6
69	60	61	64	0	3	69	5		117	93	94	97	0	3	117	8

118	93	97	96	8	3	118	8	12	0	1.	82.25
119	95	96	99	0	3	119	7	13	0	.75	90.
120	95	99	98	0	3	120	7	14	12		
121	96	103	99	0	3	121	7	15	13		
122	98	99	102	0	3	122	7	16	13		
123	99	103	102	0	3	123	7	17	14		
124	96	97	100	0	3	124	8	18	14		
125	96	100	103	0	3	125	8	19	13		
126	97	101	100	0	3	126	8	20	13		
127	100	101	104	0	3	127	8	21	13		
128	100	104	103	0	3	128	8	22	13		
129	102	103	106	0	3	129	7	23	13		
130	102	106	105	0	3	130	7	24	14		
131	103	110	106	0	3	131	7	25	14		
132	105	106	109	0	3	132	7	26	14		
133	106	110	109	0	3	133	7	27	14		
134	103	104	107	0	3	134	8	28	14		
135	103	107	110	0	3	135	8	29	13		
136	104	108	107	0	3	136	8	30	13		
137	107	108	111	0	3	137	8	31	13		
138	107	111	110	0	3	138	8	32	13		
139	109	110	113	0	3	139	7	33	13		
140	109	113	112	0	3	140	7	34	14		
141	110	111	113	0	3	141	8	35	14		
142	111	114	113	0	3	142	8	36	14		
143	113	116	115	112	4	143	7	37	14		
144	114	117	116	113	4	144	8	38	14		
145	116	119	118	115	4	145	7	39	13		
146	117	120	119	116	4	146	8	40	13		
147	119	122	121	118	4	147	7	41	0	0.	86.35
148	120	123	122	119	4	148	8	42	0	0.	82.7
149	122	125	124	121	4	149	9	43	42		
150	123	126	125	122	4	150	10	44	14		
151	125	128	127	124	4	151	9	45	0	.5	89.25
152	126	129	128	125	4	152	10	46	44		
153	128	131	130	127	4	153	9	47	0	.5	89.5
154	129	132	131	128	4	154	10	48	47		
155	131	134	133	130	4	155	9	49	42		
156	132	135	134	131	4	156	10	50	42		
1	8	1.	89.2					51	42		
2	0	1.12	69.2					52	42		
3	0	1.	89.6					53	42		
4	0	1.12	72.35					54	47		
5	0	1.25	89.6					55	47		
6	0	1.	72.35					56	47		
7	0	1.25	90.					57	47		
8	0	1.	75.5					58	47		
9	0	1.25	93.					59	42		
10	0	1.	75.5					60	42		
11	9							61	42		
								62	42		
								63	42		
								64	47		

63	47
66	47
67	47
68	47
69	42
70	42
71	42
72	42
73	42
74	47
75	47
76	47
77	47
78	47
79	42
80	42
81	42
82	42
83	42
84	47
85	47
86	47
87	47
88	47
89	0 .25 82.7
90	89
91	89
92	89
93	92
94	0 1.12 89.5
95	94
96	94
97	94
98	97
99	92
100	92
101	92
102	92
103	92
104	97
105	97
106	97
107	97
108	97
109	92
110	92
111	0 .25 79.05
112	0 .25 75.4
113	112
114	97
115	0 1.12 89.75
116	97
117	0 1.12 90.
118	117

119	0 .25 75.8
120	119
121	119
122	119
123	119
124	117
125	117
126	117
127	117
128	117
129	119
130	119
131	119
132	119
133	132
134	117
135	117
136	117
137	117
138	137
139	0 .75 75.8
140	139
141	0 1.75 90.
142	141
143	139
144	141
145	143
146	144
147	0 .75 76.2
148	146
149	0 1. 76.2
150	0 1.37 90.
151	0 1. 69.85
152	150
153	151
154	152
155	0 1. 63.5
156	154
157	11
135	1
25	0.0 -25.
109	0.0 -25.

APPENDIX C: INPUT FILE FOR STUD NO. 2

1	0	0	0											
FINITE ELEMENT ANALYSIS (SPEC 2,MESS 8)														
135	156	2	2	10	1	67	-2.	-25.	2	70	67	69	79	88
1	2102000.	142900.	.292	.020	134500.	105100.	164000.	14700.	.449	.022	.390	.287	1492900.	671400.
2	1787600.	121600.	.292	.020	114400.	89400.	139400.	12500.	.449	.022	.390	.287	1582600.	1582600.
3	1839800.	125100.	.292	.020	117700.	92000.	143500.	12900.	.449	.022	.390	.287	1334300.	287900.
4	1776900.	120800.	.292	.020	113700.	88800.	138600.	12400.	.449	.022	.390	.287	1462900.	1462900.
5	2141500.	145600.	.292	.020	137100.	107100.	167000.	15000.	.449	.022	.390	.287	1524400.	478500.
6	1776900.	120800.	.292	.020	113700.	88800.	138600.	12400.	.449	.022	.390	.287	1462900.	1462900.
7	2030000.	138000.	.292	.020	129900.	101500.	158300.	14200.	.449	.022	.390	.287	1386100.	571700.
8	1919600.	130500.	.292	.020	122900.	96000.	149700.	13400.	.449	.022	.390	.287	753500.	753500.
9	2594000.	176400.	.292	.020	166000.	129700.	202300.	18200.	.449	.022	.390	.287	1884200.	383000.
10	1725700.	117300.	.292	.020	110400.	86300.	134600.	12100.	.449	.022	.390	.287	1659500.	1659500.
157	1000.	68.	.292	.020	64.									
1	6830.	7430.	7930.											
2	6130.	7410.	8700.											
3	5140.	6710.	7910.											
4	7490.	8190.	8890.											
5	5880.	7060.	7860.											
6	7490.	8190.	8890.											
7	6250.	7120.	7710.											
8	7660.	8390.	9140.											
9	5310.	6960.	7880.											
10	7890.	8380.	8870.											
1	0.00	3.45												
2	0.	1.725												
3	0.	0.												
4	5.	3.45												
5	5.	1.725												
6	5.	0.												
7	10.	3.45												
8	10.	1.725												
9	10.	0.												
10	14.	3.45												
11	14.	1.725												
12	14.	0.												
13	18.	3.45												
14	18.	1.725												
15	18.	0.												
16	21.5	3.45												
17	21.5	1.725												
18	21.5	0.												
19	25.	3.45												
20	25.	1.725												
21	25.	0.												
22	27.5	3.45												
23	27.5	1.725												
24	27.5	0.												
25	30.	3.45												
26	30.	1.725												
27	30.	0.												
28	31.25	3.45												
29	31.25	2.587												
30	31.25	.862												
31	31.25	0.												
32	32.5	3.45												
33	32.5	1.725												
34	32.5	0.												
35	33.75	3.45												
36	33.75	2.587												
37	33.75	.862												
38	33.75	0.												
39	35.	3.45												
40	35.	1.725												
41	35.	0.												
42	36.25	3.45												
43	36.25	2.587												
44	36.25	.862												
45	36.25	0.												
46	37.5	3.45												
47	37.5	1.725												
48	37.5	0.												
49	38.75	3.45												
50	38.75	2.587												
51	38.75	.862												
52	38.75	0.												
53	40.	3.45												

54	40.	1.725
55	40.	0.
56	41.25	3.45
57	41.25	2.587
58	41.25	.862
59	41.25	0.
60	42.5	3.45
61	42.5	1.725
62	42.5	0.
63	43.75	3.45
64	43.75	2.587
65	43.75	.862
66	43.75	0.
67	45.	3.45
68	45.	1.725
69	45.	0.
70	46.25	3.45
71	46.25	2.587
72	46.25	.862
73	46.25	0.
74	47.5	3.45
75	47.5	1.725
76	47.5	0.
77	48.75	3.45
78	48.75	2.587
79	48.75	.862
80	48.75	0.
81	50.	3.45
82	50.	1.725
83	50.	0.
84	51.25	3.45
85	51.25	2.587
86	51.25	.862
87	51.25	0.
88	52.5	3.45
89	52.5	1.725
90	52.5	0.
91	53.75	3.45
92	53.75	2.587
93	53.75	.862
94	53.75	0.
95	55.	3.45
96	55.	1.725
97	55.	0.
98	56.25	3.45
99	56.25	2.587
100	56.25	.862
101	56.25	0.
102	57.5	3.45

103	57.5	1.725					
104	57.5	0.					
105	58.75	3.45					
106	58.75	2.587					
107	58.75	.862					
108	58.75	0.					
109	60.	3.45					
110	60.	1.725					
111	60.	0.					
112	62.5	3.45					
113	62.5	1.725					
114	62.5	0.					
115	65.	3.45					
116	65.	1.725					
117	65.	0.					
118	68.5	3.45					
119	68.5	1.725					
120	68.5	0.					
121	72.	3.45					
122	72.	1.725					
123	72.	0.					
124	76.	3.45					
125	76.	1.725					
126	76.	0.					
127	80.	3.45					
128	80.	1.725					
129	80.	0.					
130	85.	3.45					
131	85.	1.725					
132	85.	0.					
133	90.	3.45					
134	90.	1.725					
135	90.	0.					
1	2	5	4	1	4	1	1
2	3	6	5	2	4	2	2
3	5	8	7	4	4	3	1
4	6	9	8	5	4	4	2
5	8	11	10	7	4	5	1
6	9	12	11	8	4	6	2
7	11	14	13	10	4	7	1
8	12	15	14	11	4	8	2
9	14	17	16	13	4	9	3
10	15	18	17	14	4	10	4
11	17	20	19	16	4	11	3
12	18	21	20	17	4	12	4
13	20	23	22	19	4	13	3
14	21	24	23	20	4	14	4
15	22	23	25	0	3	15	3
16	23	26	25	0	3	16	3
17	23	27	26	0	3	17	4

18	23	24	27	0	3	18	4			66	55	59	58	0	3	66	6
19	25	26	29	0	3	19	3			67	58	59	62	0	3	67	6
20	25	29	28	0	3	20	3			68	58	62	61	0	3	68	6
21	26	33	29	0	3	21	3			69	60	61	64	0	3	69	5
22	28	29	32	0	3	22	3			70	60	64	63	0	3	70	5
23	29	33	32	0	3	23	3			71	61	68	64	0	3	71	5
24	26	27	30	0	3	24	4			72	63	64	67	0	3	72	5
25	26	30	33	0	3	25	4			73	64	68	67	0	3	73	5
26	27	31	30	0	3	26	4			74	61	62	65	0	3	74	6
27	30	31	34	0	3	27	4			75	61	65	68	0	3	75	6
28	30	34	33	0	3	28	4			76	62	66	65	0	3	76	6
29	32	33	36	0	3	29	3			77	65	66	69	0	3	77	6
30	32	36	35	0	3	30	3			78	65	69	68	0	3	78	6
31	33	40	36	0	3	31	3			79	67	68	71	0	3	79	5
32	35	36	39	0	3	32	3			80	67	71	70	0	3	80	5
33	36	40	39	0	3	33	3			81	68	75	71	0	3	81	5
34	33	34	37	0	3	34	4			82	70	71	74	0	3	82	5
35	33	37	40	0	3	35	4			83	71	75	74	0	3	83	5
36	34	38	37	0	3	36	4			84	68	69	72	0	3	84	6
37	37	38	41	0	3	37	4			85	68	72	75	0	3	85	6
38	37	41	40	0	3	38	4			86	69	73	72	0	3	86	6
39	39	40	43	0	3	39	3			87	72	73	76	0	3	87	6
40	39	43	42	0	3	40	3			88	72	76	75	0	3	88	6
41	40	47	43	0	3	41	5			89	74	75	78	0	3	89	5
42	42	43	46	0	3	42	5			90	74	78	77	0	3	90	5
43	43	47	46	0	3	43	5			91	75	82	78	0	3	91	5
44	40	41	44	0	3	44	4			92	77	78	81	0	3	92	5
45	40	44	47	0	3	45	6			93	78	82	81	0	3	93	5
46	41	45	44	0	3	46	4			94	75	76	79	0	3	94	6
47	44	45	48	0	3	47	6			95	75	79	82	0	3	95	6
48	44	48	47	0	3	48	6			96	76	80	79	0	3	96	6
49	46	47	50	0	3	49	5			97	79	80	83	0	3	97	6
50	46	50	49	0	3	50	5			98	79	83	82	0	3	98	6
51	47	54	50	0	3	51	5			99	81	82	85	0	3	99	5
52	49	50	53	0	3	52	5			100	81	85	84	0	3	100	5
53	50	54	53	0	3	53	5			101	82	89	85	0	3	101	5
54	47	48	51	0	3	54	6			102	84	85	88	0	3	102	5
55	47	51	54	0	3	55	6			103	85	89	88	0	3	103	5
56	48	52	51	0	3	56	6			104	82	83	86	0	3	104	6
57	51	52	55	0	3	57	6			105	82	86	89	0	3	105	6
58	51	55	54	0	3	58	6			106	83	87	86	0	3	106	6
59	53	54	57	0	3	59	5			107	86	87	90	0	3	107	6
60	53	57	56	0	3	60	5			108	86	90	89	0	3	108	6
61	54	61	57	0	3	61	5			109	88	89	92	0	3	109	5
62	56	57	60	0	3	62	5			110	88	92	91	0	3	110	5
63	57	61	60	0	3	63	5			111	89	96	92	0	3	111	5
64	54	55	58	0	3	64	6			112	91	92	95	0	3	112	7
65	54	58	61	0	3	65	6			113	92	96	95	0	3	113	7

114	89	90	93	0	3	114	6	7	0	1.25	17.5
115	89	93	96	0	3	115	6	8	0	1.	11.5
116	90	94	93	0	3	116	6	9	0	1.25	17.5
117	93	94	97	0	3	117	8	10	0	1.	11.5
118	93	97	96	0	3	118	8	11	0	1.5	16.85
119	95	96	99	0	3	119	7	12	0	1.	13.25
120	95	99	98	0	3	120	7	13	0	.75	16.85
121	96	103	99	0	3	121	7	14	0	.5	13.25
122	98	99	102	0	3	122	7	15	13		
123	99	103	102	0	3	123	7	16	13		
124	96	97	100	0	3	124	8	17	14		
125	96	100	103	0	3	125	8	18	14		
126	97	101	100	0	3	126	8	19	13		
127	100	101	104	0	3	127	8	20	13		
128	100	104	103	0	3	128	8	21	13		
129	102	103	106	0	3	129	7	22	13		
130	102	106	105	0	3	130	7	23	13		
131	103	110	106	0	3	131	7	24	14		
132	105	106	109	0	3	132	7	25	14		
133	106	110	109	0	3	133	7	26	14		
134	103	104	107	0	3	134	8	27	14		
135	103	107	110	0	3	135	8	28	14		
136	104	108	107	0	3	136	8	29	13		
137	107	108	111	0	3	137	8	30	13		
138	107	111	110	0	3	138	8	31	13		
139	109	110	113	0	3	139	7	32	13		
140	109	113	112	0	3	140	7	33	13		
141	110	111	113	0	3	141	8	34	14		
142	111	114	113	0	3	142	8	35	14		
143	113	116	115	112	4	143	7	36	14		
144	114	117	116	113	4	144	8	37	14		
145	116	119	118	115	4	145	7	38	14		
146	117	120	119	116	4	146	8	39	13		
147	119	122	121	118	4	147	7	40	13		
148	120	123	122	119	4	148	8	41	0	0.	17.05
149	122	125	124	121	4	149	9	42	0	0.	16.2
150	123	126	125	122	4	150	10	43	42		
151	125	128	127	124	4	151	9	44	14		
152	126	129	128	125	4	152	10	45	0	0.	15.
153	128	131	130	127	4	153	9	46	14		
154	129	132	131	128	4	154	10	47	45		
155	131	134	133	130	4	155	9	48	47		
156	132	135	134	131	4	156	10	49	0	0.	17.9
1	0	1.	24.5					50	49		
2	0	1.	13.8					51	49		
3	0	1.	21.					52	49		
4	0	1.	12.65					53	49		
5	0	1.	21.					54	0	0.	15.3
6	0	1.	12.65					55	54		

58	54		110	92
59	49		111	0 .5 18.75
60	49		112	0 .5 19.6
61	49		113	112
62	49		114	97
63	49		115	0 .0 . 15.45
64	54		116	97
65	54		117	0 .0 . 15.6
66	54		118	117
67	54		119	0 .0 . 19.2
68	54		120	119
69	49		121	119
70	49		122	119
71	49		123	119
72	49		124	0 .0 . 16.05
73	49		125	124
74	54		126	124
75	54		127	124
76	54		128	124
77	54		129	119
78	54		130	119
79	49		131	0 .75 19.2
80	49		132	0 1. 19.2
81	49		133	132
82	49		134	124
83	49		135	0 .5 16.05
84	54		136	124
85	54		137	0 1. 16.05
86	54		138	137
87	54		139	132
88	54		140	132
89	49		141	137
90	49		142	137
91	0 .5 17.9		143	0 1. 19.2
92	0 .5 17.9		144	0 1.25 16.05
93	92		145	143
94	0 .0 . 15.3		146	144
95	0 .5 15.3		147	0 1. 18.8
96	94		148	0 1.5 16.5
97	95		149	0 1. 18.8
98	97		150	0 1.5 16.5
99	92		151	149
100	92		152	0 1.25 15.45
101	92		153	149
102	92		154	152
103	93		155	149
104	97		156	0 1. 14.4
105	97		3	11
106	97		135	1.
107	97		25	0.0 -25.
108	97		109	0.0 -25.
109	92			

APPENDIX D: INPUT FILE FOR STUD NO. 3

1	0.	0.	0.
FINITE ELEMENT ANALYSIS (SPEC 3,MESS B)			
135	156	2	3.
14	15	16	17
1	135	1	156
1	2473800.	168300.	.292 .320 158300.
	17300.	.449 .022 .390	.287 1567600.
2	2285700.	155400.	.292 .020 146300.
	16600.	.449 .022 .390	.287 2089400.
3	2102600.	142800.	.292 .020 134400.
	14700.	.449 .022 .390	.287 1661000.
4	2248900.	152900.	.292 .020 143900.
	15700.	.449 .022 .390	.287 1883800.
5	2346700.	160700.	.292 .020 151500.
	16600.	.449 .022 .390	.287 1774100.
6	2134900.	145200.	.292 .020 136600.
	14900.	.449 .022 .390	.287 1991900.
7	2345700.	159500.	.292 .020 150100.
	16400.	.449 .022 .390	.287 1802300.
8	2243700.	152600.	.292 .020 143600.
	15700.	.449 .022 .390	.287 1913300.
9	1953000.	132400.	.292 .020 125000.
	13700.	.449 .022 .390	.287 1941900.
10	2238100.	151600.	.292 .020 142700.
	15600.	.449 .022 .390	.287 1639200.
157	1800.	63.	.292 .020 64.
1	5820.	7240.	6300.
2	10570.	13630.	17370.
3	6310.	7590.	9140.
4	8430.	11650.	14870.
5	6590.	7840.	8520.
6	7290.	11140.	16640.
7	5600.	7010.	8620.
8	9560.	12650.	16210.
9	6570.	7790.	8760.
10	10320.	12950.	15590.
1	0.0	3.42	
2	0.	1.71	
3	0.	0.	
4	5.	3.42	
5	5.	1.71	
6	5.	0.	
7	10.	3.42	
8	10.	1.71	
9	10.	0.	
10	14.	3.42	
11	14.	1.71	
12	14.	0.	
13	18.	3.42	
14	18.	1.71	
15	18.	0.	
16	21.5	3.42	
17	21.5	1.71	
18	21.5	0.	
19	25.	3.42	
20	25.	1.71	
21	25.	0.	
22	27.5	3.42	
23	27.5	1.71	
24	27.5	0.	
25	30.	3.42	
26	30.	1.71	
27	30.	0.	
28	31.25	3.42	
29	31.25	2.565	
30	31.25	.855	
31	31.25	0.	
32	32.5	3.42	
33	32.5	1.71	
34	32.5	0.	
35	33.75	3.42	
36	33.75	2.565	
37	33.75	.855	
38	33.75	0.	
39	35.	3.42	
40	35.	1.71	
41	35.	0.	
42	36.25	3.42	
43	36.25	2.565	
44	36.25	.855	
45	36.25	0.	
46	37.5	3.42	
47	37.5	1.71	

48 37.5 0.  
 49 38.75 3.42  
 50 38.75 2.565  
 51 38.75 .855  
 52 38.75 0.  
 53 40. 3.42  
 54 40. 1.71  
 55 40. 0.  
 56 41.25 3.42  
 57 41.25 2.565  
 58 41.25 .855  
 59 41.25 0.  
 60 42.5 3.42  
 61 42.5 1.71  
 62 42.5 0.  
 63 43.75 3.42  
 64 43.75 2.565  
 65 43.75 .855  
 66 43.75 0.  
 67 45. 3.42  
 68 45. 1.71  
 69 45. 0.  
 70 46.25 3.42  
 71 46.25 2.565  
 72 46.25 .855  
 73 46.25 0.  
 74 47.5 3.42  
 75 47.5 1.71  
 76 47.5 0.  
 77 48.75 3.42  
 78 48.75 2.565  
 79 48.75 .855  
 80 48.75 0.  
 81 50. 3.42  
 82 50. 1.71  
 83 50. 0.  
 84 51.25 3.42  
 85 51.25 2.565  
 86 51.25 .855  
 87 51.25 0.  
 88 52.5 3.42  
 89 52.5 1.71  
 90 52.5 0.  
 91 53.75 3.42  
 92 53.75 2.565  
 93 53.75 .855  
 94 53.75 0.

95	55.	3.42					
96	55.	1.71					
97	55.	0.					
98	56.25	3.42					
99	56.25	2.565					
100	56.25	.855					
101	56.25	0.					
102	57.5	3.42					
103	57.5	1.71					
104	57.5	0.					
105	58.75	3.42					
106	58.75	2.565					
107	58.75	.855					
108	58.75	0.					
109	60.	3.42					
110	60.	1.71					
111	60.	0.					
112	62.5	3.42					
113	62.5	1.71					
114	62.5	0.					
115	65.	3.42					
116	65.	1.71					
117	65.	0.					
118	68.5	3.42					
119	68.5	1.71					
120	68.5	0.					
121	72.	3.42					
122	72.	1.71					
123	72.	0.					
124	76.	3.42					
125	76.	1.71					
126	76.	0.					
127	80.	3.42					
128	80.	1.71					
129	80.	0.					
130	85.	3.42					
131	85.	1.71					
132	85.	0.					
133	90.	3.42					
134	90.	1.71					
135	90.	0.					
	1	2	3	4	5	6	7
	2	3	4	5	6	7	8
	3	4	5	6	7	8	9
	4	5	6	7	8	9	10
	5	6	7	8	9	10	11
	6	7	8	9	10	11	12

1 2 1 2 1 2

7	11	14	13	10	4	7	1			54	47	48	51	6	3	54	6
8	12	15	14	11	4	8	2			55	47	51	54	6	3	55	6
9	14	17	16	13	4	9	3			56	48	52	51	6	3	56	6
10	15	13	17	14	4	10	4			57	51	52	55	6	3	57	6
11	17	20	19	16	4	11	3			58	51	55	54	6	3	58	6
12	18	21	20	17	4	12	4			59	53	54	57	6	3	59	5
13	20	23	22	19	4	13	3			60	53	57	56	6	3	60	5
14	21	24	23	20	4	14	4			61	54	61	57	6	3	61	5
15	22	23	25	0	3	15	3			62	56	57	60	6	3	62	5
16	23	26	25	0	3	16	3			63	57	61	60	6	3	63	5
17	23	27	26	0	3	17	4			64	54	55	58	6	3	64	6
18	23	24	27	0	3	18	4			65	54	58	61	6	3	65	6
19	25	26	29	0	3	19	3			66	55	59	58	6	3	66	6
20	25	29	28	0	3	20	3			67	58	59	62	6	3	67	6
21	26	33	39	0	3	21	3			68	58	62	61	6	3	68	6
22	28	29	32	0	3	22	3			69	60	61	64	6	3	69	5
23	29	33	32	0	3	23	3			70	60	64	63	6	3	70	5
24	26	27	30	0	3	24	4			71	61	68	64	6	3	71	5
25	26	30	33	0	3	25	4			72	63	64	67	6	3	72	5
26	27	31	30	0	3	26	4			73	64	68	67	6	3	73	5
27	30	31	34	0	3	27	4			74	61	62	65	6	3	74	6
28	30	34	33	0	3	28	4			75	61	65	68	6	3	75	6
29	32	33	36	0	3	29	3			76	62	66	65	6	3	76	6
30	32	36	35	0	3	30	3			77	65	66	69	6	3	77	6
31	33	40	36	0	3	31	3			78	65	69	68	6	3	78	6
32	35	36	39	0	3	32	3			79	67	68	71	6	3	79	5
33	36	40	39	0	3	33	3			80	67	71	70	6	3	80	5
34	33	34	37	0	3	34	4			81	68	75	71	6	3	81	5
35	33	37	40	0	3	35	4			82	70	71	74	6	3	82	5
36	34	38	37	0	3	36	4			83	71	75	74	6	3	83	5
37	37	38	41	0	3	37	4			84	68	69	72	6	3	84	6
38	37	41	40	0	3	38	4			85	68	72	75	6	3	85	6
39	39	40	43	0	3	39	3			86	69	73	72	6	3	86	6
40	39	43	42	0	3	40	3			87	72	73	76	6	3	87	6
41	40	47	43	0	3	41	5			88	72	76	75	6	3	88	6
42	42	43	46	0	3	42	5			89	74	75	78	6	3	89	5
43	43	47	46	0	3	43	5			90	74	78	77	6	3	90	5
44	40	41	44	0	3	44	4			91	75	82	78	6	3	91	5
45	40	44	47	0	3	45	6			92	77	78	81	6	3	92	5
46	41	45	44	0	3	46	4			93	78	82	81	6	3	93	5
47	44	45	48	0	3	47	6			94	75	76	79	6	3	94	6
48	44	48	47	0	3	48	6			95	75	79	82	6	3	95	6
49	46	47	50	0	3	49	5			96	76	80	79	6	3	96	6
50	46	50	49	0	3	50	5			97	79	80	83	6	3	97	6
51	47	54	50	0	3	51	5			98	79	83	82	6	3	98	6
52	49	54	53	0	3	52	5			99	81	82	85	6	3	99	5
53	50	54	53	0	3	51	5			100	81	85	84	6	3	100	5

101	82	89	85	0	3	101	5			148	120	123	122	119	4	148
102	84	85	88	0	3	102	5			149	122	125	124	121	4	149
103	85	89	88	0	3	103	5			150	123	126	125	122	4	150
104	82	83	86	0	3	104	6			151	125	128	127	124	4	151
105	82	86	89	0	3	105	6			152	126	129	128	125	4	152
106	83	87	86	0	3	106	6			153	128	131	130	127	4	153
107	86	87	90	0	3	107	6			154	129	132	131	128	4	154
108	86	90	89	0	3	108	6			155	131	134	133	130	4	155
109	88	89	92	0	3	109	5			156	132	135	134	131	4	156
110	88	92	91	0	3	110	5			1	0	.5	42.			
111	89	96	92	0	3	111	5			2	0	.75	47.			
112	91	92	95	0	3	112	7			3	0	.5	48.7			
113	92	96	95	0	3	113	7			4	0	.62	48.25			
114	89	90	93	0	3	114	6			5	3					
115	89	93	96	0	3	115	6			6	0	.5	48.25			
116	90	94	93	0	3	116	6			7	0	2.25	39.4			
117	93	94	97	0	3	117	8			8	0	.75	49.5			
118	93	97	96	0	3	118	8			9	0	2.25	39.4			
119	95	96	99	0	3	119	7			10	0	.75	49.5			
120	95	99	98	0	3	120	7			11	0	4.	36.95			
121	96	103	99	0	3	121	7			12	0	1.	48.65			
122	98	99	102	0	3	122	7			13	0	2.75	36.95			
123	99	103	102	0	3	123	7			14	0	1.37	48.65			
124	96	97	100	0	3	124	8			15	13					
125	96	100	103	0	3	125	8			16	13					
126	97	101	100	0	3	126	8			17	14					
127	100	101	104	0	3	127	8			18	14					
128	100	104	103	0	3	128	8			19	13					
129	102	103	106	0	3	129	7			20	13					
130	102	106	105	0	3	130	7			21	13					
131	103	110	106	0	3	131	7			22	13					
132	105	106	109	0	3	132	7			23	13					
133	106	110	109	0	3	133	7			24	14					
134	103	104	107	0	3	134	8			25	14					
135	103	107	110	0	3	135	8			26	14					
136	104	108	107	0	3	136	8			27	14					
137	107	108	111	0	3	137	8			28	14					
138	107	111	110	0	3	138	8			29	13					
139	109	110	113	0	3	139	7			30	13					
140	109	113	112	0	3	140	7			31	13					
141	110	111	113	0	3	141	8			32	13					
142	111	114	113	0	3	142	8			33	13					
143	113	116	115	112	4	143	7			34	14					
144	114	117	116	113	4	144	8			35	14					
145	116	119	118	115	4	145	7			36	14					
146	117	120	119	116	4	146	8			37	14					
147	119	122	121	118	4	147	7			38	14					

37	43		86	47		133	132	
48	43		87	47		134	128	
41	0	1.	88	76		135	0	3.05 61.5
42	41		88	47		136	134	
43	48		89	83		137	135	
44	14		90	82		138	137	
45	0	1.5	91	0	-75 38.75	139	133	
46	44		92	91		140	132	
47	45		93	92		141	138	
48	47		94	86		142	141	
49	48		95	0	8.15 50.15	143	0	2.5 44.85
50	48		96	94		144	0	3.15 61.5
51	48		97	95		145	143	
52	43		98	97		146	144	
53	42		99	98		147	0	4. 46.7
54	47		100	92		148	0	3.25 70.5
55	47		101	92		149	0	4. 46.5
56	47		102	92		150	0	3.25 70.5
57	47		103	92		151	0	3.25 45.85
58	47		104	97		152	0	2.18 66.95
59	42		105	97		153	151	
60	42		106	97		154	152	
61	42		107	97		155	0	5 45.
62	42		108	97		156	0	1. 63.4
63	43		109	92		157	3	11
64	47		110	92		158	1	
65	47		111	0	-75 43.	159	0.0	-25.
66	47		112			160	0.0	-25.
67	47		113	97				
68	47		114	0	8.15 52.5			
69	42		115	0	8.15 52.5			
70	42		116	97				
71	42		117	115				
72	42		118	117				
73	42		119	0	-75 44.85			
74	47		120	119				
75	47		121	119				
76	47		122	119				
77	47		123	119				
78	47		124	0	8.15 61.5			
79	42		125	124				
80	42		126	124				
81	42		127	124				
82	42		128	124				
83	42		129	119				
84	47		130	119				
85	47		131	0	1. 44.85			
			132	131				

APPENDIX E: INPUT FILE FOR STUD NO. 4

## **FINITE ELEMENT ANALYSIS (SPEC 4)**

199	139.8	2.8	0.112	-2.	-25.	2.60
1	199	1	189			
1	1820600.	123800.	.292	.020	116500.	91000.
	12700.	.449	.022	.390	.287	1341000.
2	1640600.	113200.	.292	.020	106600.	83300.
	11700.	.449	.022	.390	.287	1528400.
3	2372500.	161300.	.292	.020	151600.	116600.
	16600.	.449	.022	.390	.287	1762900.
4	1936900.	131700.	.292	.020	124000.	96800.
	13600.	.449	.022	.390	.287	1585400.
5	1885700.	128200.	.292	.020	120700.	94300.
	13200.	.449	.022	.390	.287	1239500.
6	1796000.	122100.	.292	.020	114900.	89800.
	12600.	.449	.022	.390	.287	1316400.
7	1005000.	100500.	.449	.449	14100.	100500.
	14100.	.449	.449	.449	.449	73200.
8	10000.	68.	.292	.020	64.	50.
			.390	.257	700.	500.
190	10000.	68.	.292	.020	64.	
1	4810.	6020.	7920.			
2	5810.	8790.	12020.			
3	5340.	6950.	8200.			
4	4010.	5560.	6970.			
5	5230.	6860.	7930.			
6	3360.	5700.	7550.			
7	10000.	2030.	3000.			
8	10000.	2600.	3000.			
1	0.	3.4				
2	0.	1.7				
3	0.	0.				
4	3.5	3.4				
5	3.5	1.7				
6	3.5	0.				
7	5.	3.4				
8	4.75	2.48				
9	4.75	1.9				
10	5.	0.				
11	5.25	2.48				
12	5.25	1.9				
13	7.	3.4				

44	7.	1.7
15	7.	0.
16	11.	3.4
17	11.	1.7
18	11.	0.
19	15.	3.4
20	15.	1.7
21	15.	0.
22	16.67	3.4
23	16.67	3.15
24	16.67	2.07
25	17.17	0.
26	17.67	3.4
27	17.67	3.15
28	17.67	2.07
29	19.	3.4
30	19.	1.7
31	19.	0.
32	21.5	3.4
33	21.5	1.7
34	21.5	0.
35	26.	3.4
36	26.	1.7
37	26.	0.
38	28.5	3.4
39	28.5	1.7
40	28.5	0.
41	30.	3.4
42	30.	2.57
43	30.	1.7
44	30.	0.
45	30.	0.
46	31.	3.4
47	31.	2.98
48	31.	2.57
49	31.	1.7
50	31.	0.
51	31.	0.
52	31.58	3.4
53	31.58	2.9
54	31.58	2.5

55	31.58	1.7	102	42.42	2.23
56	31.58	.5	103	42.42	1.7
57	31.58	0.	104	42.42	.5
58	32.42	3.4	105	42.42	0.
59	32.42	2.98	106	43.67	3.4
60	32.42	2.57	107	43.67	2.57
61	32.42	1.7	108	43.67	2.23
62	32.42	.5	109	43.67	1.7
63	32.42	0.	110	43.67	.5
64	33.	3.4	111	43.67	0.
65	33.	2.98	112	45.	3.4
66	33.	2.57	113	45.	2.9
67	33.	1.7	114	45.	1.7
68	33.	.5	115	45.	.5
69	33.	0.	116	45.	0.
70	34.	3.4	117	46.5	3.4
71	34.	2.9	118	46.5	2.9
72	34.	1.7	119	46.5	1.7
73	34.	.5	120	46.5	.5
74	34.	0.	121	46.5	0.
75	35.	3.4	122	48.5	3.4
76	35.	2.9	123	48.5	2.9
77	35.	1.7	124	48.5	1.7
78	35.	.5	125	48.5	.5
79	35.	0.	126	48.5	0.
80	37.	3.4	127	50.5	3.4
81	37.	2.9	128	50.5	2.9
82	37.	1.7	129	50.5	1.7
83	37.	.5	130	50.5	.5
84	37.	0.	131	50.5	0.
85	39.	3.4	132	52.	3.4
86	39.	2.9	133	52.	2.9
87	39.	1.7	134	52.	1.7
88	39.	.5	135	52.	.5
89	39.	0.	136	52.	0.
90	40.5	3.4	137	53.5	3.4
91	40.5	2.9	138	53.5	2.9
92	40.5	1.7	139	53.5	1.7
93	40.5	.5	140	53.5	.5
94	40.5	0.	141	53.5	0.
95	41.5	3.4	142	55.	3.4
96	41.5	2.9	143	55.	2.9
97	41.5	1.7	144	55.	1.7
98	41.5	.5	145	55.	.5
99	41.5	0.	146	55.	0.
100	42.42	3.4	147	56.5	3.4
101	42.42	2.57	148	56.5	2.9

149	56.5	1.7		196	85.	0.	
150	56.5	.10		197	90.	3.4	
151	56.5	0.		198	90.	1.7	
152	57.	1.		199	90.	0.	
153	57.67	3.4		1	2	5	4
154	57.67	2.9		2	3	6	5
155	57.67	2.4		3	4	8	7
156	57.67	1.78		4	4	5	8
157	57.67	.10		5	5	9	8
158	57.67	0.		6	5	10	9
159	59.33	3.4		7	5	6	10
160	59.33	2.9		8	7	8	11
161	59.33	2.4		9	9	12	11
162	59.33	1.78		10	9	10	12
163	59.33	.10		11	7	11	13
164	59.33	0.		12	11	14	13
165	60.	3.4		13	11	12	14
166	60.	2.9		14	10	14	12
167	60.	2.4		15	10	15	14
168	60.	1.78		16	14	17	16
169	60.	.10		17	15	18	17
170	60.	0.		18	17	20	19
171	61.5	3.4		19	18	21	20
172	61.5	1.7		20	19	23	22
173	61.5	0.		21	19	24	23
174	64.	3.4		22	19	20	24
175	64.	1.7		23	20	25	24
176	64.	0.		24	20	21	25
177	68.5	3.4		25	23	27	26
178	68.5	1.7		26	24	28	27
179	68.5	0.		27	24	25	28
180	73.	3.4		28	26	27	29
181	73.	1.7		29	27	28	29
182	73.	0.		30	28	30	29
183	76.5	3.4		31	25	30	28
184	76.5	1.7		32	25	31	30
185	76.5	0.		33	30	33	32
186	78.83	3.4		34	31	34	33
187	78.83	1.9		35	33	36	35
188	79.5	0.		36	34	37	36
189	80.25	3.4		37	36	39	38
190	80.25	1.9		38	37	40	39
191	82.	3.4		39	38	42	41
192	82.	1.7		40	38	39	42
193	82.	0.		41	39	43	42
194	85.	3.4		42	39	44	43
195	85.	1.7		43	39	46	44

44	49	45	44	0	3	44	2	91	93	98	97	92	4	91	2
45	41	47	46	0	3	45	3	92	94	99	98	93	4	92	2
46	41	42	47	0	3	46	3	93	95	101	100	0	3	93	4
47	42	48	47	0	3	47	3	94	95	96	101	0	3	94	4
48	43	49	48	42	4	48	3	95	96	102	101	0	3	95	4
49	44	50	49	43	4	49	2	96	96	97	102	0	3	96	4
50	45	51	50	44	4	50	2	97	97	103	102	0	3	97	4
51	47	53	52	46	4	51	3	98	98	104	103	97	4	98	2
52	48	54	53	47	4	52	3	99	99	105	104	98	4	99	2
53	49	55	54	44	4	53	3	100	101	107	106	100	4	100	7
54	50	56	55	49	4	54	2	101	102	108	107	101	4	101	4
55	51	57	56	45	4	55	2	102	103	109	108	102	4	102	4
56	53	59	58	52	4	56	7	103	104	110	109	103	4	103	2
57	54	60	59	53	4	57	3	104	105	111	110	104	4	104	2
58	55	61	60	54	4	58	3	105	106	107	112	0	3	105	4
59	56	62	61	55	4	59	2	106	107	113	112	0	3	106	4
60	57	63	62	56	4	60	2	107	107	108	113	0	3	107	4
61	59	65	64	58	4	61	3	108	108	114	113	0	3	108	4
62	60	66	65	59	4	62	3	109	108	109	114	0	3	109	4
63	61	67	66	60	4	63	3	110	110	115	114	109	4	110	2
64	62	68	67	61	4	64	2	111	111	116	115	110	4	111	2
65	63	69	68	62	4	65	2	112	113	118	117	112	4	112	4
66	64	65	70	0	3	66	3	113	114	119	118	113	4	113	4
67	65	71	70	0	3	67	3	114	115	120	119	114	4	114	2
68	65	66	71	0	3	68	3	115	116	121	120	115	4	115	2
69	66	72	71	0	3	69	3	116	118	123	122	117	4	116	4
70	66	67	72	0	3	70	3	117	119	124	123	118	4	117	4
71	68	73	72	67	4	71	2	118	120	125	124	119	4	118	2
72	69	74	73	68	4	72	2	119	121	126	125	120	4	119	2
73	71	76	75	70	4	73	3	120	123	128	127	122	4	120	4
74	72	77	76	71	4	74	3	121	124	129	128	123	4	121	4
75	73	78	77	72	4	75	2	122	125	130	129	124	4	122	2
76	74	79	78	73	4	76	2	123	126	131	130	125	4	123	2
77	76	81	80	75	4	77	3	124	128	133	132	127	4	124	4
78	77	82	81	76	4	78	3	125	129	134	133	128	4	125	4
79	78	83	82	77	4	79	2	126	130	135	134	129	4	126	2
80	79	84	83	78	4	80	2	127	131	136	135	130	4	127	2
81	81	86	85	80	4	81	4	128	133	138	137	132	4	128	4
82	82	87	86	81	4	82	4	129	134	139	138	133	4	129	4
83	83	88	87	82	4	83	2	130	135	140	139	134	4	130	2
84	84	89	88	83	4	84	2	131	136	141	140	135	4	131	2
85	86	91	90	85	4	85	4	132	138	143	142	137	4	132	5
86	87	92	91	86	4	86	4	133	139	144	143	138	4	133	5
87	88	93	92	87	4	87	2	134	140	145	144	139	4	134	2
88	89	94	93	88	4	88	2	135	141	146	145	140	4	135	2
89	91	96	95	90	4	89	4	136	143	148	147	142	4	136	5
90	92	97	96	91	4	90	4	137	144	149	148	143	4	137	5

138	144	145	149	0	3	138	2		185	188	193	190	0	3	185	2
139	145	150	149	0	3	139	2		186	192	195	194	191	4	186	6
140	146	146	150	0	3	140	2		187	193	196	195	192	4	187	2
141	146	151	150	0	3	141	2		188	195	198	197	194	4	188	6
142	148	154	153	147	4	142	5		189	196	199	198	195	4	189	2
143	148	155	154	0	3	143	5		1	0	5.	70.				
144	148	149	155	0	3	144	5		2	0	5.	58.				
145	149	156	155	0	3	145	5		3	0	3.	70.				
146	149	152	156	0	3	146	2		4	0	6.	70.				
147	149	150	152	0	3	147	2		5	0	8.	70.				
148	152	157	156	0	3	148	2		6	0	6.	58.				
149	150	157	152	0	3	149	2		7	0	3.	58.				
150	151	158	157	150	4	150	2		8	0	4.	70.				
151	154	160	159	153	4	151	5		9	0	45.	45.				
152	155	161	160	154	4	152	5		10	0	4.	58.				
153	156	162	161	155	4	153	5		11	3						
154	157	163	162	156	4	154	8		12	4						
155	158	164	163	157	4	155	2		13	5						
156	160	166	165	159	4	156	5		14	6						
157	161	167	166	160	4	157	5		15	7						
158	162	168	167	161	4	158	5		16	0	2.	70.				
159	163	169	168	162	4	159	2		17	0	2.	58.				
160	164	170	169	163	4	160	2		18	1						
161	165	166	171	0	3	161	5		19	17						
162	166	167	171	0	3	162	5		20	5						
163	167	172	171	0	3	163	5		21	5						
164	167	168	172	0	3	164	5		22	0	12.	70.				
165	168	169	172	0	3	165	2		23	2						
166	169	173	172	0	3	166	2		24	15						
167	169	170	173	0	3	167	2		25	18						
168	172	175	174	171	4	168	5		26	9						
169	173	176	175	172	4	169	2		27	23						
170	175	178	177	174	4	170	5		28	0	6.	72.				
171	176	179	178	175	4	171	2		29	28						
172	178	181	180	177	4	172	5		30	0	12.	72.				
173	179	182	181	178	4	173	2		31	0	5.	60.				
174	181	184	183	180	4	174	6		32	0	3.	60.				
175	182	185	184	181	4	175	2		33	0	5.	72.				
176	183	187	186	0	3	176	6		34	0	2.	60.				
177	183	184	187	0	3	177	6		35	33						
178	184	185	187	0	3	178	2		36	34						
179	185	188	187	0	3	179	2		37	33						
180	187	190	189	186	4	180	7		38	32						
181	187	188	190	0	3	181	2		39	33						
182	189	190	191	0	3	182	6		40	33						
183	190	192	191	0	3	183	6		41	33						
184	190	193	192	0	3	184	2		42	31						

43	31		90	85		
44	31		91	87		
45	0	10.	92	87		
46	45		93	0	10.	80.
47	28		94	93		
48	0	6.	95	93		
49	42		96	90		
50	42		97	90		
51	0	15.	98	0	10.	60.
52	51		99	83		
53	48		100	9		
54	49		101	96		
55	49		102	96		
56	9		103	98		
57	48		104	99		
58	48		105	93		
59	49		106	93		
60	49		107	93		
61	51		108	101		
62	51		109	101		
63	58		110	103		
64	59		111	104		
65	59		112	108		
66	45		113	108		
67	45		114	91		
68	47		115	91		
69	37		116	112		
70	37		117	112		
71	64		118	114		
72	64		119	114		
73	66		120	0	5.	80.
74	69		121	120		
75	0	8.	122	71		
76	75		123	71		
77	73		124	0	4.	80.
78	47		125	124		
79	0	12.	126	0	4.	60.
80	79		127	126		
81	0	6.	128	120		
82	0	8.	129	120		
83	79		130	122		
84	79		131	122		
85	82		132	0	8.	89.
86	82		133	132		
87	75		134	0	8.	59.
88	75		135	134		
89	85		136	0	10.	89.

137	136		
138.	0 12.	50.	
139	138		
140	138		
141	138		
142	132		
143	0 12.	89.	
144	143		
145	0 15.	89.	
146	0 15.	50.	
147	146		
148	146		
149	146		
150	146		
151	142		
152	136		
153	152		
154	0 45.	45.	
155	0 10.	50.	
156	151		
157	143		
158	145		
159	147		
160	147		
161	152		
162	152		
163	152		
164	152		
165	138		
166	138		
167	138		
168	133		
169	134		
170	0 6.	89.	
171	0 6.	50.	
172	0 3.	89.	
173	0 3.	50.	
174	0 10.	89.	
175	0 10.	54.	
176	0 20.	89.	
177	176		
178	0 15.	54.	







48	48	53	52	47	4	48	4		95	95	100	99	94	4	95	5
49	49	54	53	48	4	49	4		96	96	101	100	95	4	96	5
50	51	56	55	50	4	50	3		97	97	102	101	96	4	97	6
51	52	57	56	51	4	51	3		98	98	103	102	97	4	98	6
52	53	58	57	52	4	52	4		99	100	105	104	99	4	99	5
53	54	59	58	53	4	53	4		100	101	106	105	100	4	100	5
54	56	61	60	55	4	54	3		101	102	107	106	101	4	101	6
55	56	62	61	59	3	55	3		102	103	108	107	102	4	102	6
56	58	57	62	59	3	56	3		103	105	110	109	104	4	103	5
57	57	63	62	59	3	57	3		104	106	111	110	105	4	104	5
58	58	64	63	57	4	58	4		105	107	112	111	106	4	105	6
59	59	65	64	58	4	59	4		106	108	113	112	107	4	106	6
60	61	67	66	60	4	60	5		107	110	115	114	109	4	107	5
61	61	62	67	60	3	61	5		108	111	116	115	110	4	108	5
62	62	68	67	60	3	62	5		109	112	117	116	111	4	109	6
63	62	63	68	60	3	63	5		110	113	118	117	112	4	110	6
64	63	69	68	60	3	64	6		111	115	120	119	114	4	111	5
65	63	64	69	60	3	65	6		112	116	121	120	115	4	112	5
66	64	70	69	60	3	66	6		113	117	122	121	116	4	113	6
67	65	71	70	64	4	67	6		114	118	123	122	117	4	114	6
68	67	73	72	66	4	68	5		115	120	125	124	119	4	115	5
69	68	74	73	67	4	69	11		116	121	126	125	120	4	116	5
70	69	75	74	68	4	70	6		117	122	127	126	121	4	117	6
71	70	76	75	69	4	71	6		118	123	128	127	122	4	118	6
72	71	77	76	70	4	72	6		119	125	130	129	124	4	119	5
73	73	79	78	72	4	73	5		120	126	131	130	125	4	120	5
74	73	80	79	70	3	74	5		121	127	132	131	126	4	121	6
75	73	74	80	70	3	75	5		122	128	133	132	127	4	122	6
76	74	81	80	70	3	76	5		123	130	135	134	129	4	123	7
77	74	75	81	70	3	77	6		124	131	136	135	130	4	124	7
78	75	82	81	70	3	78	6		125	132	137	136	131	4	125	8
79	75	76	82	70	3	79	6		126	133	138	137	132	4	126	8
80	77	83	82	76	4	80	6		127	135	140	139	134	4	127	7
81	79	85	84	78	4	81	5		128	136	141	140	135	4	128	7
82	79	80	85	70	3	82	5		129	137	142	141	136	4	129	8
83	80	86	85	70	3	83	5		130	138	143	142	137	4	130	8
84	80	81	86	70	3	84	5		131	140	145	144	139	4	131	7
85	82	87	86	81	4	85	6		132	140	146	145	140	3	132	7
86	83	88	87	82	4	86	6		133	140	141	146	140	3	133	7
87	85	90	89	84	4	87	5		134	141	147	146	140	3	134	7
88	86	91	90	85	4	88	5		135	141	148	147	142	3	135	8
89	87	92	91	86	4	89	6		136	142	148	141	140	3	136	8
90	88	93	92	87	4	90	6		137	142	143	145	140	3	137	8
91	90	95	94	89	4	91	5		138	143	149	148	143	3	138	8
92	91	96	95	90	4	92	5		139	145	151	150	144	4	139	7
93	92	97	96	91	4	93	6		140	146	152	151	145	4	140	7
94	93	98	97	92	4	94	6		141	147	153	152	146	4	141	7

142	147	148	153	0	3	142	8		16	0	15.	70.4
143	148	154	153	0	3	143	8		17	0	12.	70.4
144	148	149	154	0	3	144	8		18	0	24.	70.4
145	149	155	154	0	3	145	8		19	0	24.	27.
146	151	157	156	150	4	146	7		20	0	15.	27.
147	152	158	157	151	4	147	7		21	0	10.	27.
148	153	159	158	152	4	148	11		22	17		
149	154	160	159	153	4	149	12		23	6		
150	155	161	160	154	4	150	8		24	0	20.	27.
151	157	163	162	156	4	151	7		25	21		
152	157	158	163	0	3	152	7		26	0	12.	67.8
153	158	164	163	0	3	153	7		27	0	15.	67.8
154	158	159	164	0	3	154	7		28	0	24.	67.8
155	159	160	164	0	3	155	8		29	0	24.	26.
156	160	165	164	0	3	156	8		30	0	15.	26.
157	161	166	165	160	4	157	8		31	0	10.	26.
158	162	163	167	0	3	158	7		32	0	8.	63.2
159	163	164	168	0	3	159	7		33	0	8.	34.
160	163	168	167	0	3	160	7		34	0	6.	63.2
161	164	165	168	0	3	161	8		35	0	5.	34.
162	165	166	169	0	3	162	8		36	0	10.	63.2
163	165	169	168	0	3	163	8		37	0	12.5	63.2
164	168	171	170	167	4	164	7		38	36		
165	169	172	171	168	4	165	8		39	33		
166	171	174	173	170	4	166	9		40	0	6.	34.
167	172	175	174	171	4	167	10		41	40		
168	174	177	176	173	4	168	9		42	34		
169	175	178	177	174	4	169	10		43	34		
170	177	180	179	176	4	170	9		44	0	10.	34.
171	178	181	180	177	4	171	10		45	44		
172	180	183	182	179	4	172	9		46	34		
173	181	184	183	180	4	173	10		47	34		
1	0	3.	73.						48	44		
2	0	4.	73.						49	44		
3	0	5.5	73.						50	36		
4	0	4.2.	28.						51	32		
5	0	4.	70.4						52	39		
6	0	45.	45.						53	39		
7	0	4.	27.						54	0	12.	58.6
8	5								55	54		
9	0	3.	70.4						56	0	10.	58.6
10	0	5.5	70.4						57	56		
11	7								58	0	8.	42.
12	0	5.	70.4						59	58		
13	0	5.	27.						60	0	15.	53.6
14	0	8.	70.4						61	60		
15	0	8.	27.						62	60		

63	68		110	105		157	145				
64	0	12.	42.		111	0	2.	59.5			
65	0	10.	42.		112	111		158	146		
66	65				113	0	3.	42.9			
67	0	6.	58.6		114	113		159	151		
68	0	12.	59.5		115	99		160	158		
69	0	45.	45.		116	99		161	134		
70	0	12.	42.9		117	113		162	150		
71	0	10.	42.9		118	113		163	150		
72	3	6.	42.9		119	0	4.	69.3			
73	0	15.	59.5		120	119		165	129		
74	73				121	0	4.	43.8			
75	73				122	121		166	0	6.	37.
76	73				123	0	5.	63.3			
77	70				124	123		168	0	4.	67.1
78	71				125	0	5.	60.3			
79	71				126	125		169	0	4.	38.8
80	72				127	0	8.	63.4			
81	0	10.	59.5		128	127		170	0	2.	67.1
82	68				129	0	8.	40.4			
83	61				130	129		171	0	2.	38.8
84	61				131	0	10.	63.4			
85	0	8.	42.9		132	0	12.	63.4			
86	65				133	132		172	0	2.	67.6
87	0	6.	59.5		134	0	12.	40.4			
88	67				135	134		173	0	2.	40.6
89	0	6.	42.9		136	134			3	11	
90	69				137	134			184	1	
91	87				138	131			40	0.0	-25.
92	87				139	0	15.	63.4			
93	69				140	0	19.	63.4			
94	69				141	140			150	0.0	-25.
95	6	3.	59.5		142	0	19.	40.4			
96	95				143	142					
97	0	4.	42.9		144	142					
98	97				145	0	15.	40.4			
99	95				146	134					
100	95				147	138					
101	97				148	0	45.	45.			
102	97				149	0	45.	45.			
103	2	1.	59.5		150	0	10.	40.4			
104	103				151	132					
105	101				152	139					
106	101				153	140					
107	103				154	153					
108	103				155	144					
109	105				156	144					

## APPENDIX G: INPUT FILE FOR SIMULATION ANALYSIS

2	1	4	0
FINITE ELEMENT ANALYSIS			
1519400.	345030.	11370.	2280.
10443.	7950.	.651	.372
137	104	2	2
2	0	67	-2.
25.	2	50	1
137	1	104	
1	0.	3.5	
2	0.	1.75	
3	0.	0.	
4	2.5	3.5	
5	2.5	1.75	
6	2.5	0.	
7	5.	3.5	
8	5.	1.75	
9	5.	0.	
10	7.5	3.5	
11	7.5	1.75	
12	7.5	0.	
13	10.	3.5	
14	10.	1.75	
15	10.	0.	
16	12.5	3.5	
17	12.5	1.75	
18	12.5	0.	
19	15.	3.5	
20	15.	1.75	
21	15.	0.	
22	17.5	3.5	
23	17.5	1.75	
24	17.5	0.	
25	20.	3.5	
26	20.	1.75	
27	20.	0.	
28	22.5	3.5	
29	22.5	1.75	
30	22.5	0.	
31	25.	3.5	
32	25.	1.75	
33	25.	0.	
34	27.5	3.5	
35	27.5	1.75	
36	27.5	0.	
37	30.	3.5	
38	30.	3.	
39	30.	1.75	
40	30.	.5	
41	30.	0.	
42	32.5	3.5	
43	32.5	3.	
44	32.5	1.75	
45	32.5	.5	
46	32.5	0.	
47	35.	3.5	
48	35.	3.	
49	35.	1.75	
50	35.	.5	
51	35.	0.	
52	37.5	3.5	
53	37.5	3.	
54	37.5	1.75	
55	37.5	.5	
56	37.5	0.	
57	40.	3.5	
58	40.	3.	
59	40.	1.75	
60	40.	.5	
61	40.	0.	
62	42.5	3.5	
63	42.5	3.	
64	42.5	1.75	
65	42.5	.5	
66	42.5	0.	
67	45.	3.5	
68	45.	3.	
69	45.	1.75	
70	45.	.5	
71	45.	0.	
72	47.5	3.5	
73	47.5	3.	
74	47.5	1.75	
75	47.5	.5	
76	47.5	0.	
77	50.	3.5	
78	50.	3.	
79	50.	1.75	
80	50.	.5	
81	50.	0.	
82	52.5	3.5	
83	52.5	3.	
84	52.5	1.75	
85	52.5	.5	
86	52.5	0.	
87	55.	3.5	
88	55.	3.	

89	55.	1.75			3	5	8	7	4			54	69	74	73	68
90	55.	.5			4	6	9	8	5			55	70	75	74	69
91	55.	0.			5	8	11	10	7			56	71	76	75	70
92	57.5	3.5			6	9	12	11	8			57	73	78	77	72
93	57.5	3.			7	11	14	13	10			58	74	79	78	73
94	57.5	1.75			8	12	15	14	11			59	75	80	79	74
95	57.5	.5			9	14	17	16	13			60	76	81	80	75
96	57.5	0.			10	15	18	17	14			61	78	83	82	77
97	60.	3.5			11	17	20	19	16			62	79	84	83	78
98	60.	3.			12	18	21	20	17			63	80	85	84	79
99	60.	1.75			13	20	23	22	19			64	81	86	85	80
100	60.	.5			14	21	24	23	20			65	83	88	87	82
101	60.	0.			15	23	26	25	22			66	84	89	88	83
102	62.5	3.5			16	24	27	26	23			67	85	90	89	84
103	62.5	1.75			17	26	29	28	25			68	86	91	90	85
104	62.5	0.			18	27	30	29	26			69	88	93	92	87
105	65.	3.5			19	29	32	31	28			70	89	94	93	88
106	65.	1.75			20	30	33	32	29			71	90	95	94	89
107	65.	0.			21	32	35	34	31			72	91	96	95	90
108	67.5	3.5			22	33	36	35	32			73	93	98	97	92
109	67.5	1.75			23	34	35	38	0			74	94	99	98	93
110	67.5	0.			24	34	38	37	0			75	95	100	99	94
111	70.	3.5			25	35	39	38	0			76	96	101	100	95
112	70.	1.75			26	35	40	39	0			77	97	98	102	0
113	70.	0.			27	35	36	48	0			78	98	103	102	0
114	72.5	3.5			28	36	41	40	0			79	98	99	103	0
115	72.5	1.75			29	38	43	42	37			80	99	100	103	0
116	72.5	0.			30	39	44	43	38			81	100	104	103	0
117	75.	3.5			31	40	45	44	39			82	100	101	104	0
118	75.	1.75			32	41	46	45	40			83	103	106	105	102
119	75.	0.			33	43	48	47	42			84	104	107	106	103
120	77.5	3.5			34	44	49	48	43			85	106	109	108	105
121	77.5	1.75			35	45	50	49	44			86	107	110	109	106
122	77.5	0.			36	46	51	50	45			87	109	112	111	108
123	80.	3.5			37	48	53	52	47			88	110	113	112	109
124	80.	1.75			38	49	54	53	48			89	112	115	114	111
125	80.	0.			39	50	55	54	49			90	113	116	115	112
126	82.5	3.5			40	51	56	55	50			91	115	118	117	114
127	82.5	1.75			41	53	58	57	52			92	116	119	118	115
128	82.5	0.			42	54	59	58	53			93	118	121	120	117
129	85.	3.5			43	55	60	59	54			94	119	122	121	118
130	85.	1.75			44	56	61	60	55			95	121	124	123	120
131	85.	0.			45	58	63	62	57			96	122	125	124	121
132	87.5	3.5			46	59	64	63	58			97	124	127	126	123
133	87.5	1.75			47	63	65	64	59			98	125	128	127	124
134	87.5	0.			48	61	66	65	60			99	127	130	129	126
135	90.	3.5			49	63	68	67	62			100	128	131	130	127
136	90.	1.75			50	64	69	68	63			101	130	133	132	129
137	90.	0.			51	65	70	69	64			102	131	134	133	130
1	2	5	4	1								103	133	136	135	132
2	3	6	5	2								104	134	137	136	133

APPENDIX H: FIRST PART OF COMPUTER OUTPUT FOR ANALYSIS OF STUD NO. 2

FINITE ELEMENT ANALYSIS (SPEC 2, MESS B)

LOADS

NODE	X	Y
25	0.00	-25.00
109	0.00	-25.00

DISPLACEMENTS

NODE	X	Y
67	.52087E-02	-.78595E-01
68	.52716E-02	-.78659E-01
69	.53345E-02	-.78588E-01

ELEMENT	X-STRESS	Y-STRESS	X-Y-STRESS	STGRN
79	-.1644E+03	.1264E+01	.7003E+01	-.1644E+03
80	-.3453E+03	.3596E+01	-.5174E+01	-.3453E+03
81	.1475E+02	-.6023E+01	.2430E+01	.1475E+02
82	-.3452E+03	.3597E+01	.5245E+01	-.3452E+03
83	-.1644E+03	.1280E+01	-.6939E+01	-.1644E+03
84	.1646E+03	-.1116E+01	.5990E+01	.1646E+03
85	.1538E+02	.5321E+01	-.2525E+01	.1538E+02
86	.3150E+03	-.2990E+01	.4369E+01	.3150E+03
87	.3151E+03	-.2989E+01	.4300E+01	.3151E+03
88	.1646E+03	-.1100E+01	-.6054E+01	.1646E+03

	MAX-STRESS	MIN-STRESS	ANGLE
79	.1559E+01	-.1647E+03	2.417
80	.3673E+01	-.3454E+03	-.849
81	.1475E+02	-.6023E+01	89.933
82	.3676E+01	-.3453E+03	.861
83	.1571E+01	-.1647E+03	-2.394
84	.1648E+03	-.1332E+01	87.933
85	.1538E+02	.5321E+01	-.89.856
86	.3151E+03	-.3050E+01	-.89.213
87	.3152E+03	-.3047E+01	89.226
88	.1648E+03	-.1320E+01	-.87.911

FINITE ELEMENT ANALYSIS (SPEC 2, MESS B)

LOAD CASE 15

LOADS

NODE	X	Y
25	0.00	-375.00
109	0.00	-375.00

DISPLACEMENTS

NODE	X	Y
67	.78131E-01	-.11789E+01
68	.79075E-01	-.11799E+01
69	.80017E-01	-.11788E+01

ELEMENT	X-STRESS	Y-STRESS	X-Y-STRESS	STGRN
79	-.2466E+04	.1895E+02	.1050E+03	-.2466E+04
80	-.5180E+04	.5394E+02	-.7761E+02	-.5180E+04
81	.2212E+03	-.9035E+02	.3645E+00	.2212E+03
82	-.5178E+04	.5396E+02	.7867E+02	-.5178E+04
83	-.2466E+04	.1921E+02	-.1041E+03	-.2466E+04
84	.2459E+04	-.1674E+02	.8984E+02	.2469E+04
85	.2308E+03	.7981E+02	-.3787E+00	.2308E+03
86	.4725E+04	-.4485E+02	-.6554E+02	.4725E+04
87	.4727E+04	-.4483E+02	.6450E+02	.4727E+04
88	.2469E+04	-.1649E+02	-.9081E+02	.2469E+04

	MAX-STRESS	MIN-STRESS	ANGLE
79	.2339E+02	-.2470E+04	.162
80	.5509E+02	.5181E+04	-.057
81	.2212E+03	-.9035E+02	.017
82	.5514E+02	-.5179E+04	.058
83	.2356E+02	-.2470E+04	-.161
84	.2473E+04	-.1998E+02	17.616
85	.2308E+03	.7981E+02	.019
86	.4726E+04	-.4575E+02	-.5.834
87	.4728E+04	-.4570E+02	5.749
88	.2473E+04	-.1981E+02	-.17.932

APPENDIX I: Moisture Content and Specific Gravity of the Studs Used in the Study

Specimen Number	Moisture Content (%)	Specific Gravity
1	7.84	0.493
2	7.32	0.470
3	7.86	0.523
4	7.06	0.516
5	7.84	0.582

APPENDIX J: MODULI OF ELASTICITY AND STRESSES OF SMALL CLEAR  
SPECIMENS CUT FROM THE FIVE STUDS AFTER TEST

Specimen number*	Moduli of elasticity (psi)			Stresses (psi)		
	E <sub>1</sub>	E <sub>2</sub>	E <sub>3</sub>	S <sub>1</sub>	S <sub>2</sub>	S <sub>3</sub>
1-C-A-1	1,735,800	1,263,500	372,800	4,630	5,740	7,990
1-C-A-2	2,130,200	1,705,400	1,074,800	4,990	6,020	8,060
Average (1-C-A)	1,933,000	1,484,500	723,800	4,810	5,880	8,030
1-C-B-1	2,408,500	1,627,100	626,100	4,930	6,680	8,490
1-C-B-2	3,097,000	1,861,500	790,700	6,260	7,380	8,360
Average (1-C-B)	2,752,800	1,744,300	708,400	5,600	7,030	8,430
1-C-C-1	2,758,800	1,959,900	1,111,000	4,270	6,220	8,580
1-C-C-2	2,490,200	2,018,100	1,998,000	5,720	6,830	8,420
1-C-C-3	1,775,200	1,538,500	827,200	5,760	6,340	8,460
Average (1-C-C)	2,341,400	1,838,800	1,312,100	5,250	6,460	8,490
Average (1-C)	2,342,300	1,710,600	971,500	5,220	6,460	8,340
1-T-A-1	1,609,100	1,609,100	1,609,100	10,990	10,990	10,990
1-T-A-2	1,923,800	1,559,100	1,559,100	8,510	9,240	9,970
1-T-A-3	1,636,800	1,086,800	1,033,700	8,920	9,390	10,100
Average (1-T-A)	1,723,300	1,418,300	1,400,600	9,470	9,870	10,350

Specimen number	Moduli of elasticity (psi)			Stresses (psi)		
	E <sub>1</sub>	E <sub>2</sub>	E <sub>3</sub>	S <sub>1</sub>	S <sub>2</sub>	S <sub>3</sub>
1-T-B-1	1,896,300	1,620,600	1,620,600	11,120	11,440	11,760
1-T-B-2	1,441,300	1,255,500	1,255,500	10,110	10,870	11,630
Average (1-T-B)	1,668,800	1,438,100	1,438,100	10,620	11,160	11,700
1-T-D	1,833,300	1,787,200	1,787,200	10,240	11,050	11,870
1-T-E-1	2,215,500	1,927,000	1,462,000	8,630	13,640	15,500
1-T-E-2	2,313,100	1,831,100	1,037,500	12,310	13,380	14,080
1-T-E-3	2,142,000	2,002,900	2,002,900	9,530	10,430	11,340
Average (1-T-E)	2,223,500	1,920,300	1,500,800	10,160	12,480	13,640
Average (1-T)	1,890,100	1,631,000	1,485,300	10,040	11,160	11,920
2-C-A	2,102,000	1,492,900	671,400	6,830	7,430	7,930
2-C-B	1,839,800	1,334,300	287,900	5,140	6,710	7,910
2-C-D	2,115,200	1,670,900	1,037,400	3,250	6,250	7,710
2-C-E	2,594,000	1,884,200	383,000	5,310	6,960	7,880
Average (2-C)	2,162,700	1,595,600	594,900	5,130	6,840	7,860

Specimen number	Moduli of elasticity (psi)			Stresses (psi)		
	E <sub>1</sub>	E <sub>2</sub>	E <sub>3</sub>	S <sub>1</sub>	S <sub>2</sub>	S <sub>3</sub>
2-T-A	1,787,600	1,582,600	1,582,600	6,130	7,410	8,700
2-T-D	1,919,600	753,500	753,500	7,660	8,390	9,140
2-T-E-1	1,687,700	1,584,600	1,584,600	5,810	6,870	7,930
2-T-E-2	1,712,000	1,616,500	1,616,500	8,720	9,130	9,540
2-T-E-3	1,777,400	1,777,400	1,777,400	9,140	9,140	9,140
Average (2-T-E)	1,725,700	1,659,500	1,659,500	7,890	8,380	8,870
Average (2-T)	1,776,900	1,462,900	1,462,900	7,490	8,190	8,890
3-C-A-1	2,507,900	1,469,900	458,100	6,960	7,660	8,330
3-C-A-2	2,439,800	1,665,300	333,900	4,690	6,810	8,280
Average (3-C-A)	2,473,800	1,567,600	396,000	5,820	7,240	8,300
3-C-B-1	1,734,600	1,548,800	618,200	5,190	6,440	8,540
3-C-B-2	2,466,500	1,773,200	434,200	7,420	8,730	9,730
Average (3-C-B)	2,100,600	1,661,000	526,200	6,310	7,590	9,140
3-C-C-1	2,515,700	1,794,500	680,700	6,730	7,810	8,300
3-C-C-2	2,757,800	2,127,900	1,369,700	6,270	7,750	8,740
3-C-C-3	1,826,500	1,399,900	507,600	6,760	7,950	8,530
Average (3-C-C)	2,366,700	1,774,100	852,700	6,590	7,840	8,520

Specimen number	Moduli of elasticity (psi)			Stresses (psi)		
	E <sub>1</sub>	E <sub>2</sub>	E <sub>3</sub>	S <sub>1</sub>	S <sub>2</sub>	S <sub>3</sub>
3-C-D-1	2,635,000	1,799,800	373,300	4,930	6,810	8,680
3-C-D-2	2,056,300	1,804,800	1,746,600	6,260	7,210	8,560
Average (3-C-D)	2,345,700	1,802,300	1,060,000	5,600	7,010	8,620
3-C-E-1	2,009,800	1,678,200	425,000	6,030	7,410	8,730
3-C-E-2	1,896,200	1,405,700	267,300	7,110	8,170	8,790
Average (3-C-E)	1,953,000	1,541,900	346,100	6,570	7,790	8,760
Average (3-C)	2,258,800	1,678,900	655,900	6,220	7,530	8,650
3-T-A-1	2,542,700	2,316,600	1,464,600	10,910	14,820	16,370
3-T-A-2	2,205,000	1,933,300	1,769,100	11,150	13,280	17,660
3-T-A-3	2,109,400	2,018,200	1,740,500	9,640	12,800	18,090
Average (3-T-A)	2,285,700	2,089,400	1,658,100	10,570	13,630	17,370
3-T-B-1	2,288,800	1,917,800	1,917,800	8,090	11,140	14,190
3-T-B-2	2,209,100	1,849,900	1,849,900	8,770	12,160	15,560
Average (3-T-B)	2,248,900	1,883,800	1,883,800	8,430	11,650	14,870
3-T-C	2,134,900	1,991,900	1,652,900	7,290	11,140	16,640
3-T-E-1	2,018,900	1,915,200	1,915,200	6,630	11,180	15,730

Specimen number	Moduli of elasticity (psi)			Stresses (psi)		
	E <sub>1</sub>	E <sub>2</sub>	E <sub>3</sub>	S <sub>1</sub>	S <sub>2</sub>	S <sub>3</sub>
3-T-E-2	2,441,400	1,363,300	1,363,300	14,020	14,730	15,460
Average (3-T-E)	2,230,100	1,639,200	1,639,200	10,320	12,950	15,590
Average (3-T)	2,243,700	1,913,300	1,709,100	9,560	12,650	16,210
4-C-A	1,820,600	1,341,000	363,000	4,010	6,020	7,920
4-C-B-1	2,319,000	1,698,400	542,400	4,870	6,610	8,200
4-C-B-2	2,426,100	1,827,500	604,300	5,820	7,100	8,200
Average (4-C-B)	2,372,500	1,762,900	573,300	5,340	6,850	8,200
4-C-C	1,936,900	1,585,400	753,700	4,010	5,560	6,970
4-C-D-1	2,329,600	1,458,800	510,300	5,770	7,040	7,920
4-C-D-2	1,441,800	1,020,200	310,600	4,690	6,680	7,950
Average (4-C-D)	1,885,700	1,239,500	410,400	5,230	6,860	7,930
4-C-E	1,796,000	1,316,400	315,000	3,860	5,700	7,550
Average (4-C)	2,010,000	1,463,900	485,600	4,720	6,390	7,810
4-T-B-1	1,580,100	1,429,700	1,348,500	6,630	9,610	13,300
4-T-B-2	1,662,200	1,649,000	1,649,000	4,050	7,430	10,810

Specimen number	Moduli of elasticity (psi)			Stresses (psi)		
	E <sub>1</sub>	E <sub>2</sub>	E <sub>3</sub>	S <sub>1</sub>	S <sub>2</sub>	S <sub>3</sub>
4-T-B-3	1,679,400	1,506,500	1,506,500	6,750	9,340	11,940
Average (4-T)	1,640,600	1,528,400	1,501,300	5,810	8,790	12,020
5-C-A	2,518,800	1,489,900	414,600	5,290	6,970	8,920
5-C-B-1	1,598,200	1,362,700	335,600	5,910	7,450	9,130
5-C-B-2	1,630,300	1,393,300	534,500	5,340	7,050	8,800
Average (5-C-B)	1,614,200	1,378,000	435,000	5,620	7,250	8,960
5-C-D-1	1,632,600	897,200	151,100	6,330	7,920	9,080
5-C-D-2	1,653,200	1,174,300	313,200	4,540	7,030	9,580
Average (5-C-D)	1,642,900	1,035,700	232,100	5,430	7,480	9,330
5-C-E-1	1,551,700	1,286,300	283,100	4,530	6,910	9,640
5-C-E-2	1,945,200	1,403,900	174,300	5,390	7,140	8,730
Average (5-C-E)	1,748,400	1,345,100	228,700	4,960	7,020	9,190
Average (5-C)	1,790,000	1,286,800	315,200	5,330	7,210	9,130
5-T-A-1	1,570,600	1,463,300	1,463,300	8,650	10,260	11,880
5-T-A-2	1,511,600	1,470,700	1,470,700	5,400	7,710	10,020
Average (5-T-A)	1,541,100	1,467,000	1,467,000	7,020	8,980	10,950